

TABLE OF CONTENTS

LIST OF FIGURES	ix
LIST OF TABLES	xv
I. INTRODUCTION	1
A. THE SLICE CONCEPT	1
B. SEAKEEPING.....	2
II. MODELING.....	5
A. OVERVIEW	5
B. PROGRAM DESCRIPTION.....	5
C. PROGRAM INPUT.....	6
1. Station Profiles.....	6
2. Weight Curve Generation	7
3. Regular and Irregular Waves.....	8
4. Damping Coefficients	9
III. RESULTS	23
A. OVERVIEW	23
B. REGULAR WAVE RESULTS	24
C. IRREGULAR WAVE RESULTS	66
D. SEAKEEPING EVALUATION.....	67
IV. DISCUSSION.....	78
A. CONCLUSIONS	78
B. RECOMMENDATIONS.....	79
LIST OF REFERENCES	81
APPENDIX A.....	83
INITIAL DISTRIBUTION LIST	91

LIST OF FIGURES

Figure (1). A Typical SWATH Configuration.	1
Figure (2). The SLICE Configuration Without Payload Module.	2
Figure (3). Representative Station Profile (Forward Pod near Frame 11).	6
Figure (4). SLICE Weight Curve.	7
Figure (5). Full Scale Resistance Based on Model Tests, From LMSC, 1994.	10
Figure (6). Roll Characteristics, 30 Degree Wave Angle. Damping = 0.02.....	10
Figure (7). Roll Characteristics, 60 Degree Wave Angle. Damping = 0.02.....	11
Figure (8). Roll Characteristics, 90 Degree Wave Angle. Damping = 0.02.....	11
Figure (9). Roll Characteristics, 120 Degree Wave Angle. Damping = 0.02.....	12
Figure (10). Roll Characteristics, 150 Degree Wave Angle. Damping = 0.02.....	12
Figure (11). Roll Characteristics as a Function of Wave Angle, 0 Knots. Damping = 0.02.	13
Figure (12). Roll Characteristics as a Function of Wave Angle, 5 Knots. Damping = 0.02.	13
Figure (13). Roll Characteristics as a Function of Wave Angle, 10 Knots. Damping = 0.02.	14
Figure (14). Roll Characteristics as a Function of Wave Angle, 15 Knots. Damping = 0.02.	14
Figure (15). Roll Characteristics as a Function of Wave Angle, 20 Knots. Damping = 0.02.	15
Figure (16). Roll Characteristics as a Function of Wave Angle, 30 Knots. Damping = 0.02.	15
Figure (17). Significant Double Amplitudes Roll, From LMSC, 1994.....	16
Figure (18). Comparison of Roll Damping Factors.	16
Figure (19). Roll Characteristics as a Function of Wave Angle, 0 Knots. No Viscous Damping.....	17
Figure (20). Roll Characteristics as a Function of Wave Angle, 5 Knots. No Viscous Damping.....	18
Figure (21). Roll Characteristics as a Function of Wave Angle, 10 Knots. No Viscous Damping.....	18
Figure (22). Roll Characteristics as a Function of Wave Angle, 15 Knots. No Viscous Damping.....	19
Figure (23). Roll Characteristics as a Function of Wave Angle, 20 Knots. No Viscous Damping.....	19
Figure (24). Roll Characteristics as a Function of Wave Angle, 30 Knots. No Viscous Damping.....	20

Figure (25). Roll Characteristics, 30 Degree Wave Angle. No Viscous Damping.....	20
Figure (26). Roll Characteristics, 60 Degree Wave Angle. No Viscous Damping.....	21
Figure (27). Damping Effects on Roll Motion , 60 Degree Wave Angle at 10 Knots.....	21
Figure (28). Wave Angle Definitions.....	24
Figure (29). Surge Characteristics as a Function of Wave Angle, 0 Knots.	25
Figure (30). Heave Characteristics as a Function of Wave Angle, 0 Knots.	26
Figure (31). Pitch Characteristics as a Function of Wave Angle, 0 Knots.	26
Figure (32). Sway Characteristics as a Function of Wave Angle, 0 Knots.....	27
Figure (33). Roll Characteristics as a Function of Wave Angle, 0 Knots.....	27
Figure (34). Yaw Characteristics as a Function of Wave Angle, 0 Knots.	28
Figure (35). Surge Characteristics as a Function of SLICE Speed, 0 Degree Wave Angle.	28
Figure (36). Surge Characteristics as a Function of SLICE Speed, 30 Degree Wave Angle.	29
Figure (37). Surge Characteristics as a Function of SLICE Speed, 60 Degree Wave Angle.	29
Figure (38). Surge Characteristics as a Function of SLICE Speed, 90 Degree Wave Angle.	31
Figure (39). Surge Characteristics as a Function of SLICE Speed, 120 Degree Wave Angle.	31
Figure (40). Surge Characteristics as a Function of SLICE Speed, 150 Degree Wave Angle.	32
Figure (41). Surge Characteristics as a Function of SLICE Speed, 180 Degree Wave Angle.	32
Figure (42). Surge Characteristics as a Function of Wave Angle, 5 Knots.	33
Figure (43). Surge Characteristics as a Function of Wave Angle, 10 Knots.	33
Figure (44). Surge Characteristics as a Function of Wave Angle, 15 Knots.	34
Figure (45). Surge Characteristics as a Function of Wave Angle, 20 Knots.	34
Figure (46). Surge Characteristics as a Function of Wave Angle, 30 Knots.	35
Figure (47). Sway Characteristics as a Function of SLICE Speed, 30 Degree Wave Angle.	35
Figure (48). Sway Characteristics as a Function of SLICE Speed, 60 Degree Wave Angle.	36
Figure (49). Sway Characteristics as a Function of SLICE Speed, 90 Degree Wave Angle.	36
Figure (50). Sway Characteristics as a Function of SLICE Speed, 120 Degree Wave Angle.	37

Figure (51). Sway Characteristics as a Function of SLICE Speed, 150 Degree Wave Angle.	37
Figure (52). Sway Characteristics as a Function of Wave Angle, 5 Knots.	38
Figure (53). Sway Characteristics as a Function of Wave Angle, 10 Knots.	38
Figure (54). Sway Characteristics as a Function of Wave Angle, 15 Knots.	39
Figure (55). Sway Characteristics as a Function of Wave Angle, 20 Knots.	39
Figure (56). Sway Characteristics as a Function of Wave Angle, 30 Knots.	40
Figure (57). Yaw Characteristics as a Function of SLICE Speed, 30 Degree Wave Angle.	40
Figure (58). Yaw Characteristics as a Function of SLICE Speed, 60 Degree Wave Angle.	41
Figure (59). Yaw Characteristics as a Function of SLICE Speed, 90 Degree Wave Angle.	41
Figure (60). Yaw Characteristics as a Function of SLICE Speed, 120 Degree Wave Angle.	42
Figure (61). Yaw Characteristics as a Function of SLICE Speed, 150 Degree Wave Angle.	42
Figure (62). Yaw Characteristics as a Function of Wave Angle, 5 Knots.	43
Figure (63). Yaw Characteristics as a Function of Wave Angle, 10 Knots.	43
Figure (64). Yaw Characteristics as a Function of Wave Angle, 15 Knots.	44
Figure (65). Yaw Characteristics as a Function of Wave Angle, 20 Knots.	44
Figure (66). Yaw Characteristics as a Function of Wave Angle, 30 Knots.	45
Figure (67). Heave Characteristics as a Function of SLICE Speed, 0 Degree Wave Angle.	46
Figure (68). Heave Characteristics as a Function of SLICE Speed, 30 Degree Wave Angle.	46
Figure (69). Heave Characteristics as a Function of SLICE Speed, 60 Degree Wave Angle.	47
Figure (70). Heave Characteristics as a Function of SLICE Speed, 90 Degree Wave Angle.	47
Figure (71). Heave Characteristics as a Function of SLICE Speed, 120 Degree Wave Angle.	48
Figure (72). Heave Characteristics as a Function of SLICE Speed, 150 Degree Wave Angle.	48
Figure (73). Heave Characteristics as a Function of SLICE Speed, 180 Degree Wave Angle.	49
Figure (74). Heave Characteristics as a Function of Wave Angle, 5 Knots.	49
Figure (75). Heave Characteristics as a Function of Wave Angle, 10 Knots.	50
Figure (76). Heave Characteristics as a Function of Wave Angle, 15 Knots.	50

Figure (77). Heave Characteristics as a Function of Wave Angle, 20 Knots.	51
Figure (78). Heave Characteristics as a Function of Wave Angle, 30 Knots.	51
Figure (79). Pitch Characteristics as a Function of SLICE Speed, 0 Degree Wave Angle.....	52
Figure (80). Pitch Characteristics as a Function of SLICE Speed, 30 Degree Wave Angle.....	52
Figure (81). Pitch Characteristics as a Function of SLICE Speed, 60 Degree Wave Angle.....	53
Figure (82). Pitch Characteristics as a Function of SLICE Speed, 90 Degree Wave Angle.....	53
Figure (83). Pitch Characteristics as a Function of SLICE Speed, 120 Degree Wave Angle.....	54
Figure (84). Pitch Characteristics as a Function of SLICE Speed, 150 Degree Wave Angle.....	54
Figure (85). Pitch Characteristics as a Function of SLICE Speed, 180 Degree Wave Angle.....	55
Figure (86). Pitch Characteristics as a Function of Wave Angle, 5 Knots.	55
Figure (87). Pitch Characteristics as a Function of Wave Angle, 10 Knots.	56
Figure (88). Pitch Characteristics as a Function of Wave Angle, 15 Knots.	56
Figure (89). Pitch Characteristics as a Function of Wave Angle, 20 Knots.	57
Figure (90). Pitch Characteristics as a Function of Wave Angle, 30 Knots.	57
Figure (91). Roll Characteristics as a Function of SLICE Speed, 30 Degree Wave Angle.	59
Figure (92). Roll Characteristics as a Function of SLICE Speed, 60 Degree Wave Angle.	60
Figure (93). Roll Characteristics as a Function of SLICE Speed, 90 Degree Wave Angle.	60
Figure (94). Roll Characteristics as a Function of SLICE Speed, 120 Degree Wave Angle.	61
Figure (95). Roll Characteristics as a Function of SLICE Speed, 150 Degree Wave Angle.	61
Figure (96). Roll Characteristics as a Function of Wave Angle, 5 Knots.	62
Figure (97). Roll Characteristics as a Function of Wave Angle, 10 Knots.	62
Figure (98). Roll Characteristics as a Function of Wave Angle, 15 Knots.	63
Figure (99). Roll Characteristics as a Function of Wave Angle, 20 Knots.	63
Figure (100). Roll Characteristics as a Function of Wave Angle, 30 Knots.	64
Figure (101). Resonant Peak Locations for Surge.	64
Figure (102). Resonant Peak Locations for Heave.	65

Figure (103). Resonant Peak Locations for Pitch.....	65
Figure (104). Resonant Peak Locations for Roll.....	66
Figure(105). Pitch Characteristics, 0 Knots.....	69
Figure(107). Pitch Characteristics, 10 Knots.....	69
Figure(106). Pitch Characteristics, 5 Knots.....	69
Figure(108). Pitch Characteristics, 15 Knots.....	69
Figure(109). Pitch Characteristics, 20 Knots.....	70
Figure(111). Roll Characteristics, 0 Knots.....	70
Figure(110). Pitch Characteristics, 30 Knots.....	70
Figure(112). Roll Characteristics, 5 Knots.....	70
Figure(113). Roll Characteristics, 10 Knots.....	71
Figure(115). Roll Characteristics, 20 Knots.....	71
Figure(114). Roll Characteristics, 15 Knots.....	71
Figure(116). Roll Characteristics, 30 Knots.....	71
Figure(117). Pitch Characteristics, Sea State 2.	72
Figure(119). Pitch Characteristics, Sea State 4.	72
Figure(118). Pitch Characteristics, Sea State 3.	72
Figure(120). Pitch Characteristics, Sea State 5.	72
Figure(121). Pitch Characteristics, Sea State 6.	73
Figure(123). Roll Characteristics, Sea State 2.	73
Figure(122). Pitch Characteristics, Sea State 7.	73
Figure(124). Roll Characteristics, Sea State 3.	73
Figure(125). Roll Characteristics, Sea State 4.	74
Figure(127). Roll Characteristics, Sea State 6.	74
Figure(126). Roll Characteristics, Sea State 5.	74
Figure(128). Roll Characteristics, Sea State 7.	74

Figure(129). Vertical Acceleration, 0 Knots.	75
Figure(131). Vertical Acceleration, 10 Knots.	75
Figure(130). Vertical Acceleration, 5 Knots.	75
Figure(132). Vertical Acceleration, 15 Knots.	75
Figure(133). Vertical Acceleration, 20 Knots.	76
Figure(135). Vertical Acceleration, Sea State 2.	76
Figure(134). Vertical Acceleration, 30 Knots.	76
Figure(136). Vertical Acceleration, Sea State 3.	76
Figure(137). Vertical Acceleration, Sea State 4.	77
Figure(139). Vertical Acceleration, Sea State 6.	77
Figure(138). Vertical Acceleration, Sea State 5.	77
Figure(140). Vertical Acceleration, Sea State 7.	77

LIST OF TABLES

TABLE (1). SLICE PRINCIPAL DIMENSIONS, FROM LMSC, 1994.....	2
TABLE (2). SEAKEEPING CRITERIA IN TRANSIT, FROM MCCREIGHT, 1987.....	3
TABLE (3). SUMMARY OF DISPLACEMENTS.....	8
TABLE (5). REGIONS OF NEGATIVE ENCOUNTER FREQUENCIES.....	30
TABLE (6). RELATIONSHIP BETWEEN SEA SEVERITY AND WAVE TO SHIP LENGTH RATIOS. AFTER PAPOULIAS, 1993.	58
TABLE (7). LEGEND FOR POLAR PLOTS.....	67

I. INTRODUCTION

A. THE SLICE CONCEPT

The SLICE ATD (Advanced Technology Demonstration) is an advancement of conventional small waterplane area twin hull (SWATH) design. The main advantages to SWATH vessels lie in their improved seakeeping abilities over monohulls of similar displacement. This improvement is attributed to the reduced waterplane area which provides for longer natural periods of heave and pitch motions as well as less wave exciting forces. A typical SWATH configuration is shown in Figure (1).

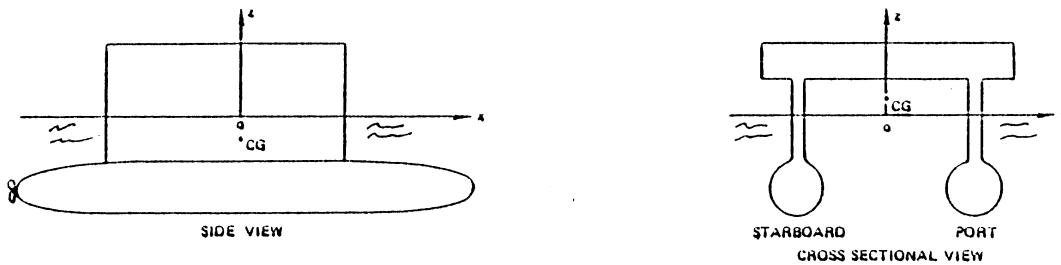


Figure (1). A Typical SWATH Configuration.

The reduced waterplane area of a SWATH vessel is typically twenty percent of that of a similar monohull (Fein, 1987). The SLICE concept further reduces the waterplane area by separating the two streamlined submerged hulls of the SWATH into four torpedo-shaped pods. These pods are individually connected to the above water structural box by separate wing-shaped struts. Other striking modifications include the offset of forward and after pods and the modular payload capacity. Figure (2) shows the SLICE configuration and Table (1) is a summary of typical dimensions.

B. SEAKEEPING

The seakeeping performance of a ship is often quantified by crew comfort, mission accomplishment, and operability/maintainability of shipboard systems. All of these factors can be improved by reducing the adverse motions and accelerations of the platform. The SWATH

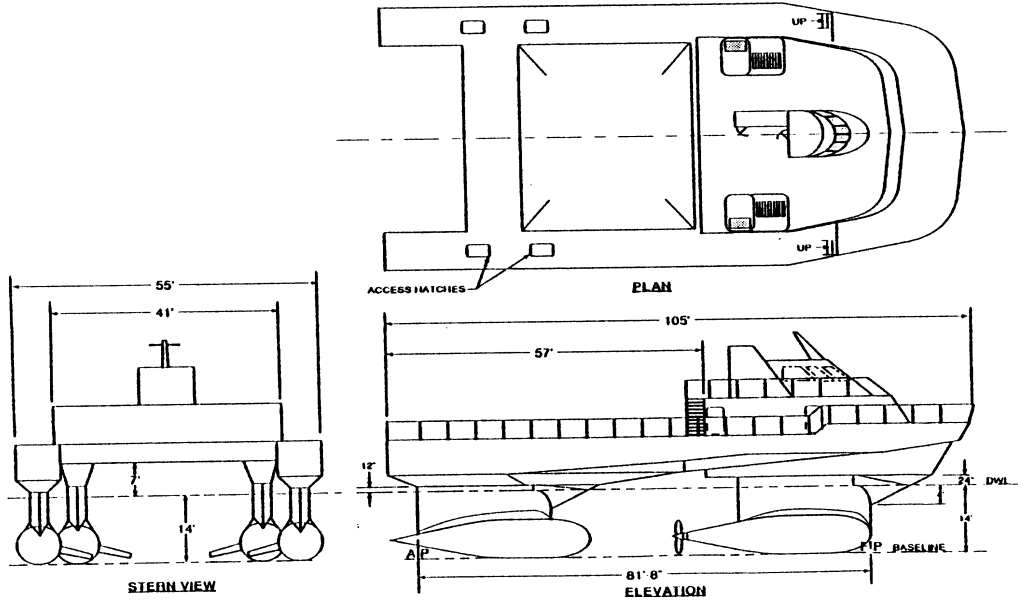


Figure (2). The SLICE Configuration Without Payload Module.

Length Overall	105' - 0"
Length Between Perpendiculars	81' - 8"
Length of Fwd Lower Hull	33' - 9"
Length of Aft Lower Hull	36' - 0"
Length of Struts	24' - 0"
Breadth Overall	55' - 0"
Diameter (max.) Lower Hulls	8' - 0"
Depth Molded to Main Deck	25' - 0"
Depth Molded to DWL	14' - 0"
Length on Design Waterline	89' - 1 1/2"
Fwd Hull Offset From Centerline	16' - 6"
Aft Hull Offset From Centerline	23' - 6"

Table (1). SLICE Principal Dimensions, From LMSC, 1994.

hullform exhibits reduced motions due to its small waterplane area, which minimizes wave exciting forces. Another benefit is provided by the increased natural periods in heave and pitch. This tends to reduce the occurrence of resonant motions resulting from wave excitation forces in normally encountered seas. There is a distinct disadvantage to small waterplane area vessels. Most exhibit vertical plane instabilities above certain speeds. This has been successfully countered by the use of active and passive stabilizing fins. These fins also provide additional damping. For conventional hulls, wavemaking damping dominates. For SWATH and SLICE hulls, wavemaking damping is roughly the same magnitude as the viscous damping due to their reduced waterplane areas. Because of this, viscous effects cannot be neglected in the modeling process.

Evaluation of a vessel's seakeeping characteristics in the early stages of design is an important milestone in the creation of a product that will perform as desired without costly design changes during and after construction. Key to this process is the computer modeling of ship motions and accelerations over the range of sea conditions that may be encountered in service.

The evaluation of a vessel's seakeeping capability is largely dependent on the mission areas that will dominate its operation. The SLICE is, by design, capable of multiple missions. The predominant intended use of the SLICE, to date, is as a passenger ferry; therefore, one might apply seakeeping criteria that emphasize passenger comfort. Such criteria would limit the motions of pitch and roll, deck wetness and deck slamming events, and accelerations in the vertical plane. Specific criteria may be set as in Table (2).

Roll (deg.) ^a	8.0
Pitch (deg.) ^a	3.0
Vertical acceleration (g's) ^a	0.4
Slams/hr	20
Wetnesses/hr	30

^aSignificant Amplitudes.

Table (2). Seakeeping Criteria in Transit, From McCreight, 1987.

Chapter II discusses the modeling of the SLICE and the necessary assumptions to complete this study. In Chapter III, the results are presented and discussed. Chapter IV

completes the study with recommendations for continued research.

II. MODELING

A. OVERVIEW

The SLICE ATD concept incorporates multipurpose missions through the use of modular payloads. The following studies are based on the passenger ferry application. The SHIPMO.BM program, written by Robert F. Beck and Armin W. Troesch (1989), is utilized to conduct motion studies and predict wave loading due to motions in both regular and irregular waves. Motion data is compiled for all six degrees of freedom over a speed range from zero to thirty knots. The modeling process includes generation of the underwater hull offsets; generation of the weight curve for this application; regular and irregular wave model selection and parameters; and, the determination of appropriate damping in surge and roll.

B. PROGRAM DESCRIPTION

The SHIPMO.BM program is a FORTRAN 77 based code that employs numerous subroutines to determine the motions, velocities, accelerations, shear loads, and bending moments of a given underwater hull model. It employs the strip theory of Salvesen, et al (1970), in the determination of motions in six degrees of freedom, and a two-dimensional potential theory source distribution technique similar to that of Frank (1967). The usefulness of this program in dealing with the SLICE design has been previously demonstrated for vertical plane motions (Peffer, 1995).

The mentioned calculations are based on slender body theory in an ideal fluid. To obtain more realistic motion predictions, the user can supply additional viscous damping factors for both surge and roll. Alternatively, the roll damping can be calculated by the program using the method of Himeno (1981). This method employs an equivalent linearization to the nonlinear roll moment-roll angle relationship.

C. PROGRAM INPUT

The program input file consists of data too numerous to devote a full description. However, there are a few sections that deserve detailed mention. The complete input file is included as Appendix [A].

1. Station Profiles

The model consists of twenty stations along the length of the hull. The required offsets are determined from ship drawings (LMSC, 1994) to describe the shape of the underwater portion of the hull based on the design waterline. Stations are located to best characterize the hull form and, therefore; are not spaced at even intervals. Each station is restricted to a maximum of fifteen offset points. While this may prove to be a limitation on the accuracy of underwater volume calculations for geometrically difficult hull shapes, redimensioning of the program was deemed not necessary. Figure (3) shows a representative station profile.

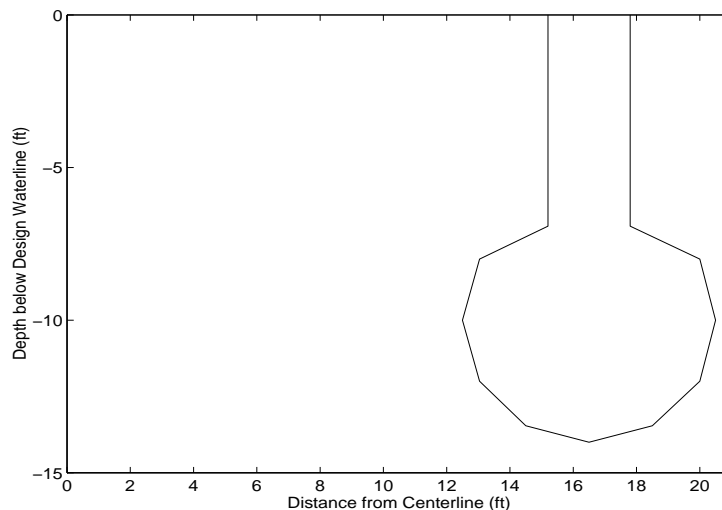


Figure (3). Representative Station Profile (Forward Pod near Frame 11).

2. Weight Curve Generation

A copy of the weight report for the ferry application served as the foundation for the construction of the weight curve (Roberts, 1995). The weight per unit length at various locations along the hull is determined by assuming an even distribution of equipment loads across each machinery space. This assumption is necessary since detailed drawings of equipment footprints were not available. Another simplifying assumption deals with the distribution of the weight of the hull structure along the length of the SLICE. This distribution is assumed to be twenty-five percent for the forward and after pod structures and fifty percent for the remaining structure up to and including the main deck. Forecastle, superstructure, and ferry module weights are considered as separate loads. These weights are also assumed to be constant along the lengths of their application. The program assumes port and starboard symmetry, along the centerline, for the weight curve at a given location; therefore, the only other required input is the vertical center of gravity at each weight curve ordinate. This is obtained through composite area calculations of all unit weights at a longitudinal location. The generated weight curve, ignoring the ten percent design margin, is shown in Figure (4). Table (3) summarizes calculated displacements.

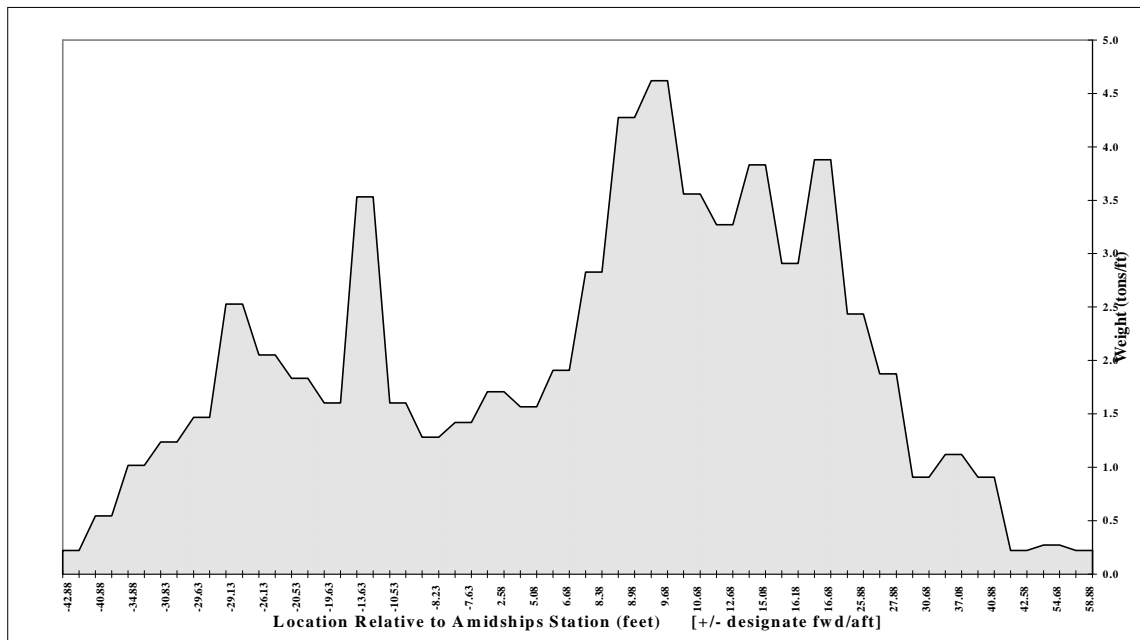


Figure (4). SLICE Weight Curve.

Weight Report Value	165.57 tons
Hydrostatic Value (based on station data)	164.57 tons
Weight Curve Value (area under curve)	167.08 tons

Table (3). Summary of Displacements.

3. Regular and Irregular Waves

Regular wave motions are developed based on several input parameters. Wave amplitude, the range of wavelengths or frequencies and their increment, and the wave angle are all required to determine the velocity potential in the global coordinate system. In the moving coordinate system, fixed to the ship, the vessel speed is also required.

In addition to the supplied regular wave data, motions in a seaway can be modeled with irregular waves. Six wave spectrum types are available for use in the program. The two spectra for this study are generated utilizing the Pierson-Moskowitz and ITTC wave spectrum models based on annual sea state data for the open oceans provided in Table (4).

Sea State	1	2	3	4	5	6	7
Significant Wave Height (ft)	0-0.3	0.3-1.6	1.6-4.1	4.1-8.2	8.2-13.1	13.1-19.7	19.7-29.5
Modeled Wave Height (ft)	0.3	0.95	2.85	6.15	10.65	16.4	24.6
Most Probable Modal Wave Period (sec)	-	7	8	9	10	12	14
Model Utilized	P.M.	ITTC	ITTC	ITTC	ITTC	ITTC	ITTC

Table (4). Annual Sea States in the Open Ocean, Northern Hemisphere, After Gilmer, 1982.

a. Pierson - Moskowitz Wave Spectrum

This model predicts fully developed seas, assuming steady winds and no detrimental effects from the underlying swell. Wave spectra are developed based on a single input parameter, the significant wave height as follows:

$$S_I^+(\omega) = \frac{0.0081g^2}{\omega^5} \exp\left[-0.032\left(\frac{g}{H_s\omega^2}\right)^2\right] \quad (1)$$

where: $S_I^+(\omega)$ is the one-sided incident wave spectrum.
 g is the acceleration of gravity.
 H_s is the significant wave height.
 ω is the wave frequency.

The Pierson - Moskowitz model generates a wave spectrum that can only be approached asymptotically in the seaway.

b. ITTC Spectrum Based on Modal Period

This model belongs to a two parameter spectrum family allowing the input of both significant wave height and mean period data. This provides more realistic wave spectra accounting for developing, fully developed, and decaying seas, depending on the magnitude of the parameters provided. The general form of this model is:

$$S_I^+(\omega) = \frac{0.3125H_s^2\omega_p^4}{\omega^5} \exp\left[-1.25\left(\frac{\omega_p}{\omega}\right)^4\right] \quad (2)$$

where: $\omega_p = 2\pi/T_p$
 T_p is the period of spectral peak

4. Damping Coefficients

Additional damping factors for both surge and roll are employed to provide more realistic motion results for these modes. The program allows the input of eight terms for surge and one for roll. The surge damping terms are determined from the slope of the resistance versus

speed curve, at up to eight different speeds, in consistent units of force per velocity. These values were obtained from Figure (5).

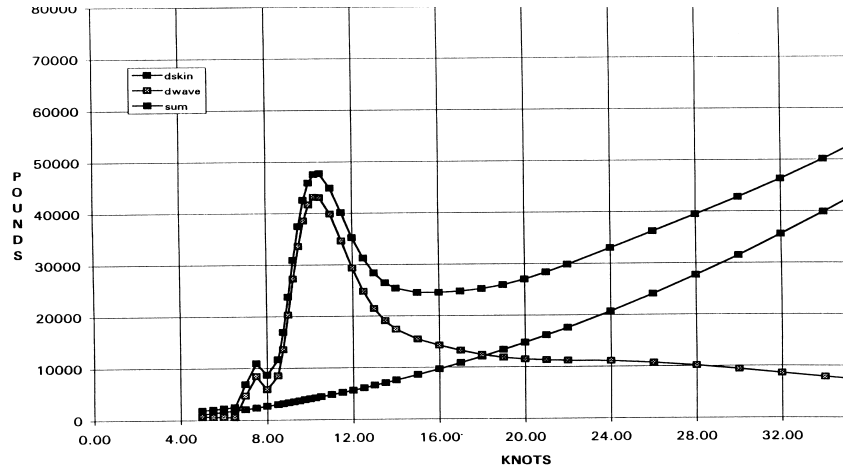


Figure (5). Full Scale Resistance Based on Model Tests, From LMSC, 1994.

The additional roll damping term is expressed as the percent of overall critical damping for roll. According to Reilly (1988), this value should be near two percent to only account for viscosity effects. Roll results based on this assumption are shown in Figures (6) through (16).

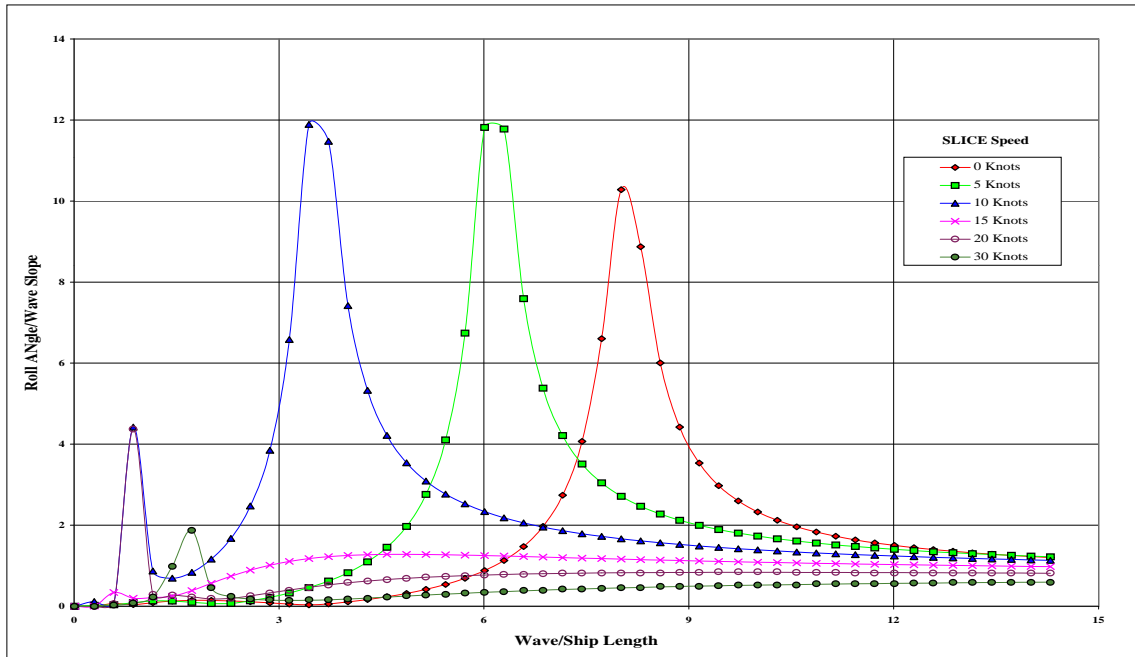


Figure (6). Roll Characteristics, 30 Degree Wave Angle. Damping = 0.02.

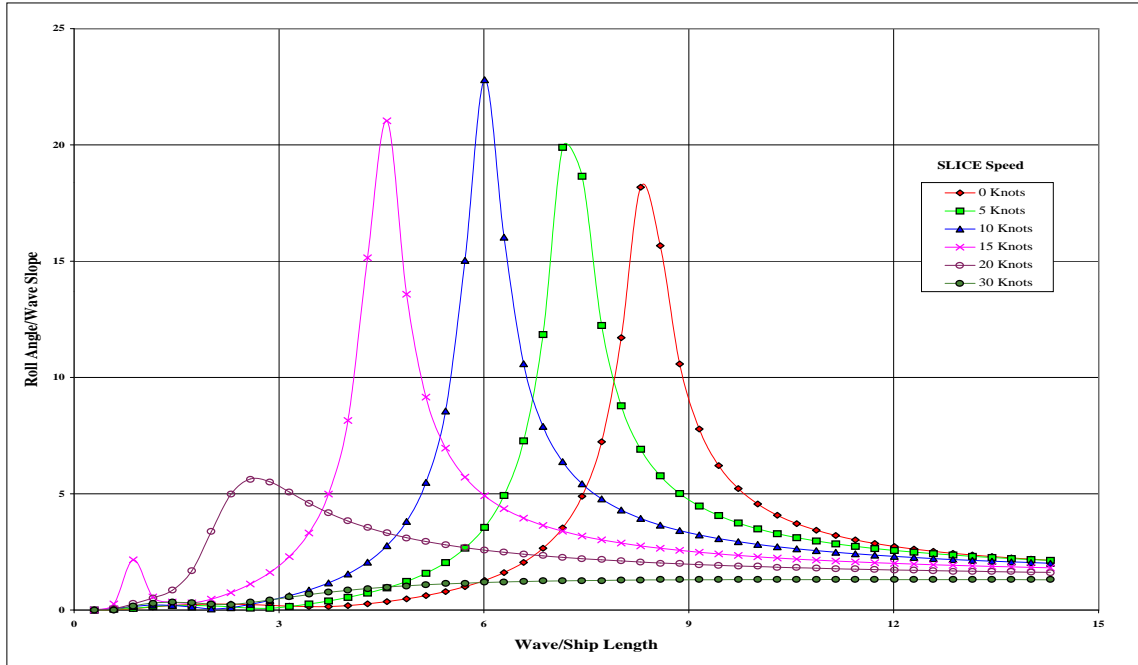


Figure (7). Roll Characteristics, 60 Degree Wave Angle. Damping = 0.02.

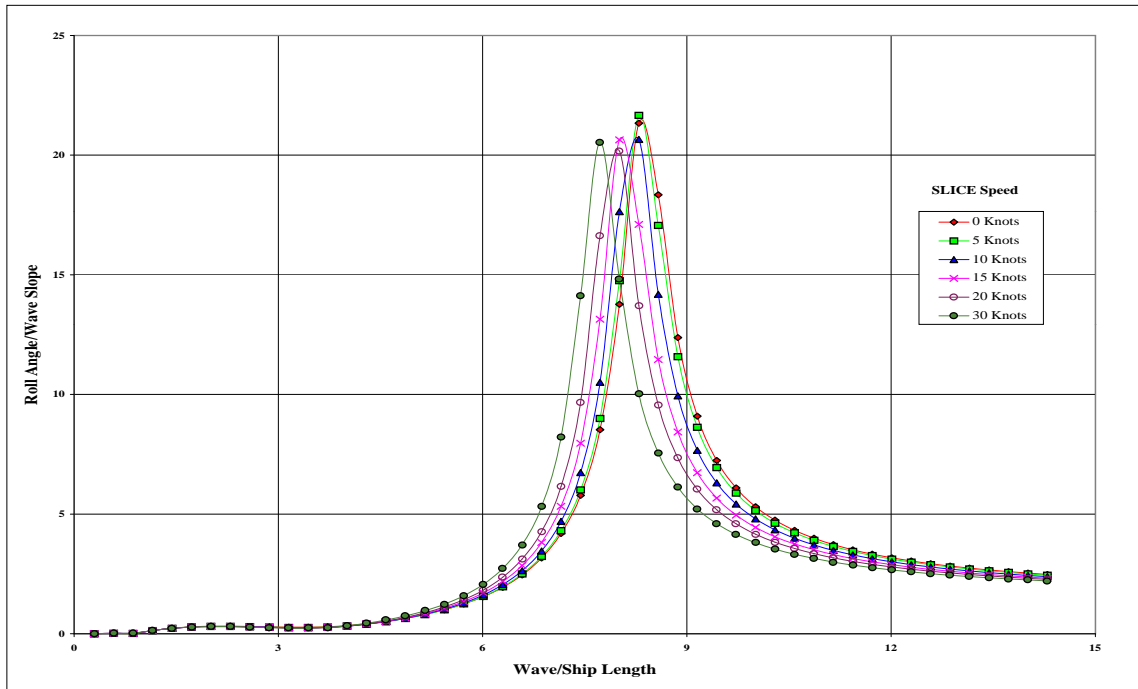


Figure (8). Roll Characteristics, 90 Degree Wave Angle. Damping = 0.02.

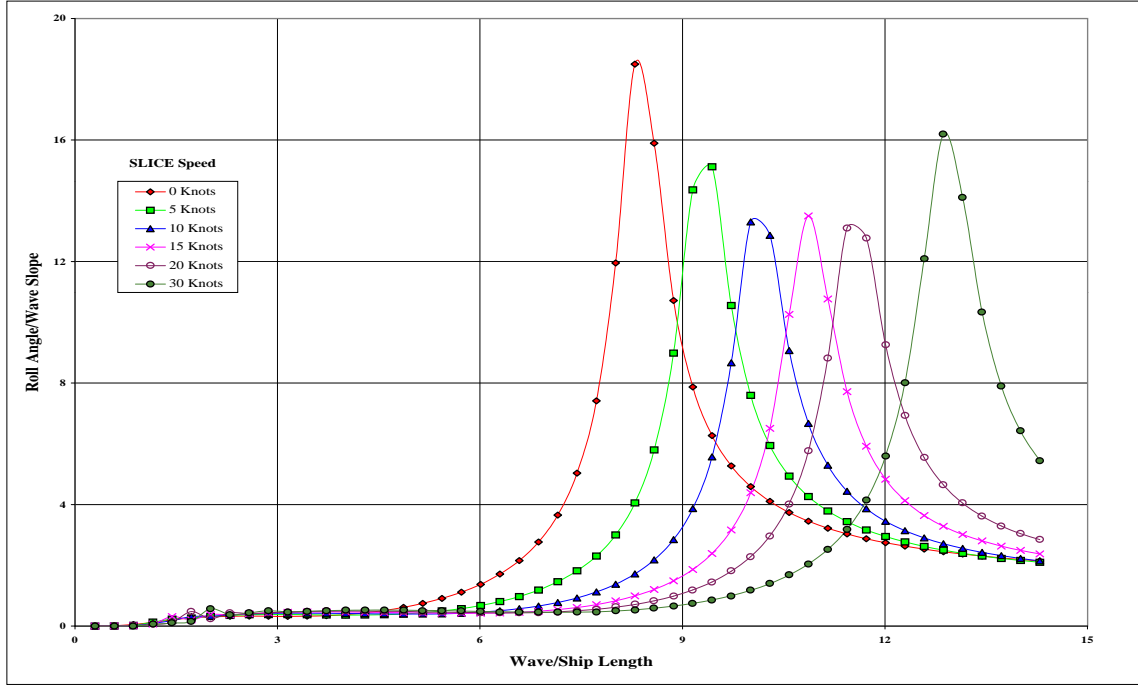


Figure (9). Roll Characteristics, 120 Degree Wave Angle. Damping = 0.02.

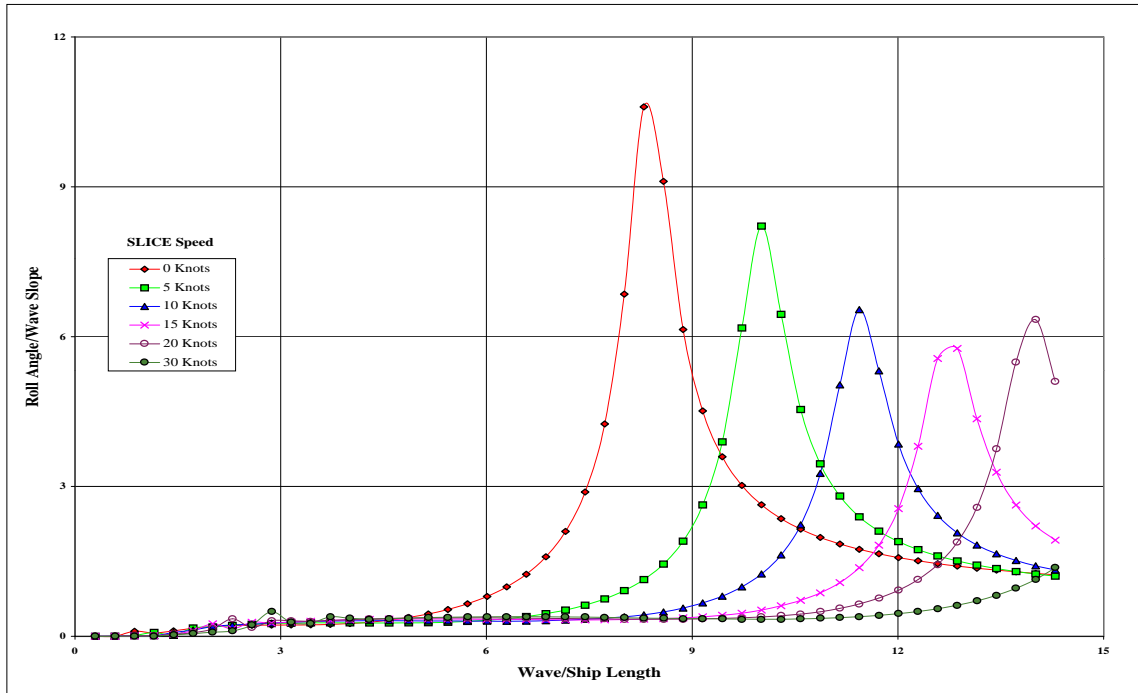


Figure (10). Roll Characteristics, 150 Degree Wave Angle. Damping = 0.02.

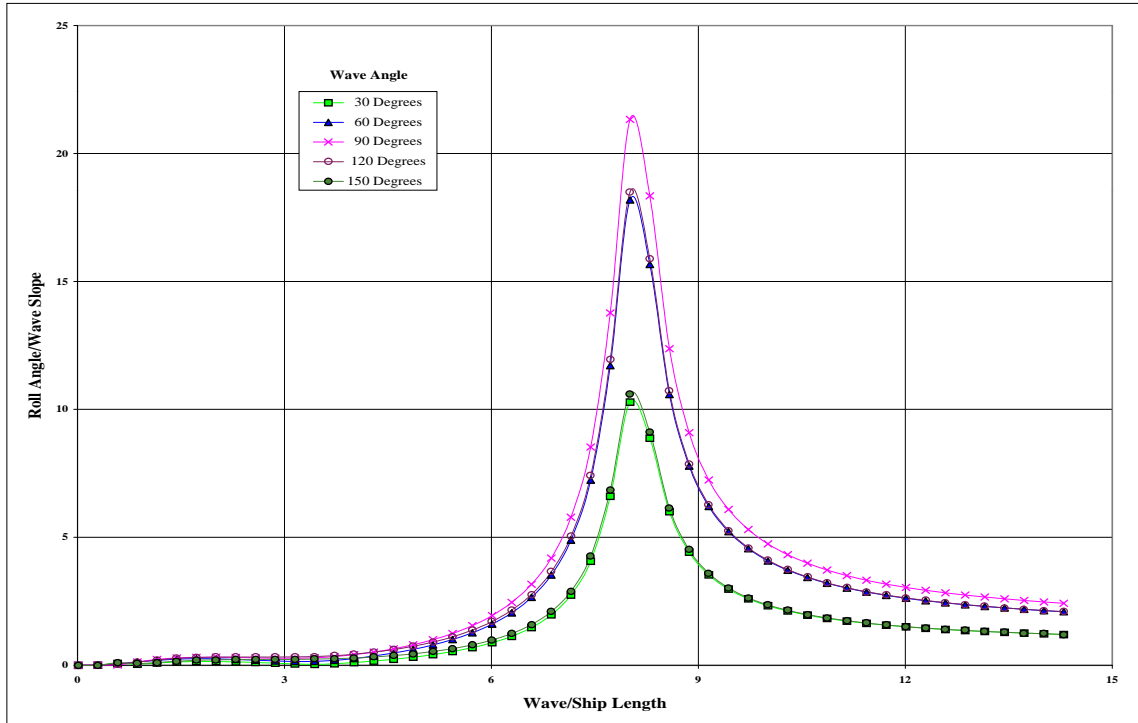


Figure (11). Roll Characteristics as a Function of Wave Angle, 0 Knots. Damping = 0.02.

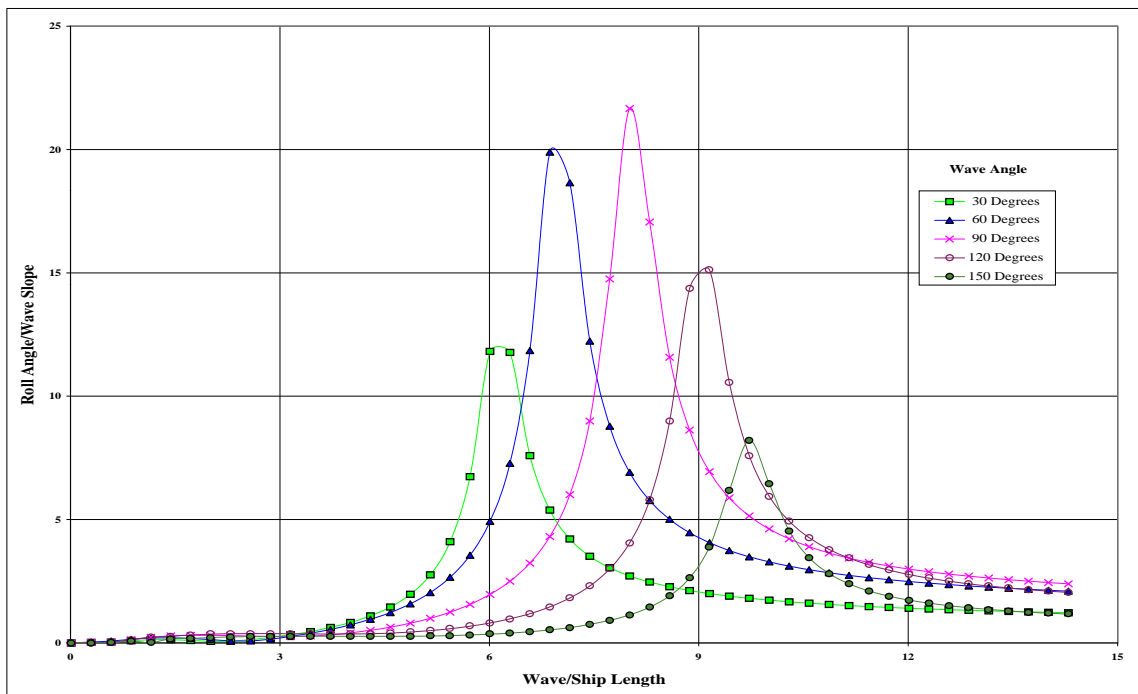


Figure (12). Roll Characteristics as a Function of Wave Angle, 5 Knots. Damping = 0.02.

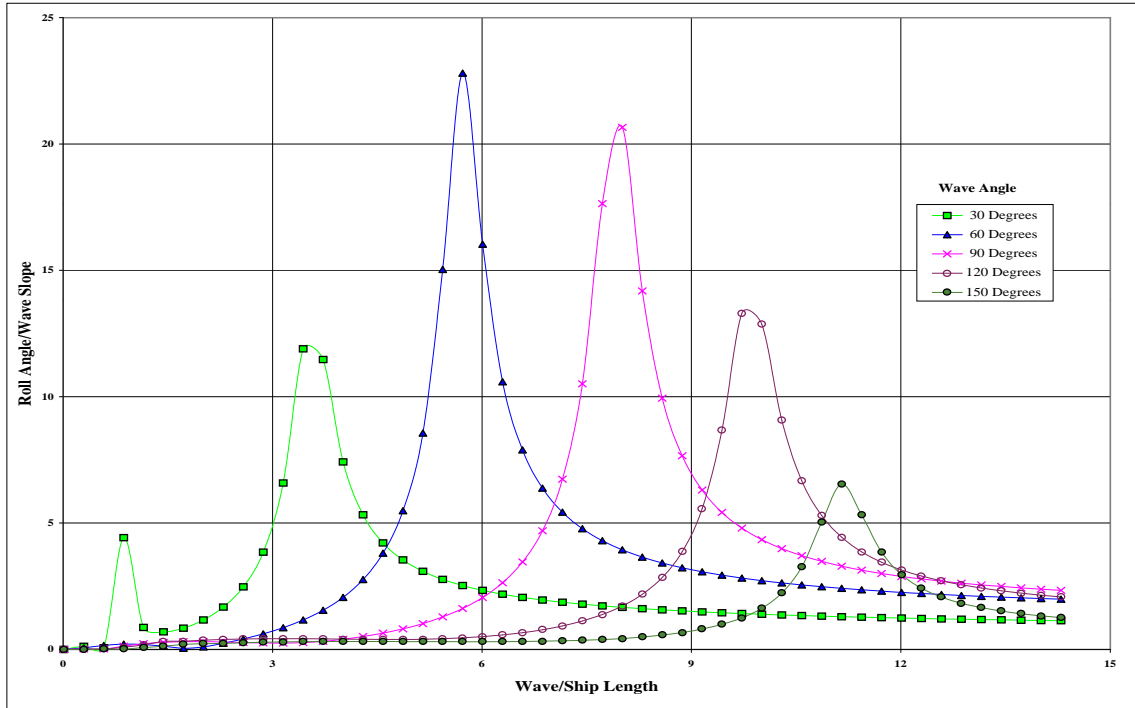


Figure (13). Roll Characteristics as a Function of Wave Angle, 10 Knots. Damping = 0.02.

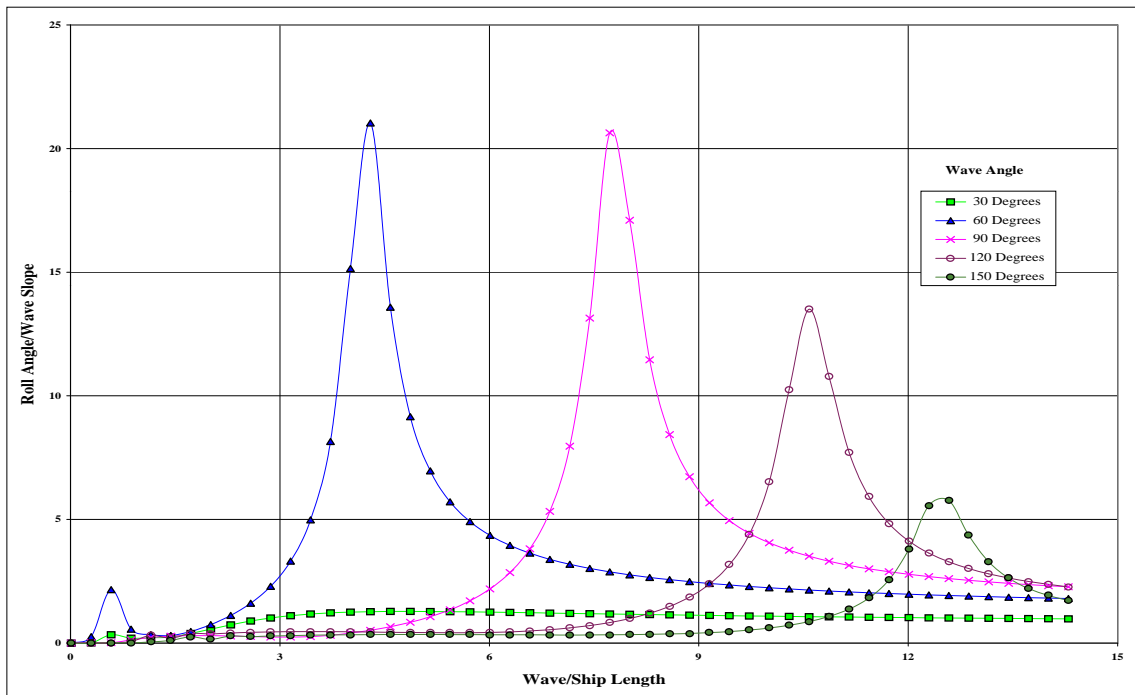


Figure (14). Roll Characteristics as a Function of Wave Angle, 15 Knots. Damping = 0.02.

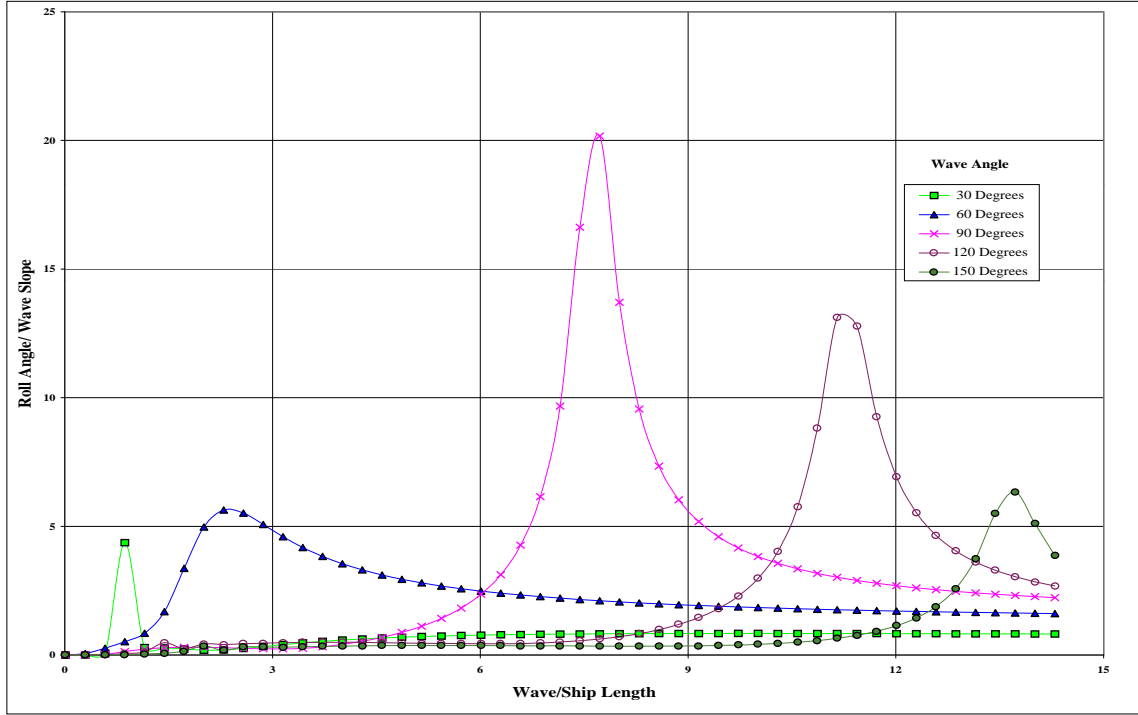


Figure (15). Roll Characteristics as a Function of Wave Angle, 20 Knots. Damping = 0.02.

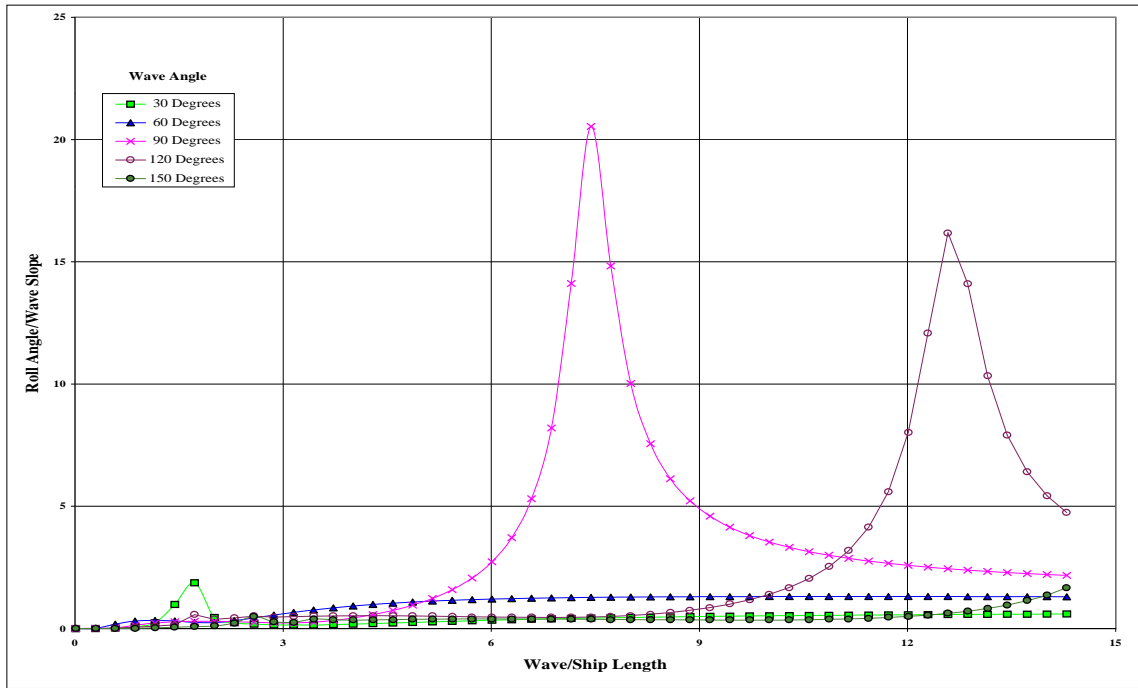


Figure (16). Roll Characteristics as a Function of Wave Angle, 30 Knots. Damping = 0.02.

When compared to the experimental results of Figure(17), the roll response is substantially greater, refer to Figure (18). This indicates there is substantially more damping present in roll. An iterative process was employed to replicate the data presented in Figure (17). This process

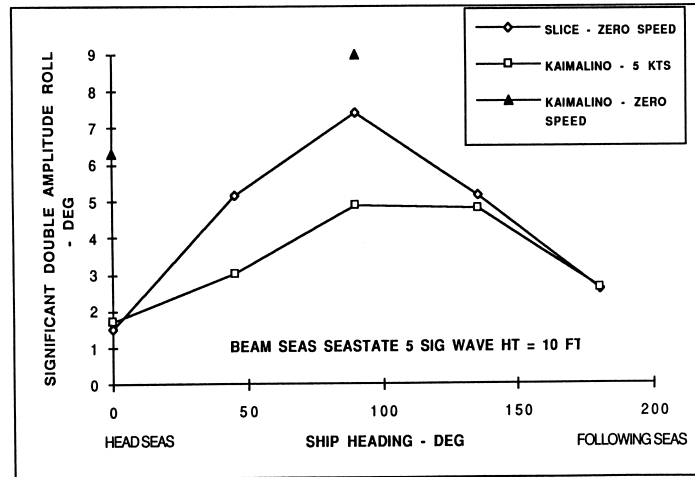


Figure (17). Significant Double Amplitudes Roll, From LMSC, 1994.

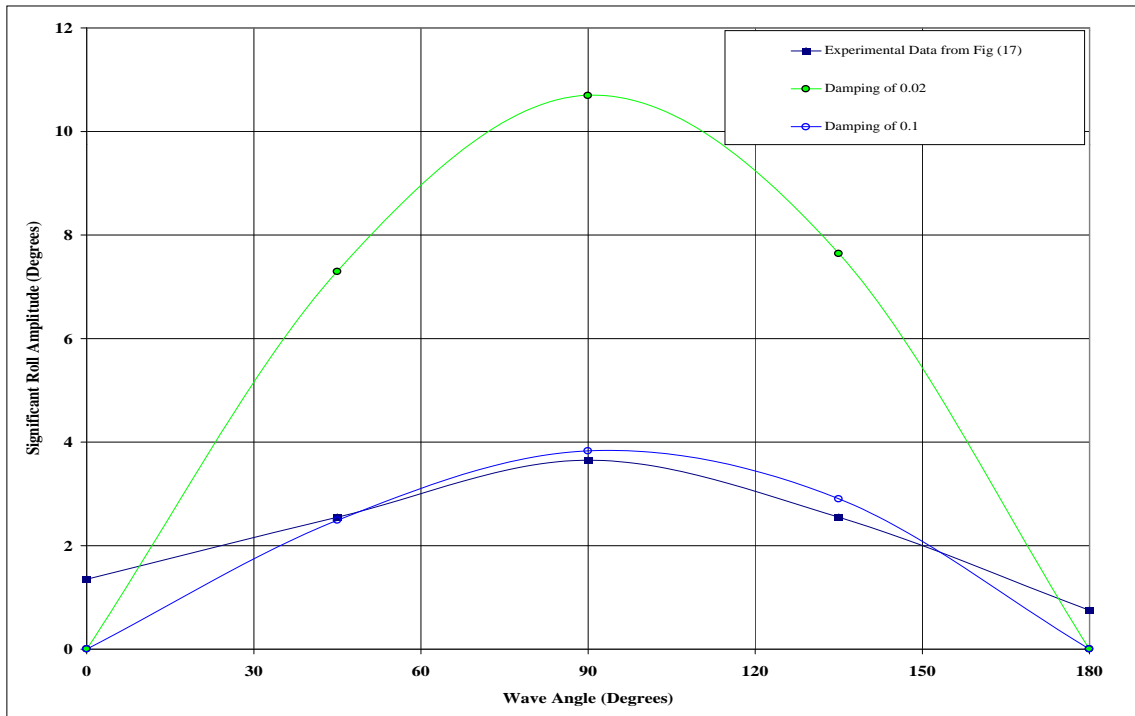


Figure (18). Comparison of Roll Damping Factors.

included simulating an undamped model to determine a representative peak in the roll response of the SLICE. Figures (19) through (26) depict this response in quartering seas, where motions are expected to be maximized. Once found, the effects of damping are modeled as shown in Figure (27). It is immediately obvious that this damping factor should be less than 0.3 for the system to remain underdamped. Since the boundary has been established on the range of acceptable values, the appropriate damping factor can be more easily determined. Hull forms like the SLICE/SWATH are considered lightly damped as reflected in the determined value of close to ten percent.

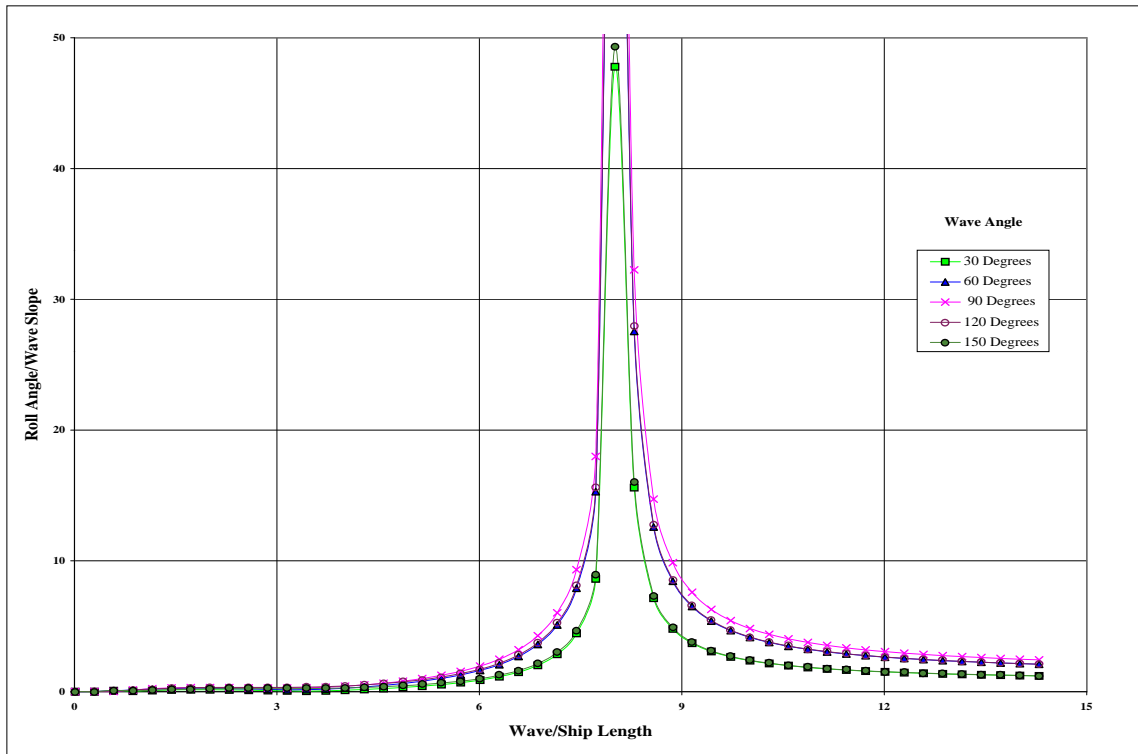


Figure (19). Roll Characteristics as a Function of Wave Angle, 0 Knots. No Viscous Damping.

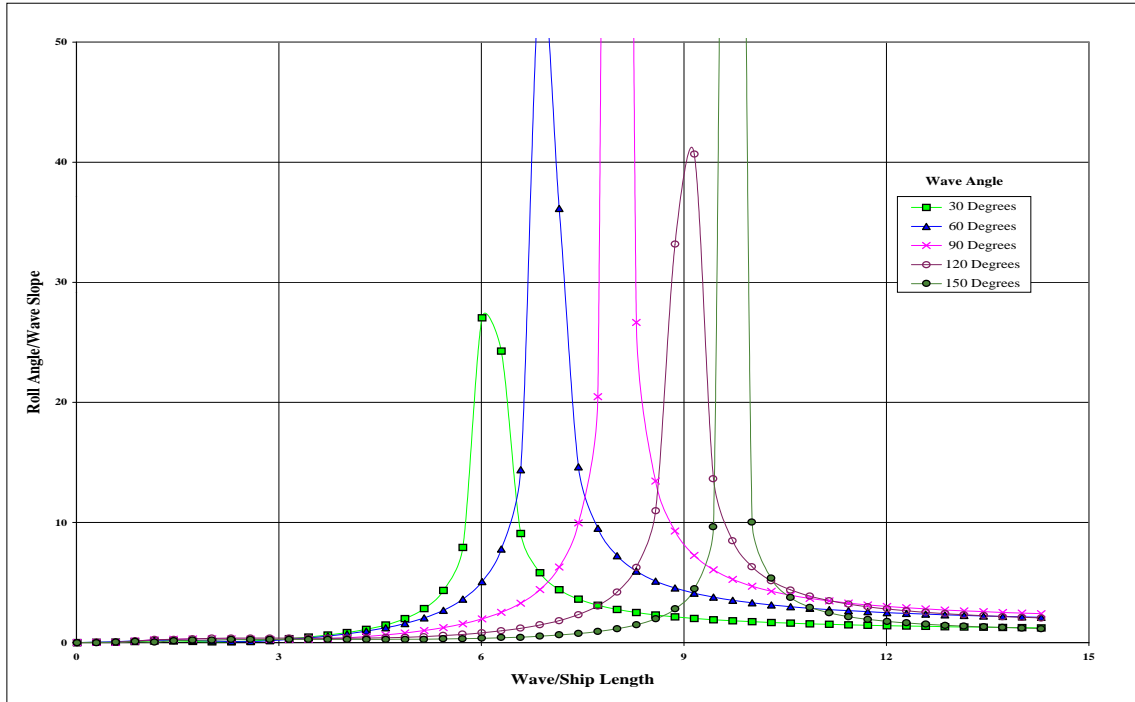


Figure (20). Roll Characteristics as a Function of Wave Angle, 5 Knots. No Viscous Damping.

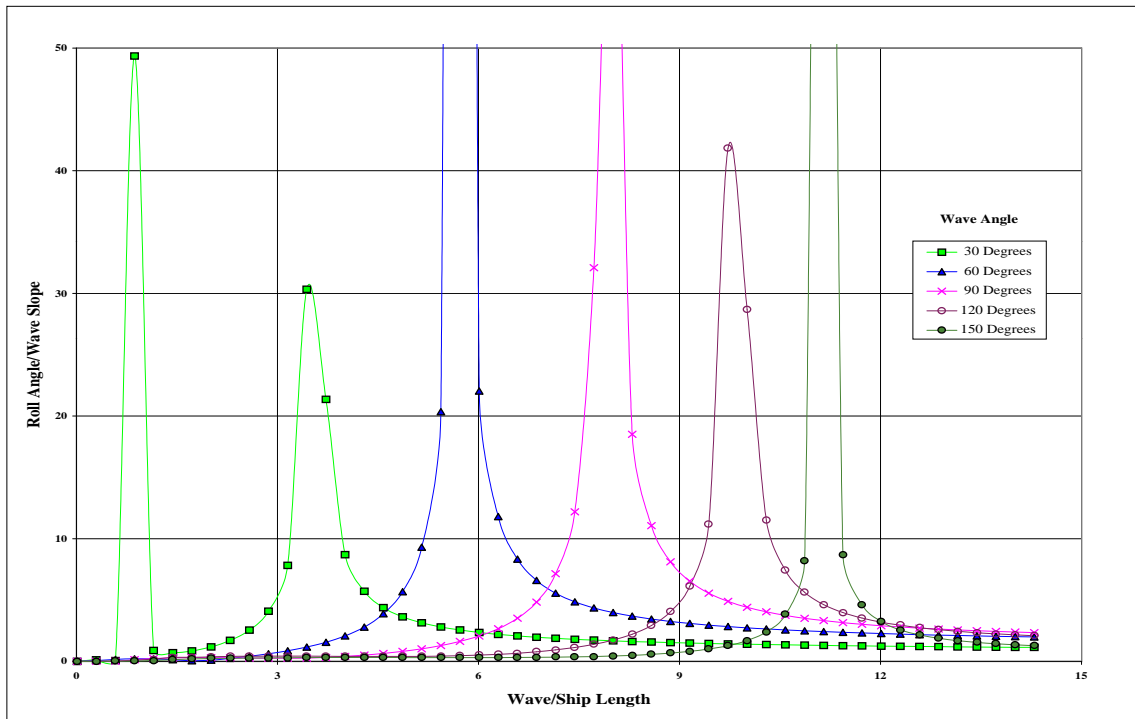


Figure (21). Roll Characteristics as a Function of Wave Angle, 10 Knots. No Viscous Damping.

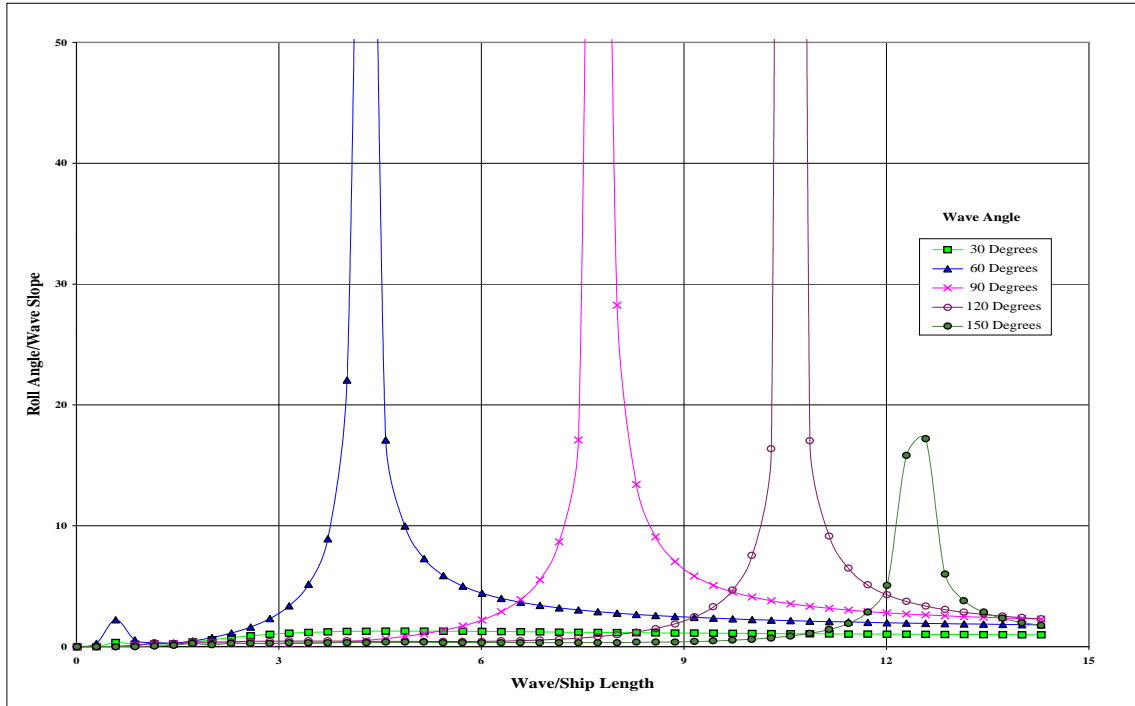


Figure (22). Roll Characteristics as a Function of Wave Angle, 15 Knots. No Viscous Damping.

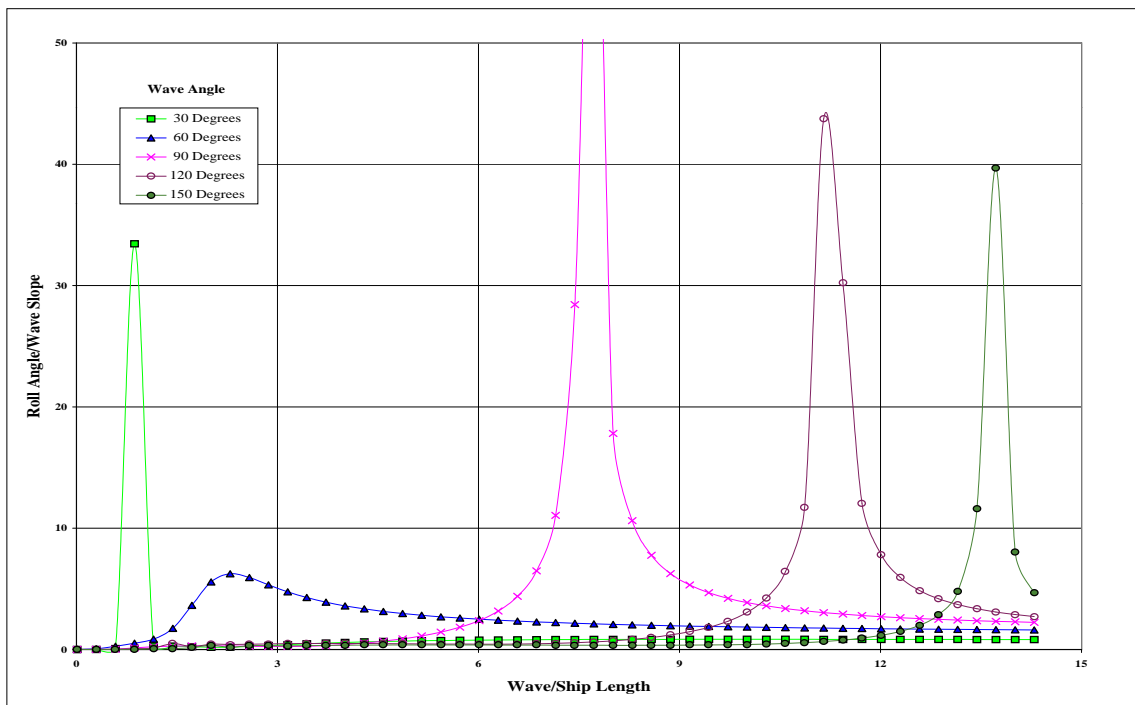


Figure (23). Roll Characteristics as a Function of Wave Angle, 20 Knots. No Viscous Damping.

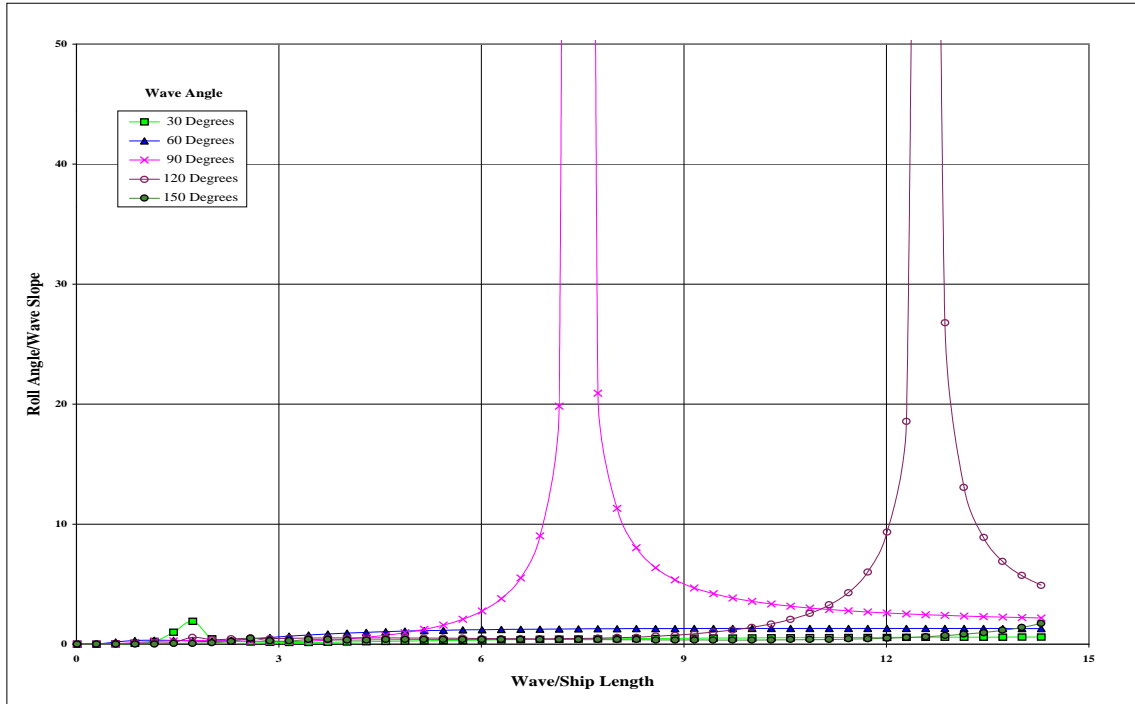


Figure (24). Roll Characteristics as a Function of Wave Angle, 30 Knots. No Viscous Damping.

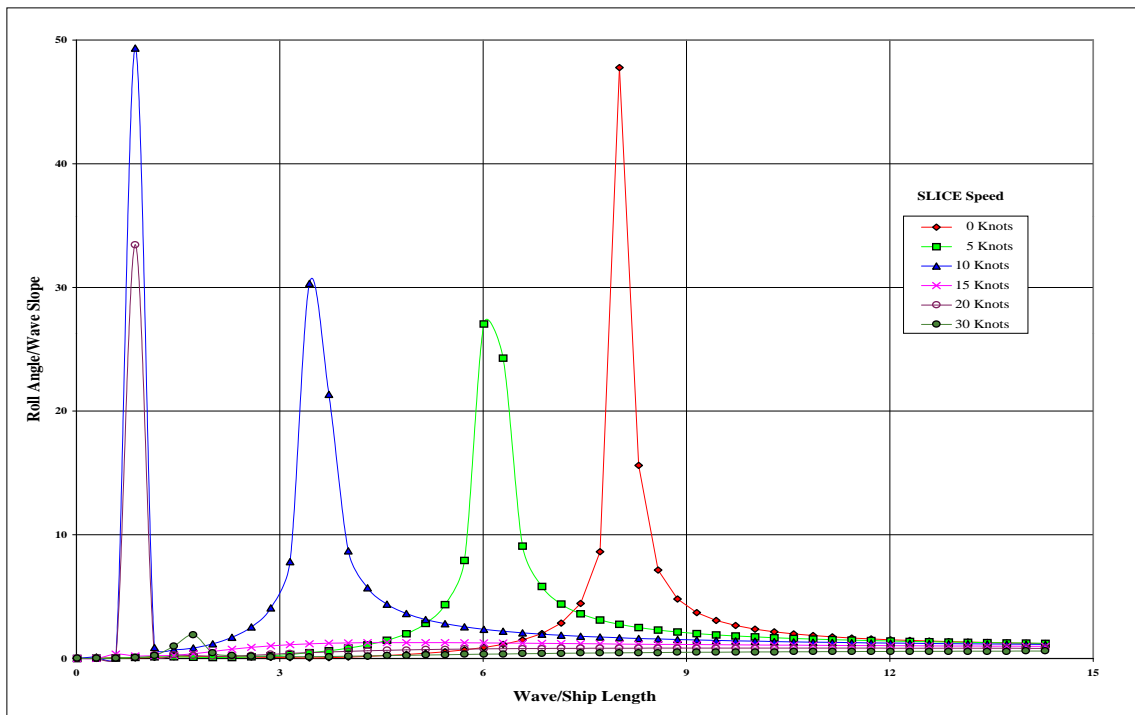


Figure (25). Roll Characteristics, 30 Degree Wave Angle. No Viscous Damping.

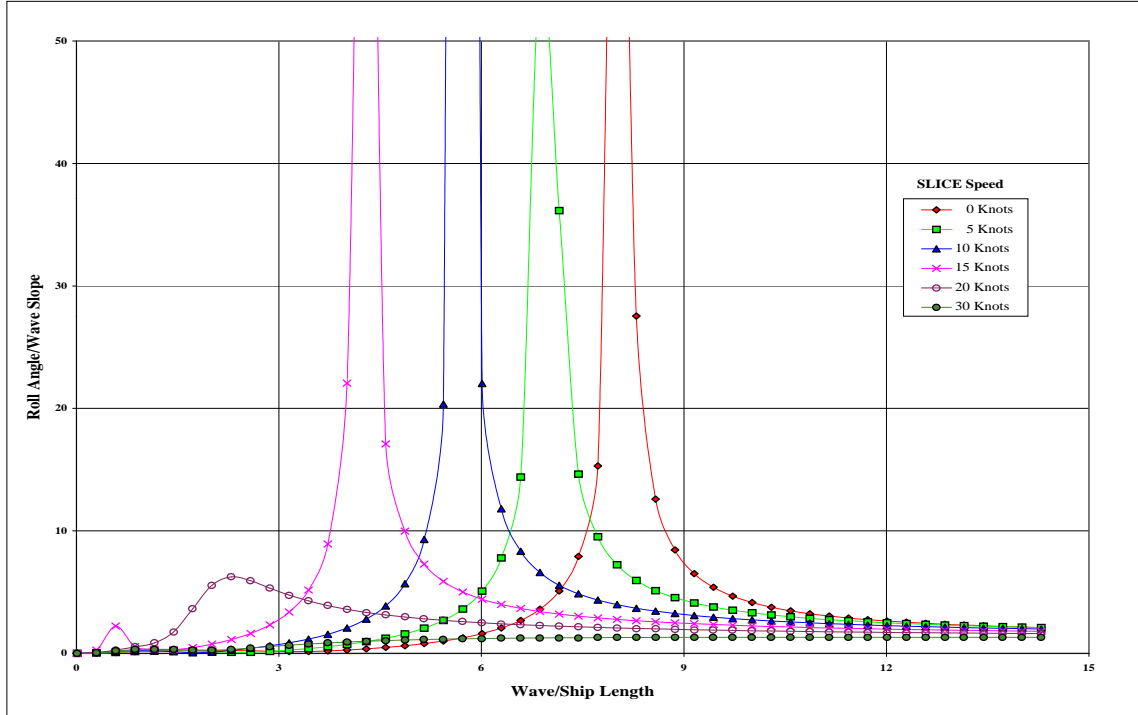


Figure (26). Roll Characteristics, 60 Degree Wave Angle. No Viscous Damping.

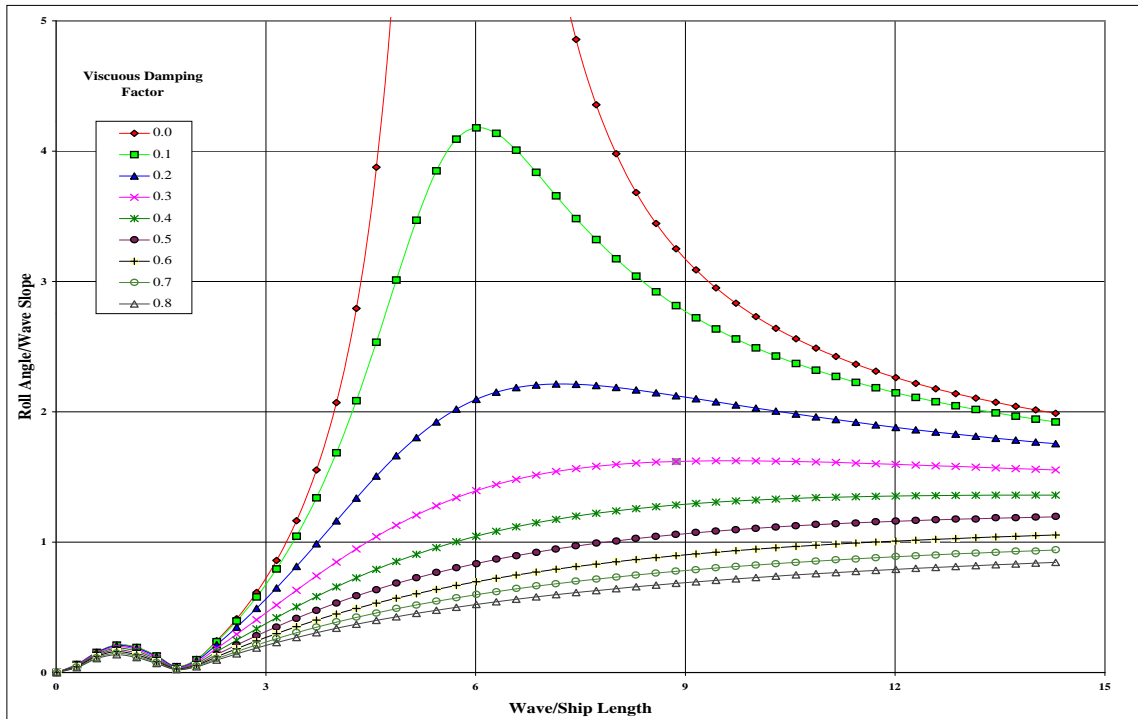


Figure (27). Damping Effects on Roll Motion, 60 Degree Wave Angle at 10 Knots.

The reason for the five fold increase in this parameter, as compared to the literature, stems from the nature of the roll damping coefficient. SHIPMO.BM utilizes the following relationship in regular seas:

$$\text{---} \tag{3}$$

- where: B_{44} is the roll damping coefficient.
 ζ_4 is the complex roll amplitude.
 ω_e is the wave encounter frequency.
 $B_1 = B_F + B_W + B_L$
 $B_2 = B_E + B_{BK}$
 B_F is the frictional damping component.
 B_W is the wave generation damping component.
 B_L is the hull lift damping component.
 B_E is the hull eddy damping component.
 B_{BK} is the bilge keel damping component.

The literature value of 0.02 may only be sufficient to describe the frictional component, thus underestimating system damping in roll. Additionally, the data we are attempting to duplicate includes the damping effect of the control surfaces (stabilizer/rudders and canards). For these reasons, the value of ten percent was utilized for the remainder of the data presented in this study.

III. RESULTS

A. OVERVIEW

The regular wave results of this study are presented in terms of a non-dimensional quantity called the response amplitude operator (RAO); simply stated, a transfer function. The RAO's are presented in two forms to describe both translation (Surge, Sway, and Heave) and rotational (Roll, Pitch, and Yaw) motions encountered through excitement with a wave of unit amplitude, given frequency, and direction of approach, or wave angle. In translation, the operator describes a given motion per wave height. For instance, heave/wave amplitude. Rotational motions are in terms of the given motion with reference to the slope of the incident wave. For instance, roll angle/wave slope. The nondimensionalizations are as follows:

$$- \quad \text{---} \quad (4)$$

$$- \quad \text{---} \quad (5)$$

where: $\zeta_{1,2,3,4,5,6}$ are the nondimensional RAO's.
 $\zeta_{1,2,3}$ are the translation motions of surge, sway, and heave.
 $\zeta_{4,5,6}$ are the rotational motions of roll, pitch, and yaw.
 A is the wave amplitude.
 k is the wave number based on encounter frequency.

The magnitude of these operators are commonly plotted against a non-dimensional length quantity defined as the wave/ship length ratio. The range of wave/ship lengths was determined to cover the average wavelength of a seaway up to sea state seven (Papoulias, 1993).

Regular wave studies are presented using the RAO's. Two main effects are investigated; the influence of wave angle, and vessel speed, on the motions of the SLICE. Wave angles of

zero degrees represent following seas, while those of 180 degrees represent head seas. Data were compiled for wave angles of zero to 180 degrees at 30 degree increments as shown in Figure (28). Full coverage (360 degrees) was not necessary due to port and starboard symmetry of the SLICE design.

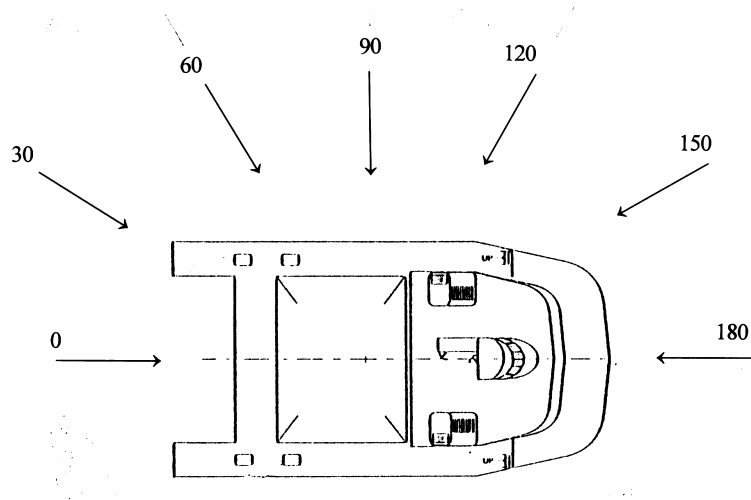


Figure (28). Wave Angle Definitions.

In the irregular wave analysis, the significant motion amplitudes are plotted as a function of wave angle on polar plots. A significant amplitude is defined as the average of the highest one-third of all motions for the given wave spectrum encountered. Data were compiled for wave angles from zero to 180 degrees at ten degree increments. In addition to the effects studied in the regular waves, the influence of sea state, as described in Table (4), is investigated.

As mentioned previously, the SHIPMO.BM program utilizes computations based on an ideal fluid assumption. Viscous corrections are input for the motions of surge and roll. However; for the other four motions, no corrections can be supplied. Because of this, motions can be over predicted and periods of motion can be under predicted.

B. REGULAR WAVE RESULTS

In general, vertical plane motions are greater for head and following seas, while horizontal plane motions are maximized in beam seas. This observation is consistent with

intuition. With the SLICE at rest, 0 knots forward speed, the RAO's for surge, heave, and pitch show a single characteristic resonant peak at wave/ship lengths near 2.01 for surge and heave, and 2.30 for pitch; at all wave angles. These correspond to wave excitation frequencies of 0.98 and 0.92 hertz, respectively. Based on the data analyzed, it is predicted that the SLICE will exhibit natural periods near 6.42 seconds in surge and heave, and 6.86 seconds in pitch. The motions of sway and yaw did not exhibit any resonant phenomena; however, a consistent peak was seen in roll at a wave/ship length of 8.58 which corresponds to frequency and period of motion of 0.47 hertz and 13.26 seconds respectively. This too was present at all wave angles. Figures (29) through (34) illustrate the above points.

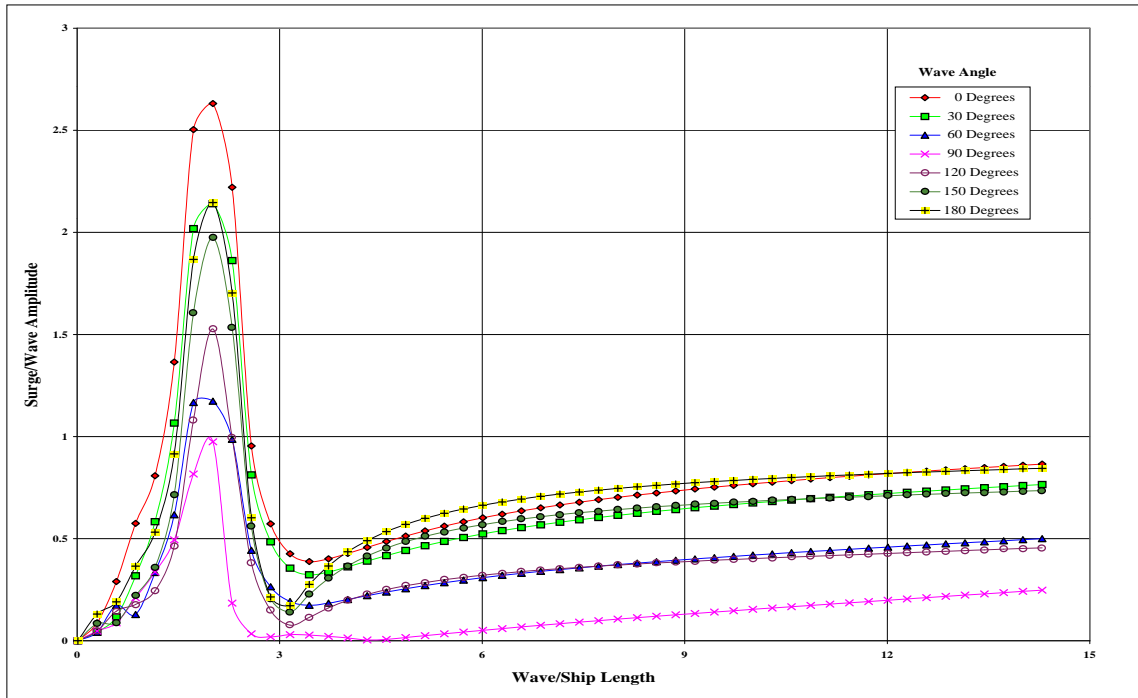


Figure (29). Surge Characteristics as a Function of Wave Angle, 0 Knots.

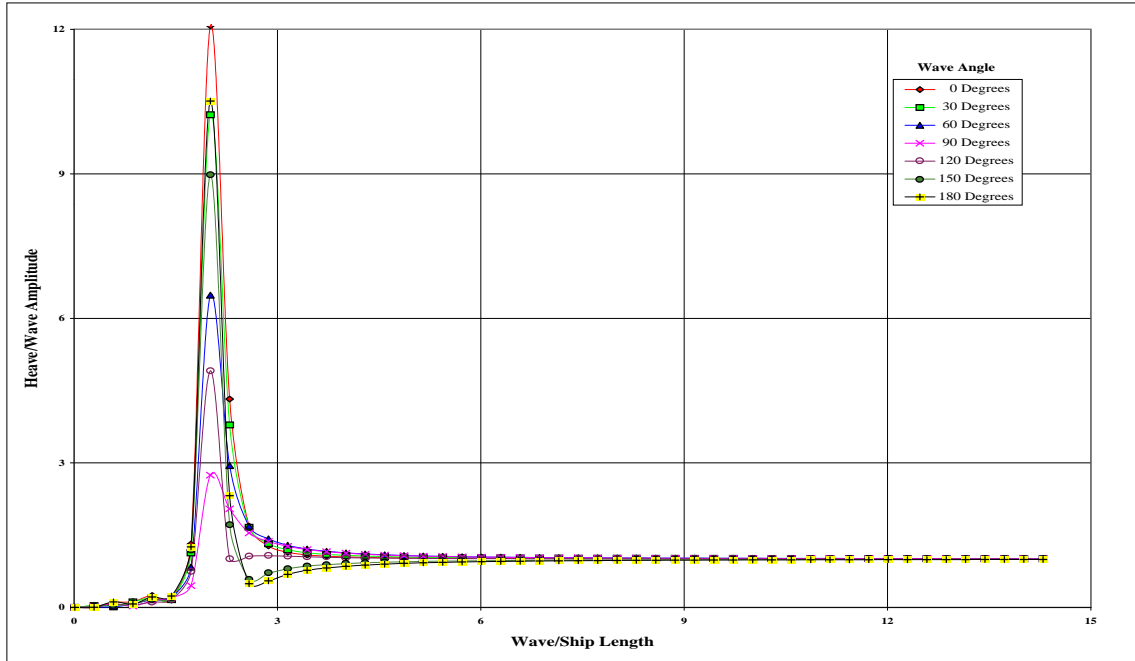


Figure (30). Heave Characteristics as a Function of Wave Angle, 0 Knots.

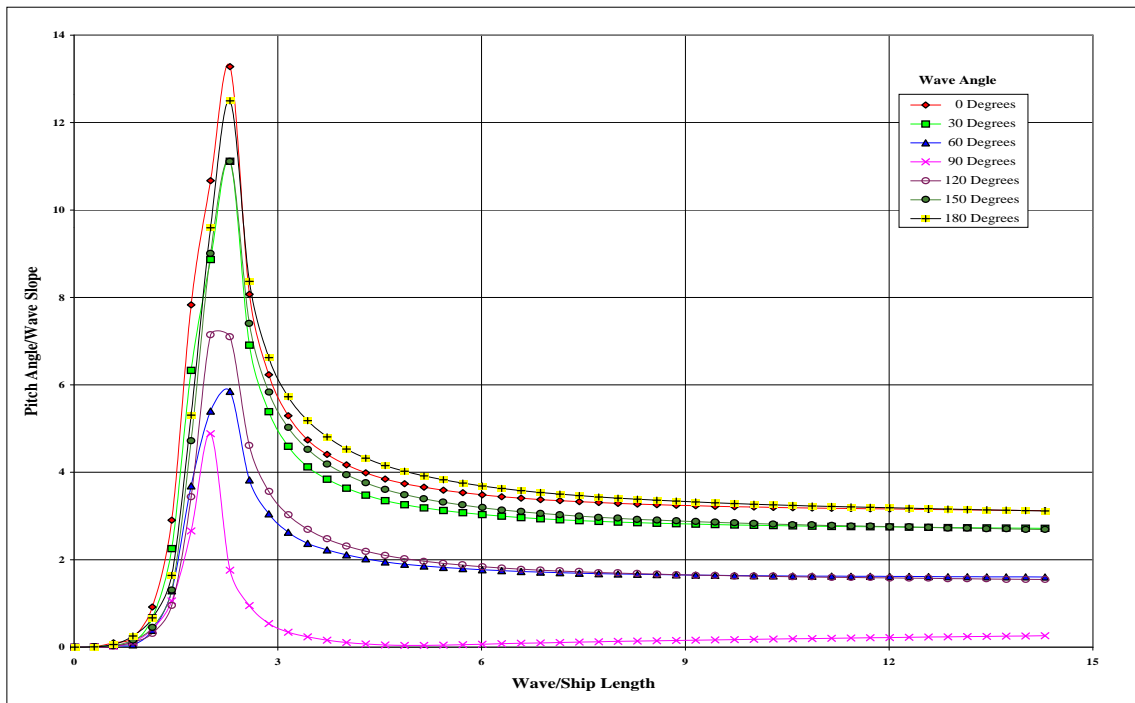


Figure (31). Pitch Characteristics as a Function of Wave Angle, 0 Knots.

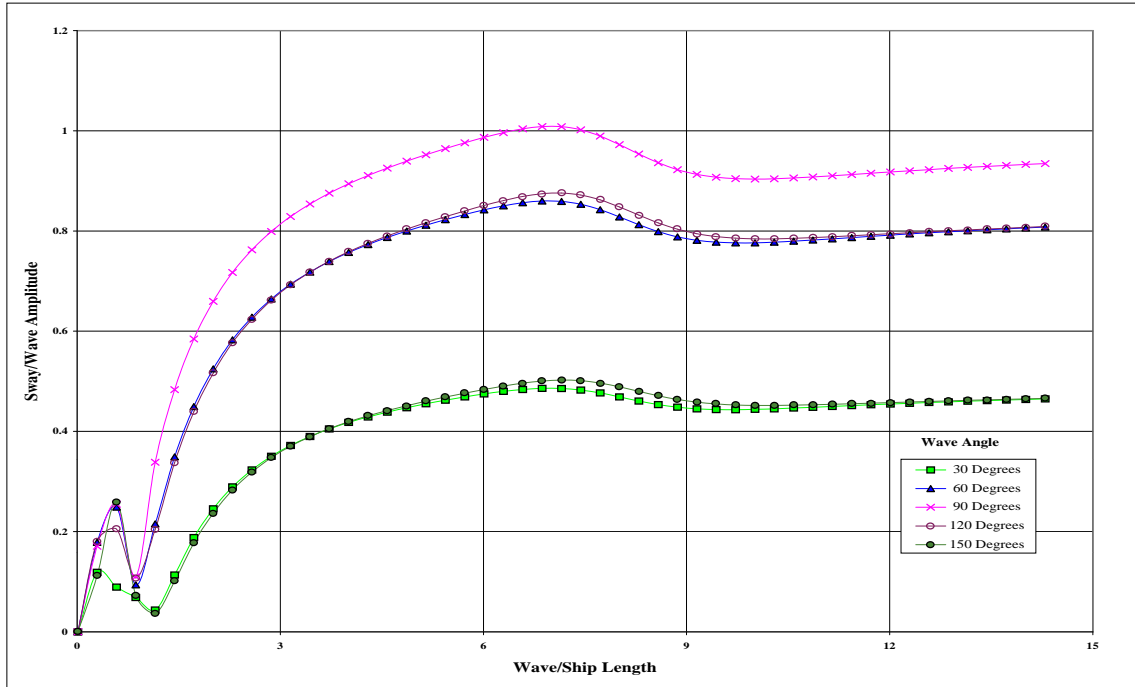


Figure (32). Sway Characteristics as a Function of Wave Angle, 0 Knots.

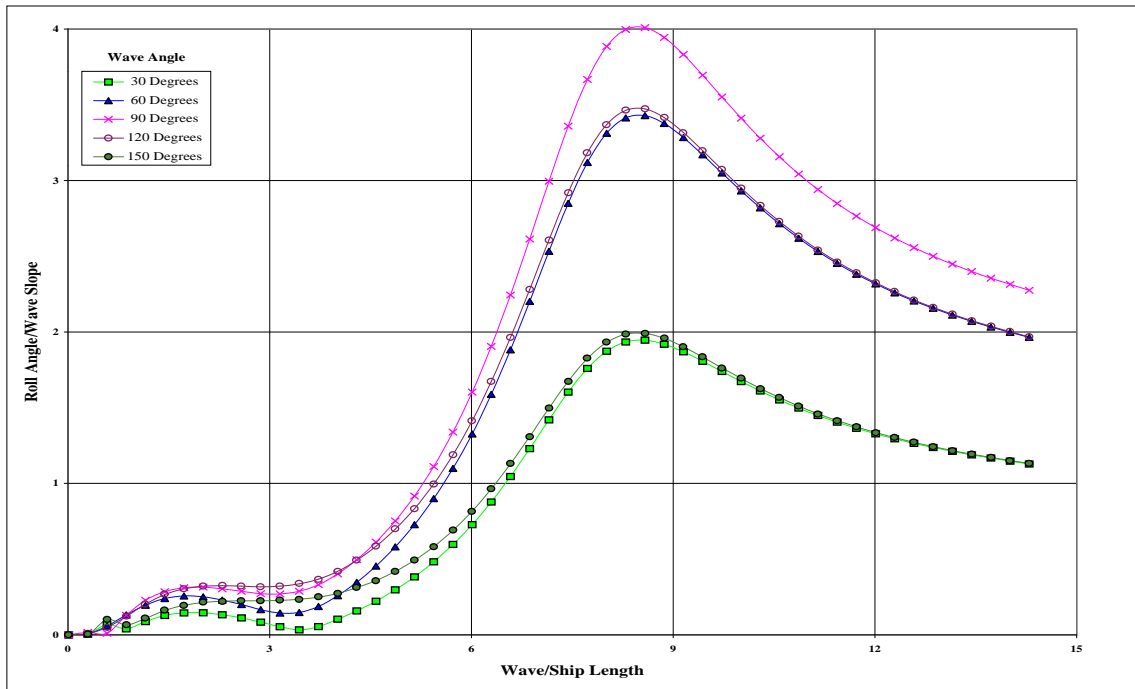


Figure (33). Roll Characteristics as a Function of Wave Angle, 0 Knots.

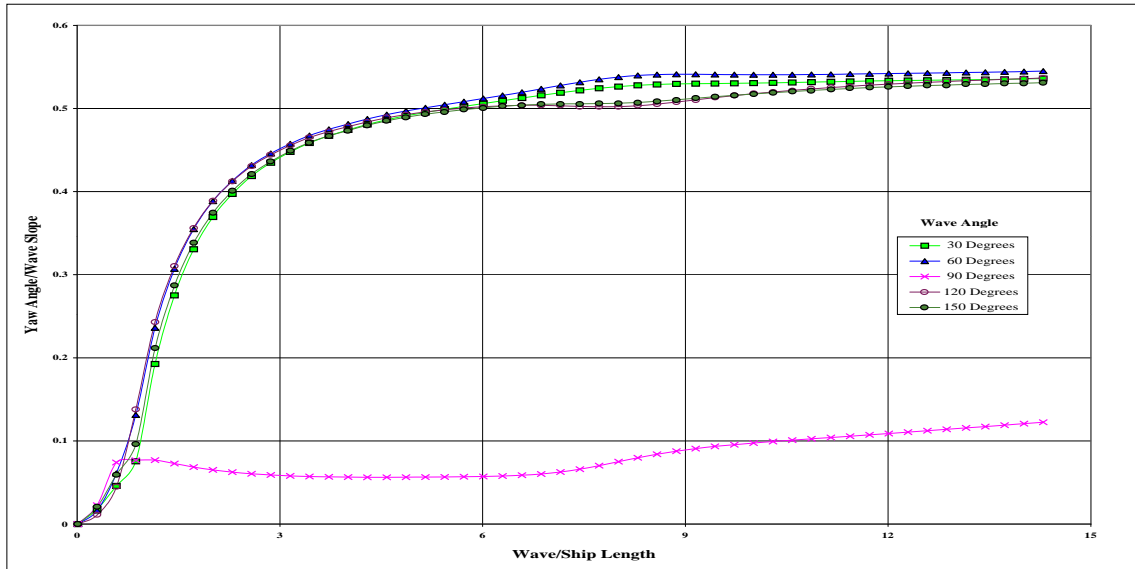


Figure (34). Yaw Characteristics as a Function of Wave Angle, 0 Knots.

As the SLICE begins to make headway, the resonant peak locations migrate as a function of the wave angle. As speed increases above ten knots; the resonant motions in surge increase drastically, for wave angles of 0 to 60 degrees. The same trend can be seen in the motions of sway and yaw. Refer to Figures (35) through (66). This results from instabilities in the strip

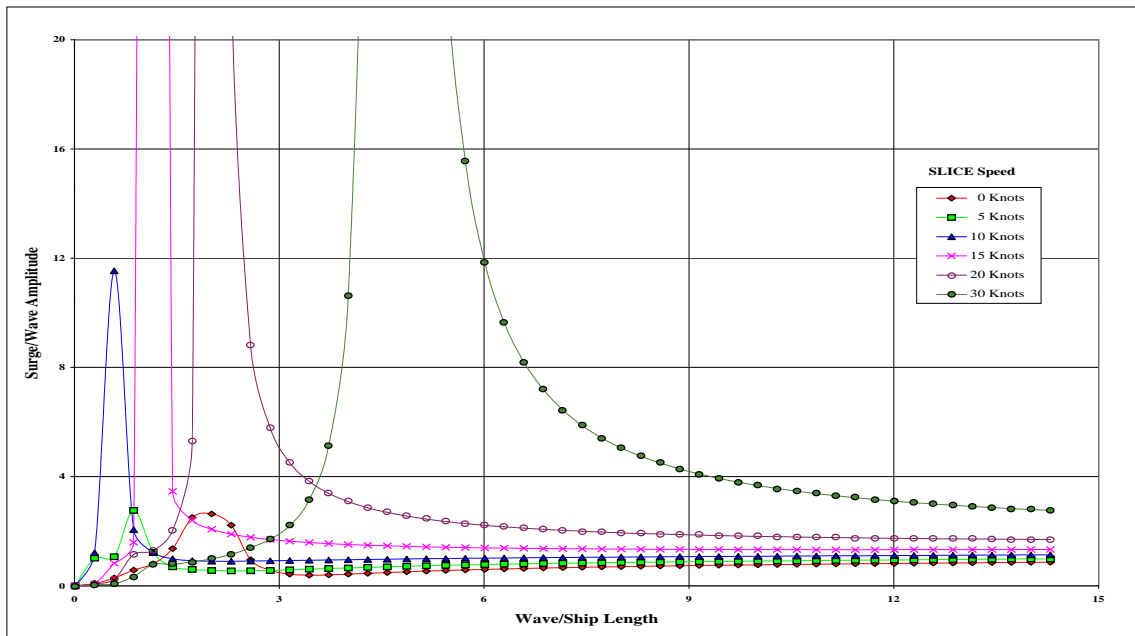


Figure (35). Surge Characteristics as a Function of SLICE Speed, 0 Degree Wave Angle.

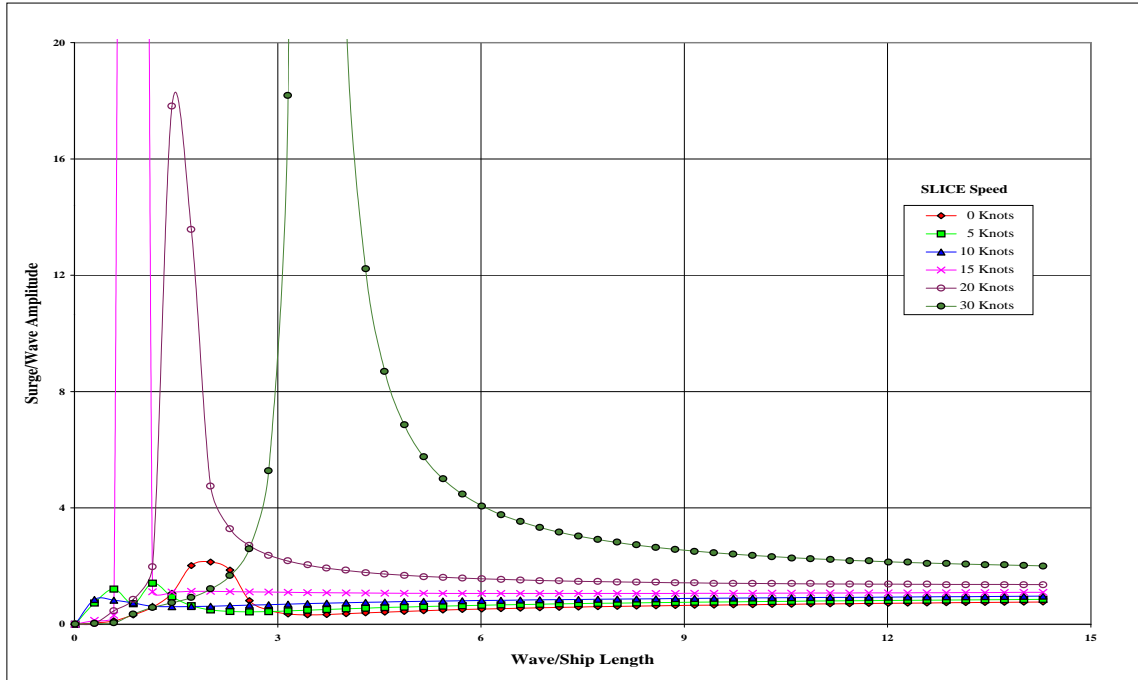


Figure (36). Surge Characteristics as a Function of SLICE Speed, 30 Degree Wave Angle.

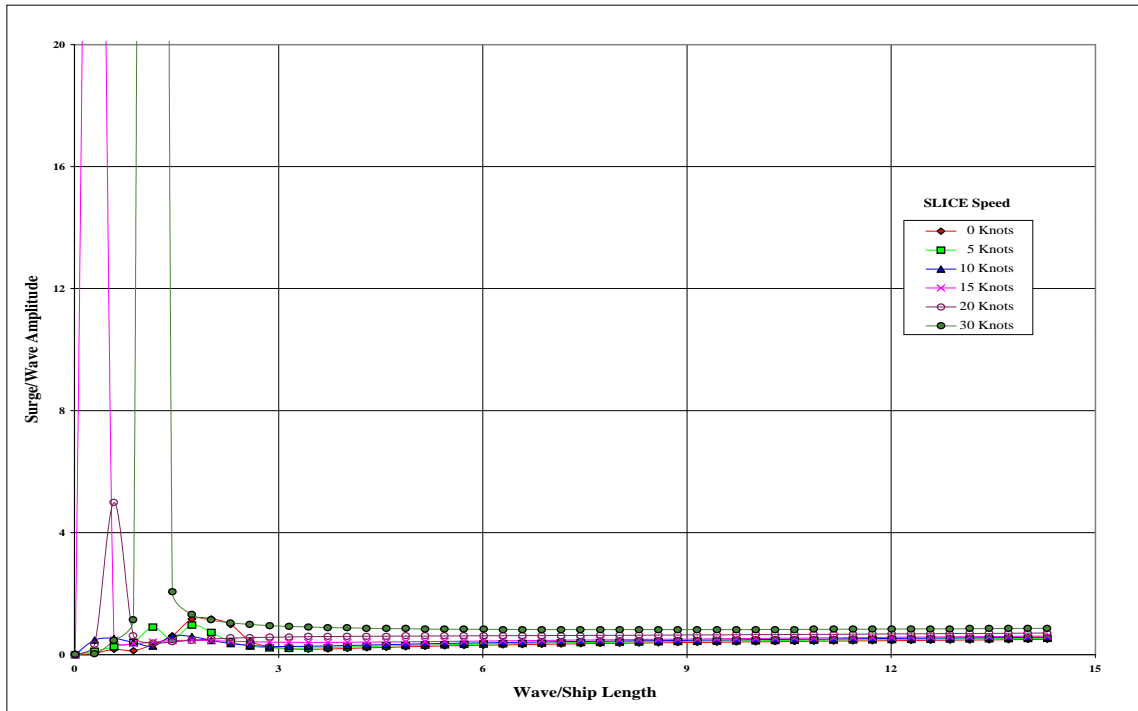


Figure (37). Surge Characteristics as a Function of SLICE Speed, 60 Degree Wave Angle.

theory due to negative encounter frequencies (Lee, 1976; Hong, 1986; McCreight, 1987). The encounter frequency is determined by:

$$\omega_e = \omega - U \sin \theta \tag{6}$$

where: ω_e is the encounter frequency.
 ω is the wave frequency.
 g is the acceleration due to gravity.
 U is the ship forward speed.
 θ is the wave angle.

For negative encounter frequencies, the nontrivial root of equation (6) is:

$$\omega_e = -\sqrt{g \sin \theta} \tag{7}$$

or,

$$\omega_e = -\sqrt{g \sin \theta} \tag{8}$$

Since wave frequencies and ship speeds are never less than zero, we may rule out wave angles greater than 90 degrees. Equation (8) allows us to determine the range of wave frequencies which will result in negative encounter frequencies. From this, the applicable wave to ship length ratios can be specified. Table (5) summarizes these results. The clear section shows the minimum wave frequencies that will generate negative encounter frequencies; while, the shaded section shows corresponding maximum wave to ship length ratio values.

Speed \ Wave Angle	0 (deg.)	30 (deg.)	60 (deg.)	0 (deg.)	30 (deg.)	60 (deg.)
5 knots	3.864	4.462	7.728	0.0095	0.0095	0.0095
10 knots	1.932	2.231	3.864	0.2952	0.2952	0.0095
15 knots	1.288	1.487	2.576	1.1524	0.8667	0.0095
20 knots	0.966	1.115	1.932	2.0095	1.4381	0.2952
30 knots	0.644	0.744	1.288	4.5810	3.4381	1.1524

Table (5). Regions of Negative Encounter Frequencies.

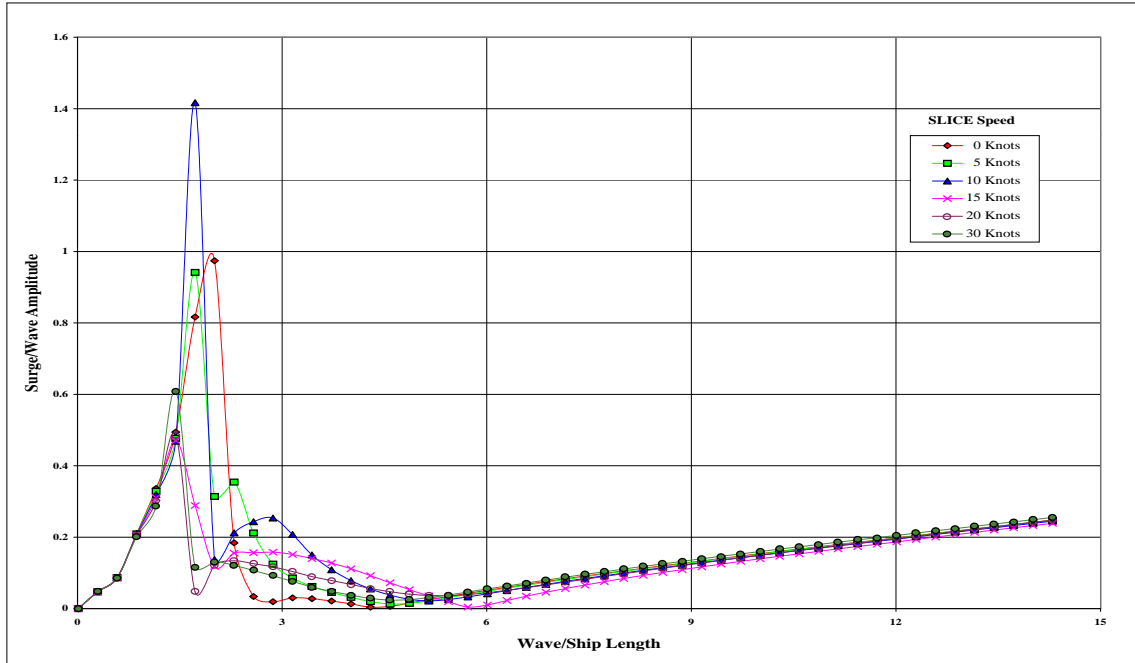


Figure (38). Surge Characteristics as a Function of SLICE Speed, 90 Degree Wave Angle.

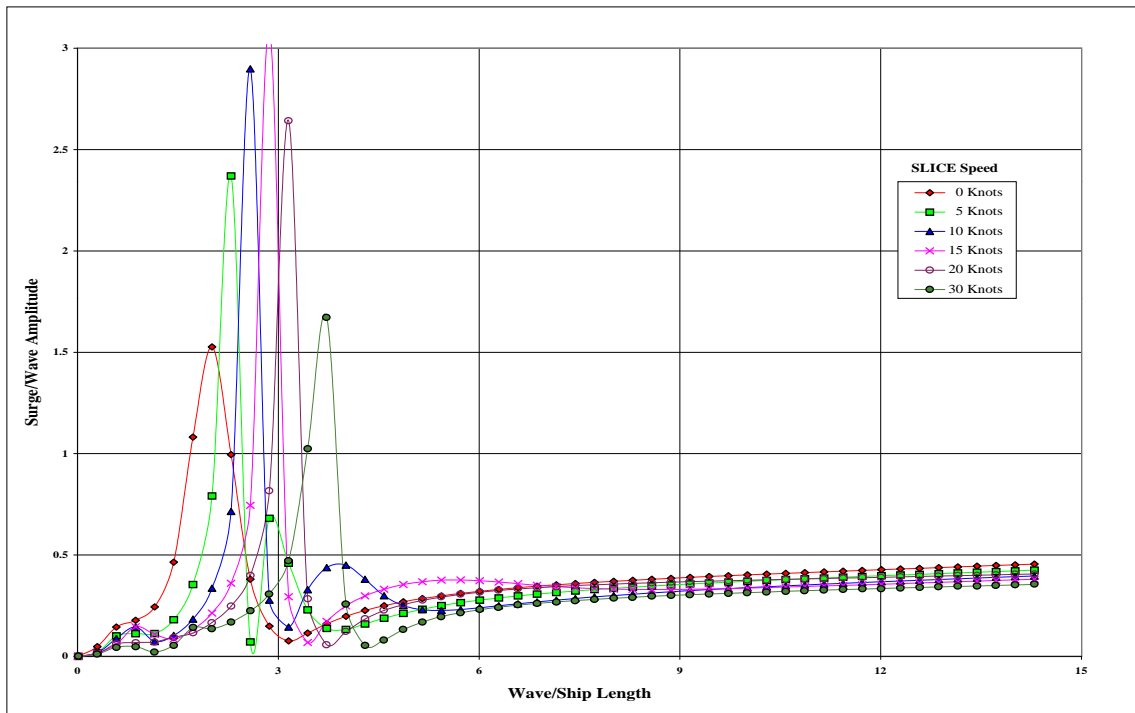


Figure (39). Surge Characteristics as a Function of SLICE Speed, 120 Degree Wave Angle.

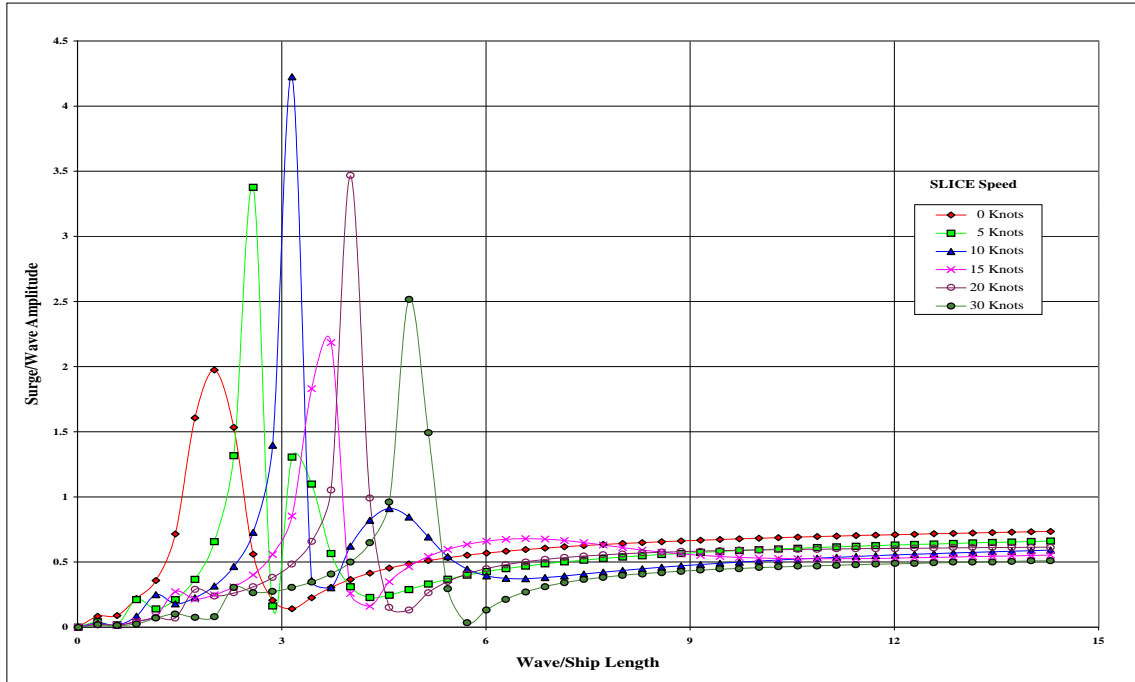


Figure (40). Surge Characteristics as a Function of SLICE Speed, 150 Degree Wave Angle.

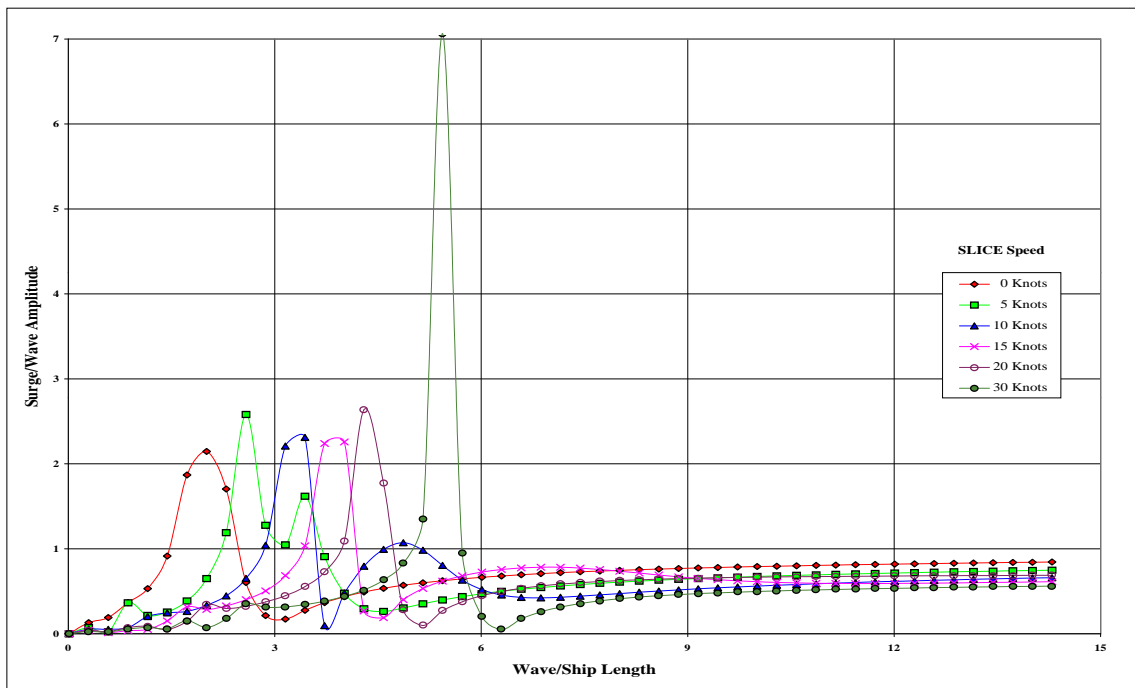


Figure (41). Surge Characteristics as a Function of SLICE Speed, 180 Degree Wave Angle.

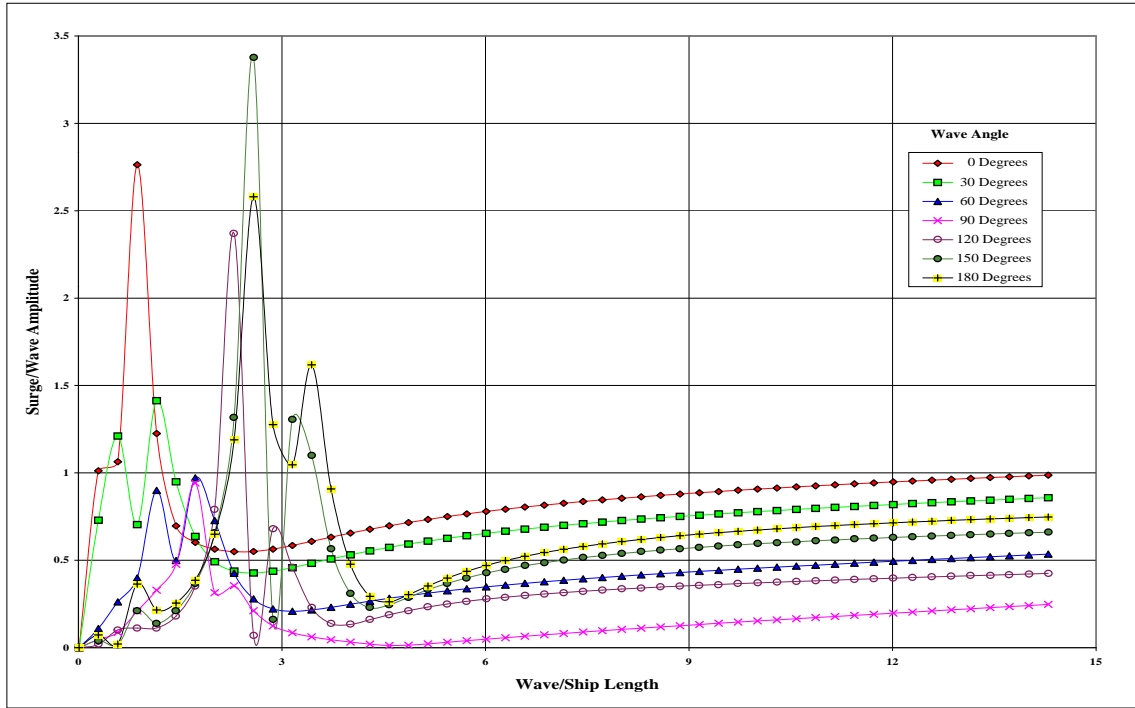


Figure (42). Surge Characteristics as a Function of Wave Angle, 5 Knots.

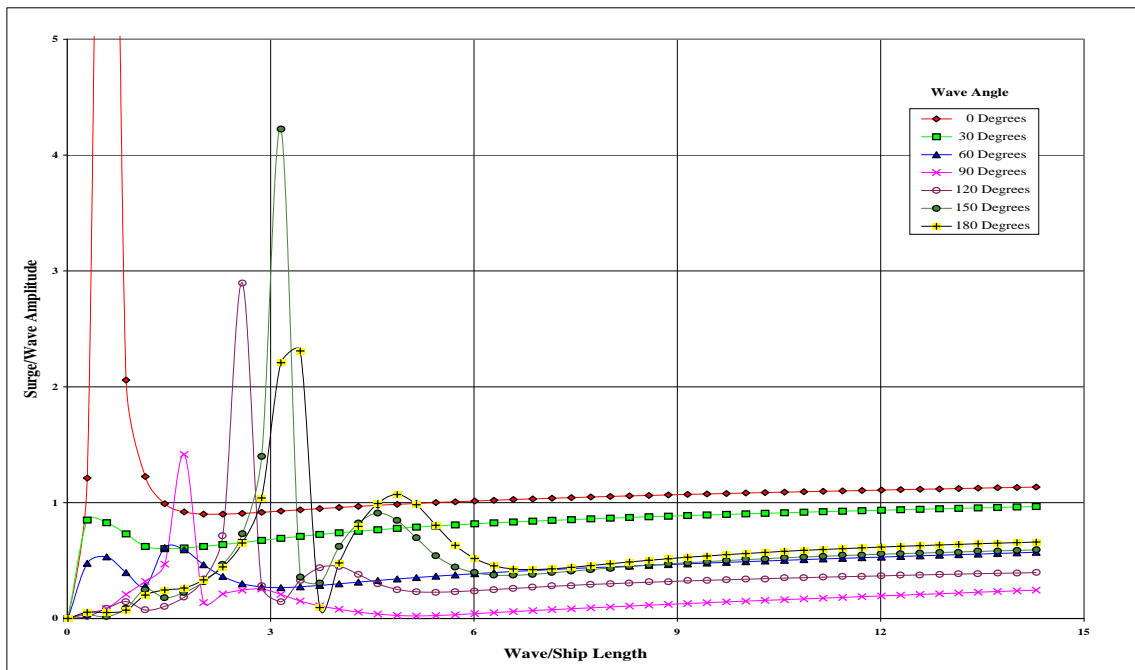


Figure (43). Surge Characteristics as a Function of Wave Angle, 10 Knots.

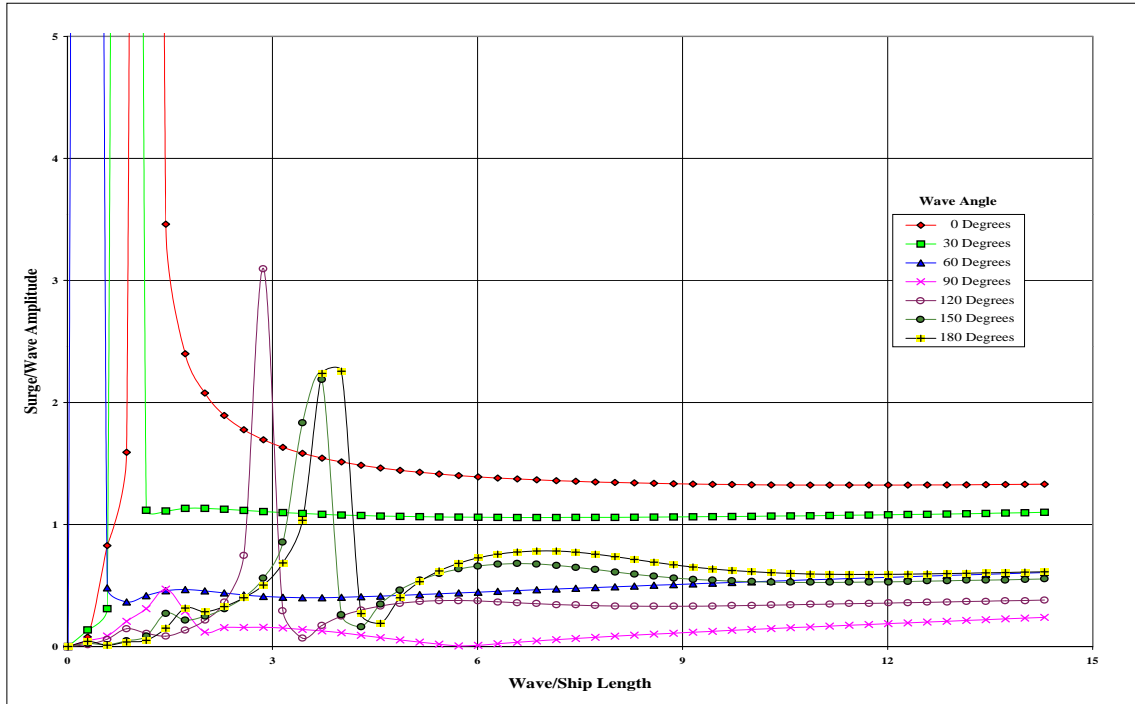


Figure (44). Surge Characteristics as a Function of Wave Angle, 15 Knots.

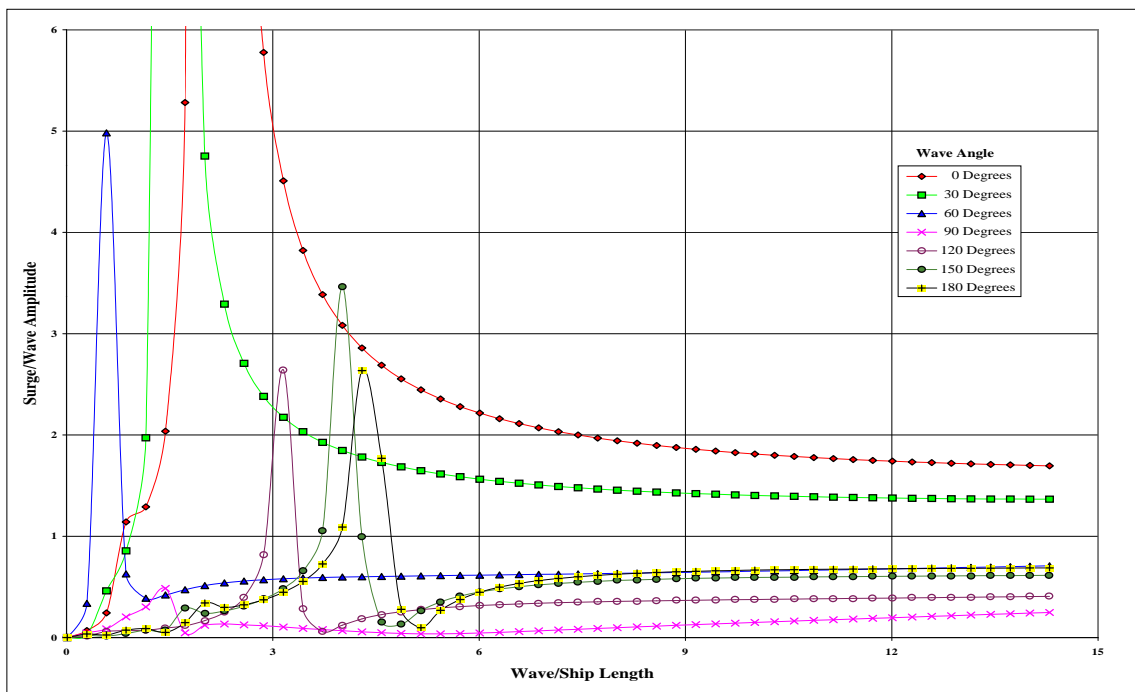


Figure (45). Surge Characteristics as a Function of Wave Angle, 20 Knots.

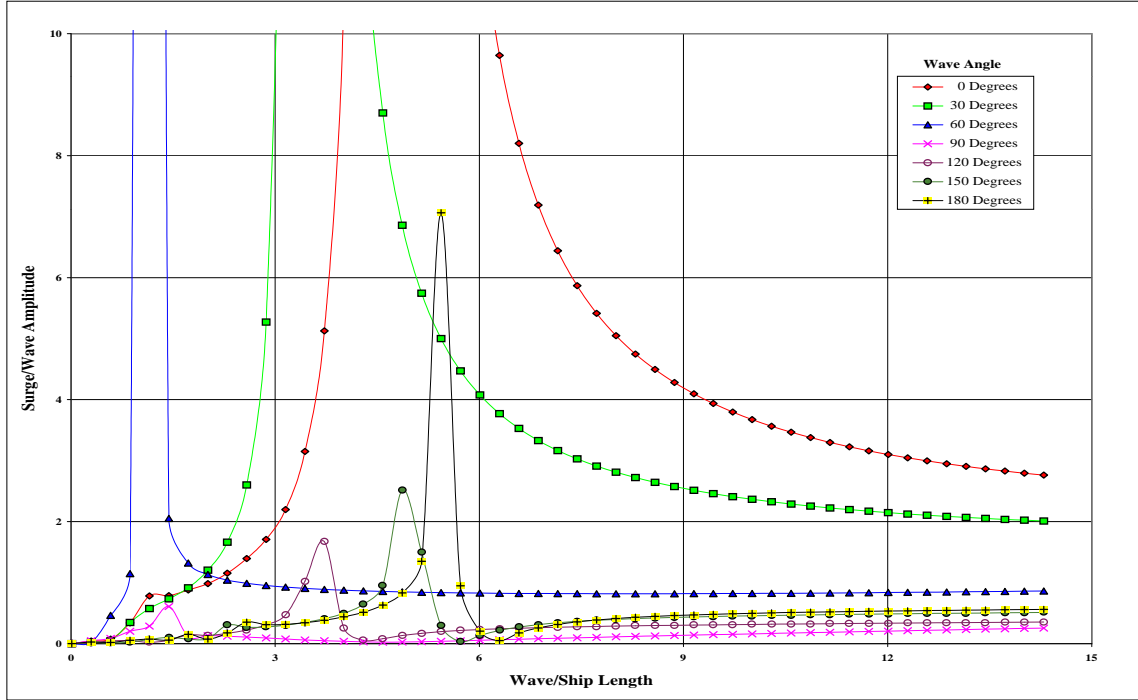


Figure (46). Surge Characteristics as a Function of Wave Angle, 30 Knots.

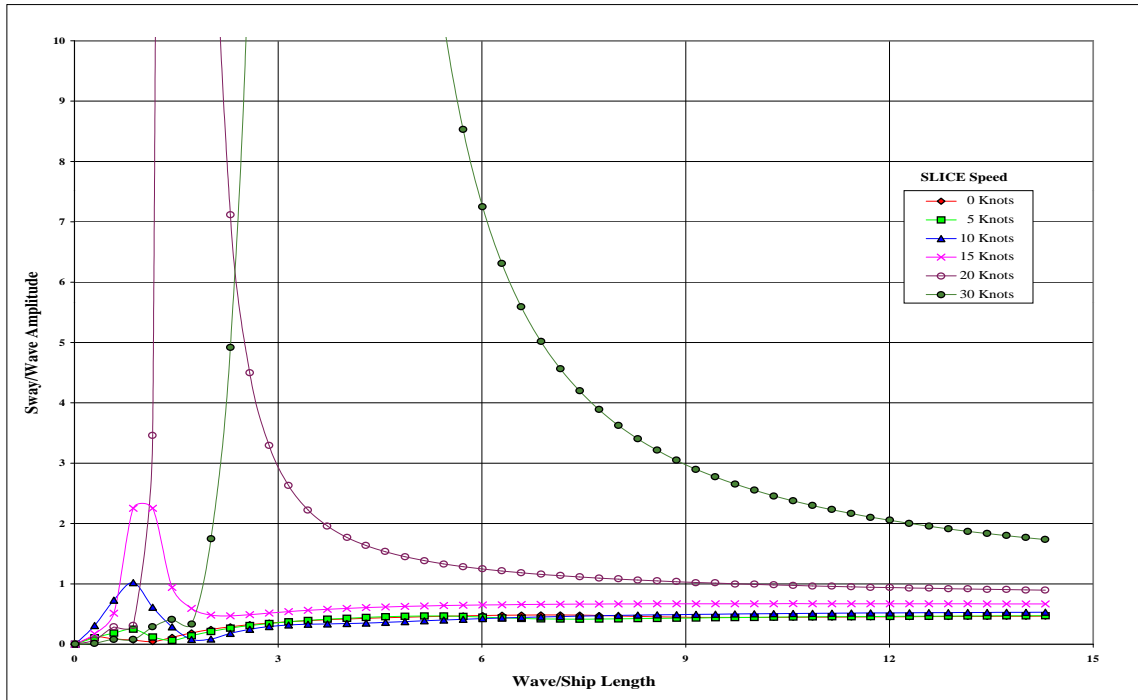


Figure (47). Sway Characteristics as a Function of SLICE Speed, 30 Degree Wave Angle.

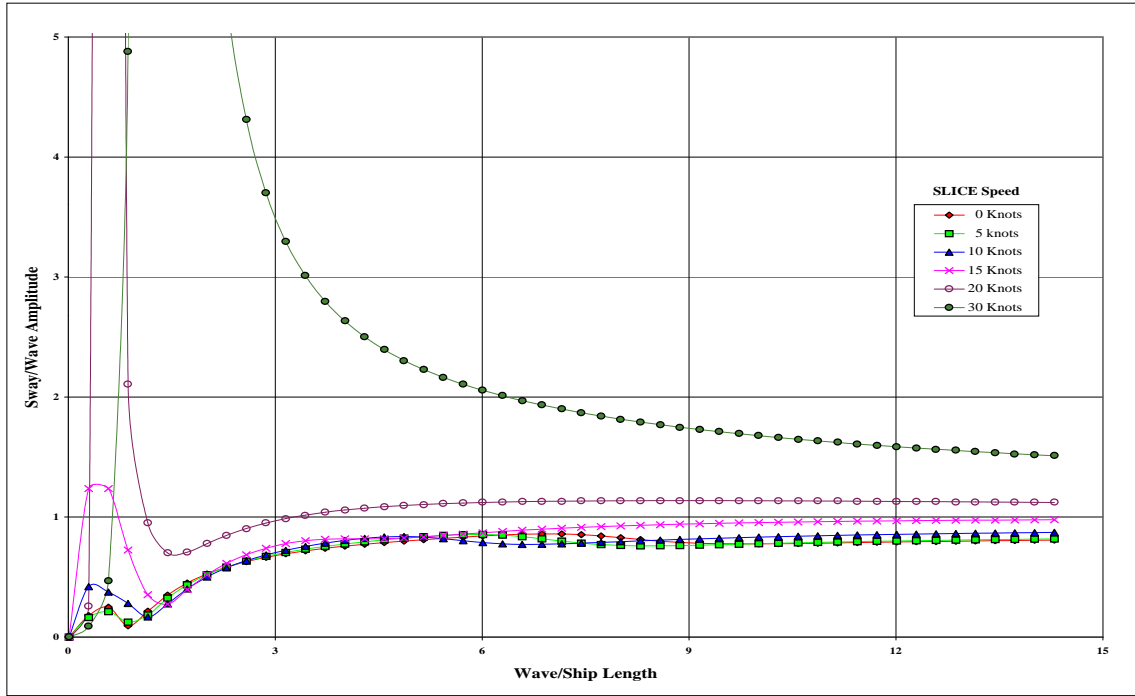


Figure (48). Sway Characteristics as a Function of SLICE Speed, 60 Degree Wave Angle.

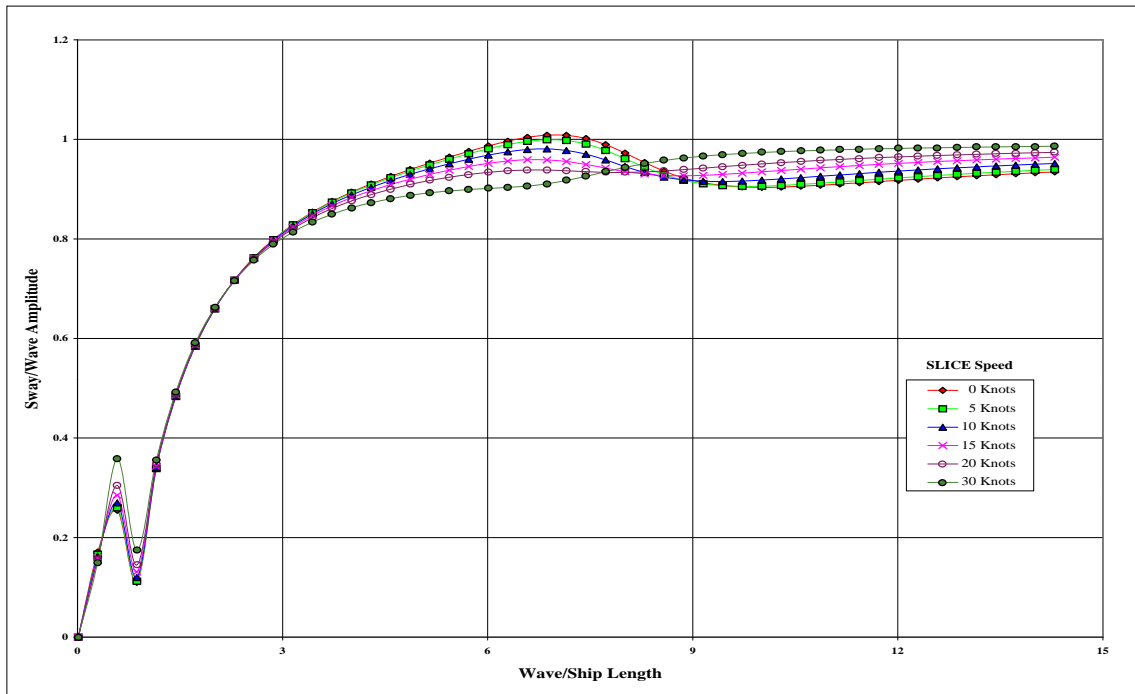


Figure (49). Sway Characteristics as a Function of SLICE Speed, 90 Degree Wave Angle.

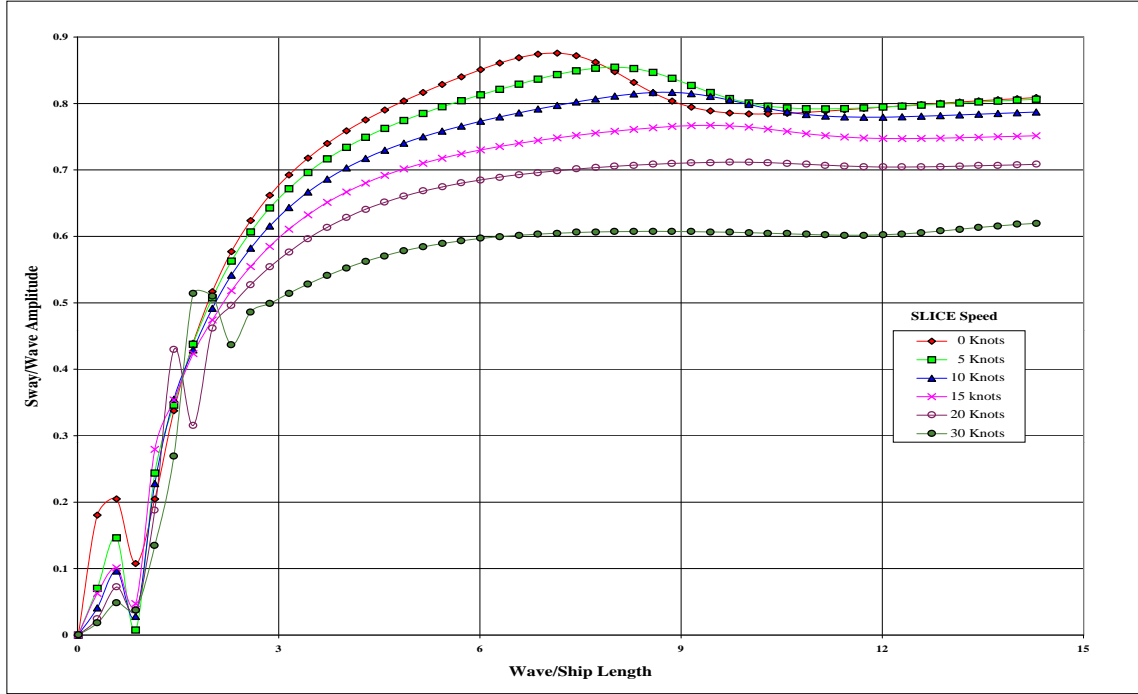


Figure (50). Sway Characteristics as a Function of SLICE Speed, 120 Degree Wave Angle.

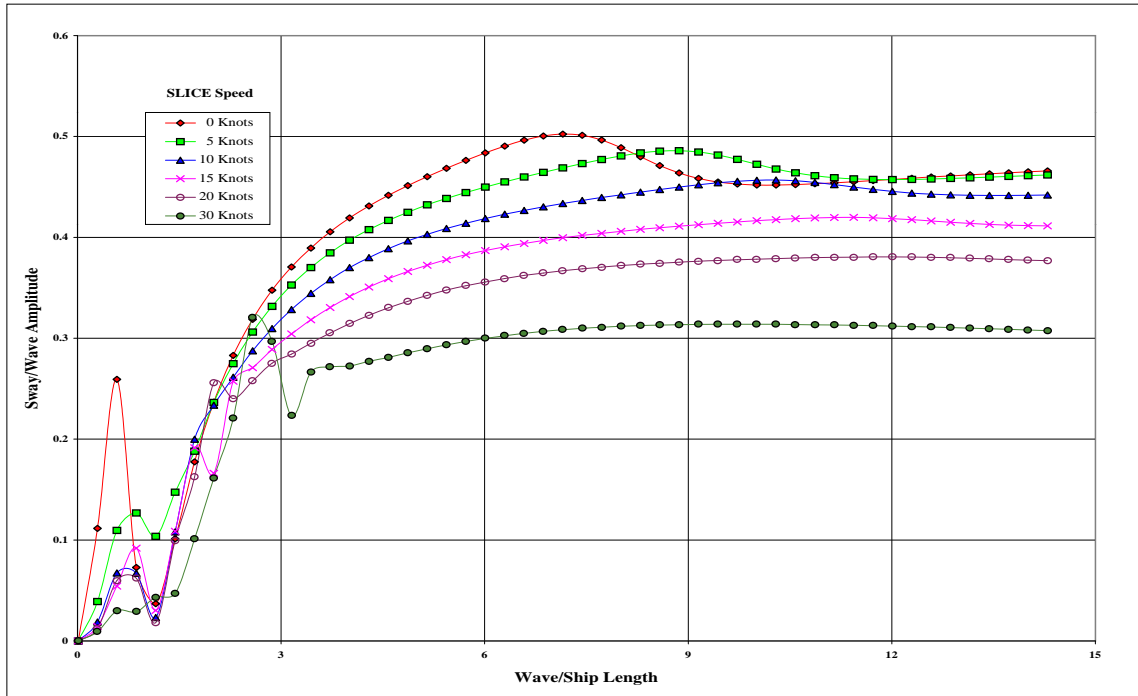


Figure (51). Sway Characteristics as a Function of SLICE Speed, 150 Degree Wave Angle.

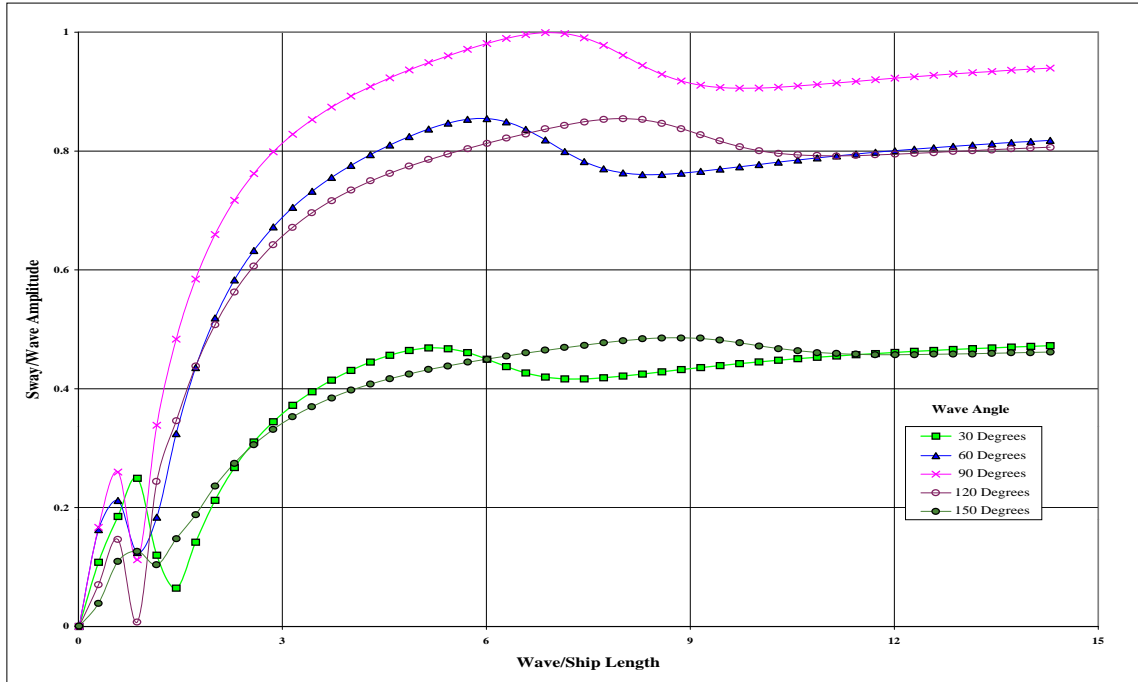


Figure (52). Sway Characteristics as a Function of Wave Angle, 5 Knots.

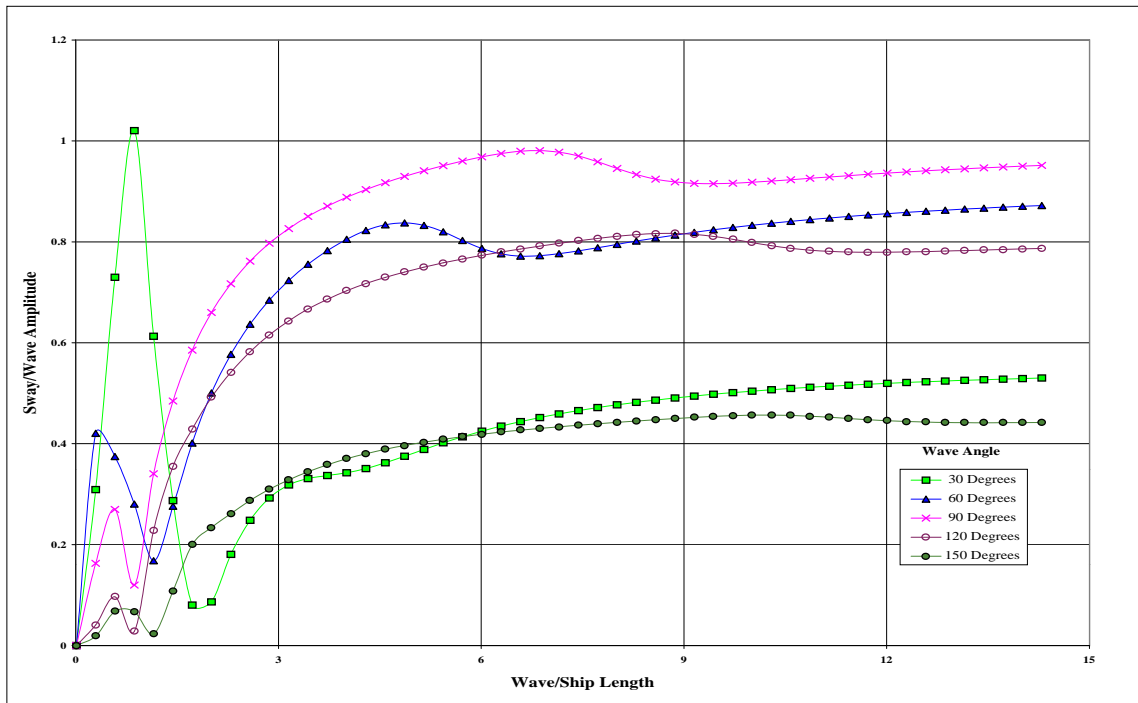


Figure (53). Sway Characteristics as a Function of Wave Angle, 10 Knots.

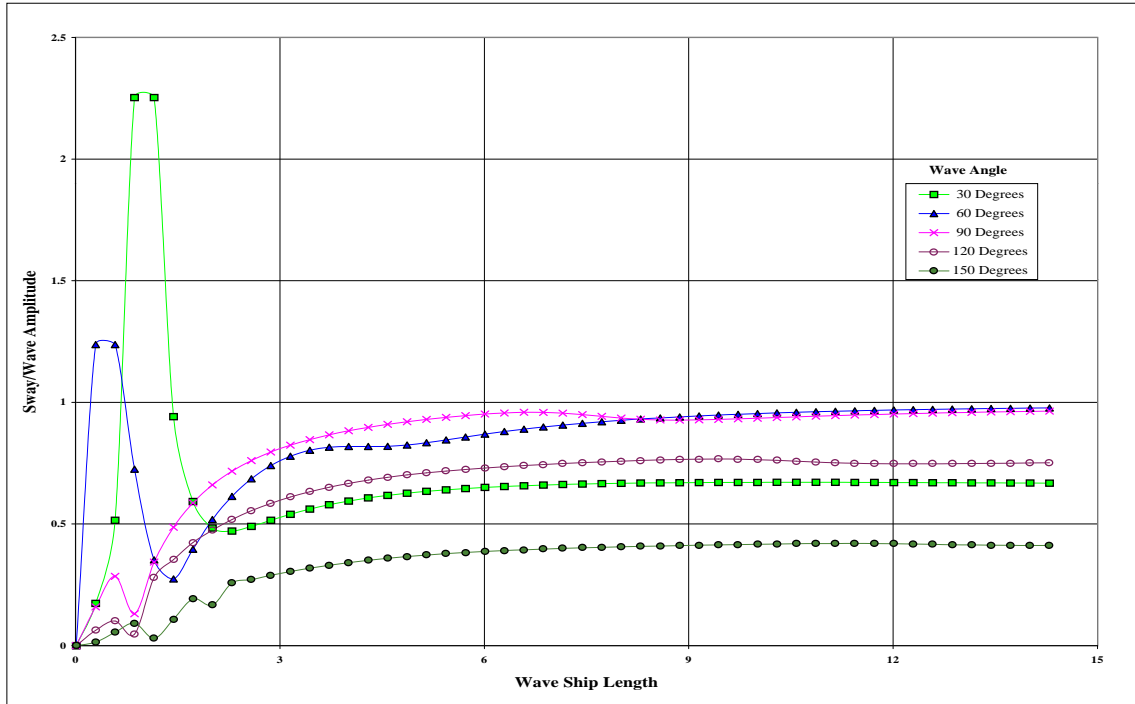


Figure (54). Sway Characteristics as a Function of Wave Angle, 15 Knots.

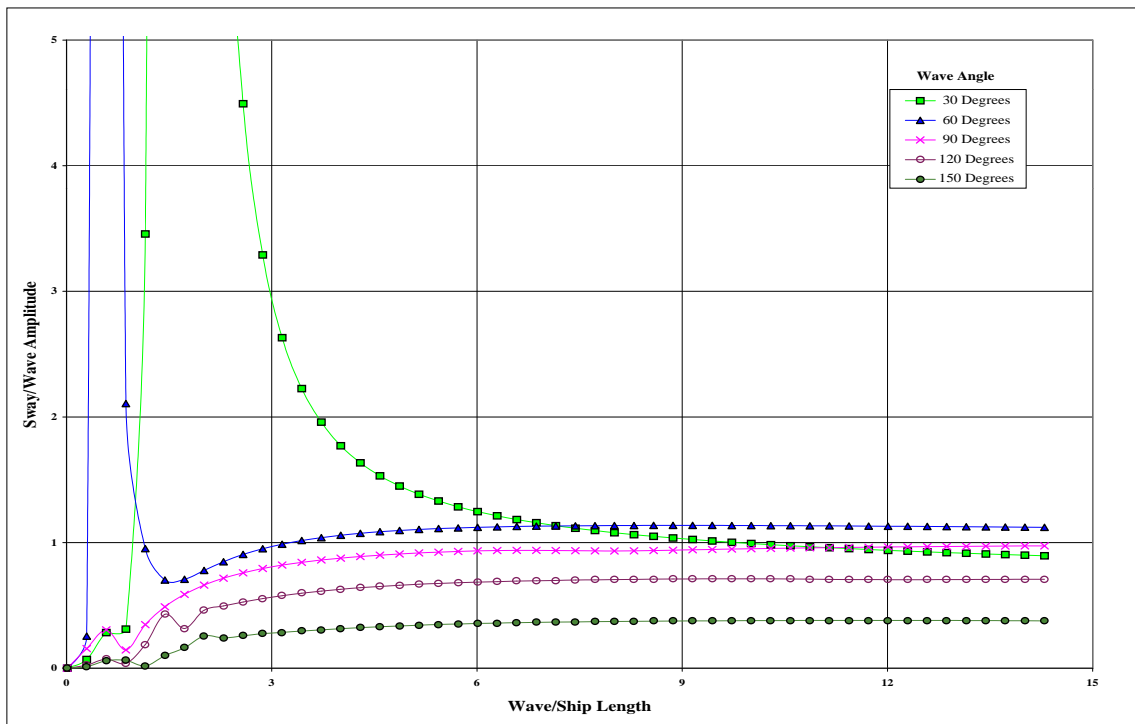


Figure (55). Sway Characteristics as a Function of Wave Angle, 20 Knots.

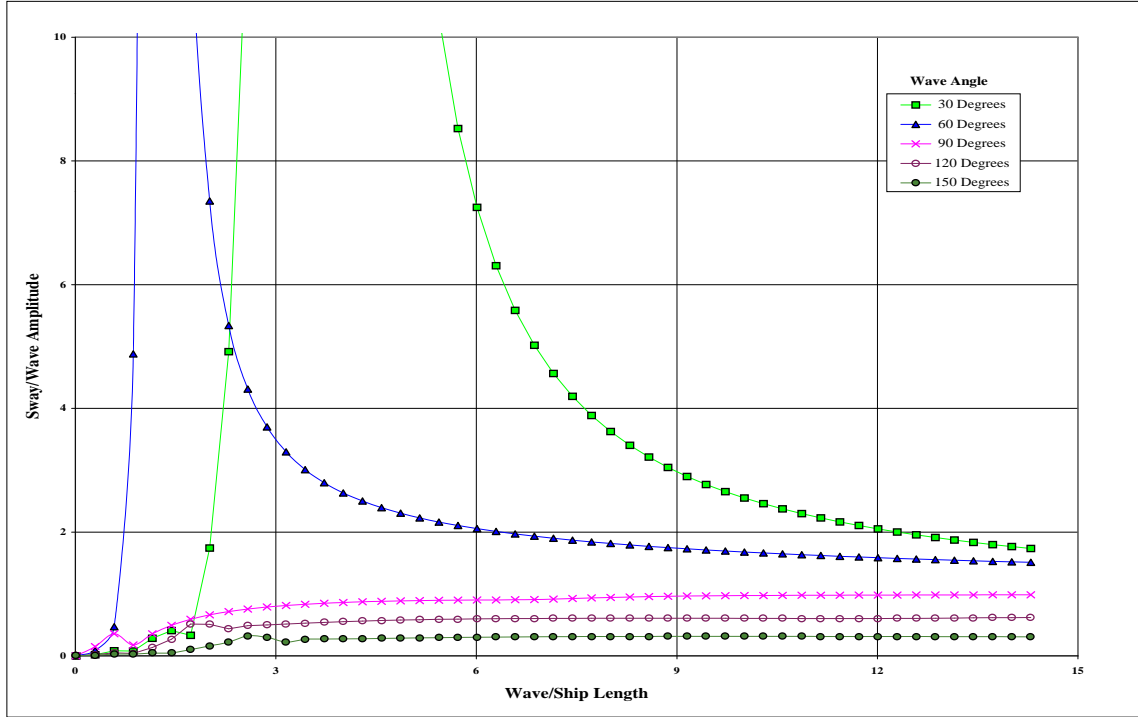


Figure (56). Sway Characteristics as a Function of Wave Angle, 30 Knots.

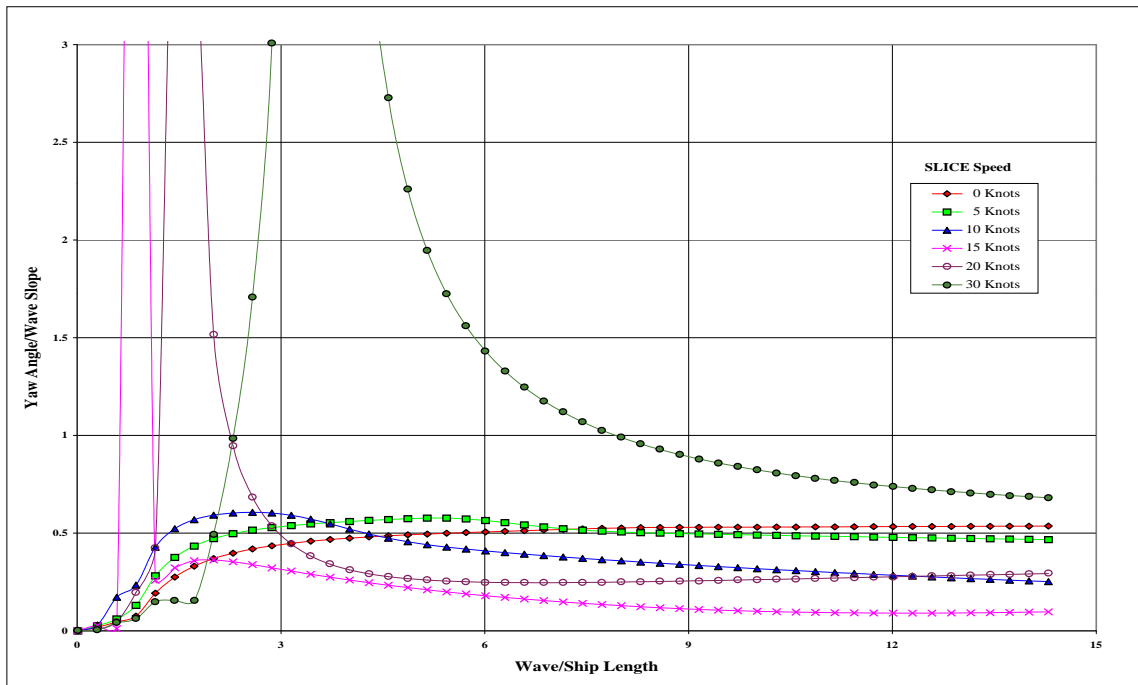


Figure (57). Yaw Characteristics as a Function of SLICE Speed, 30 Degree Wave Angle.

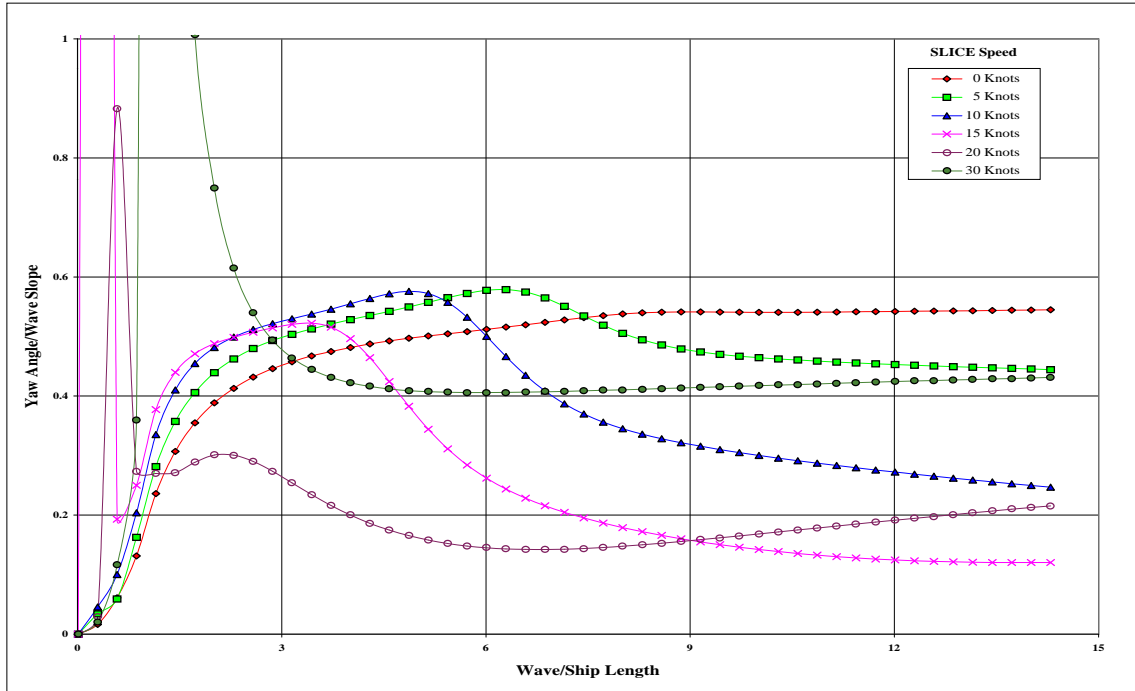


Figure (58). Yaw Characteristics as a Function of SLICE Speed, 60 Degree Wave Angle.

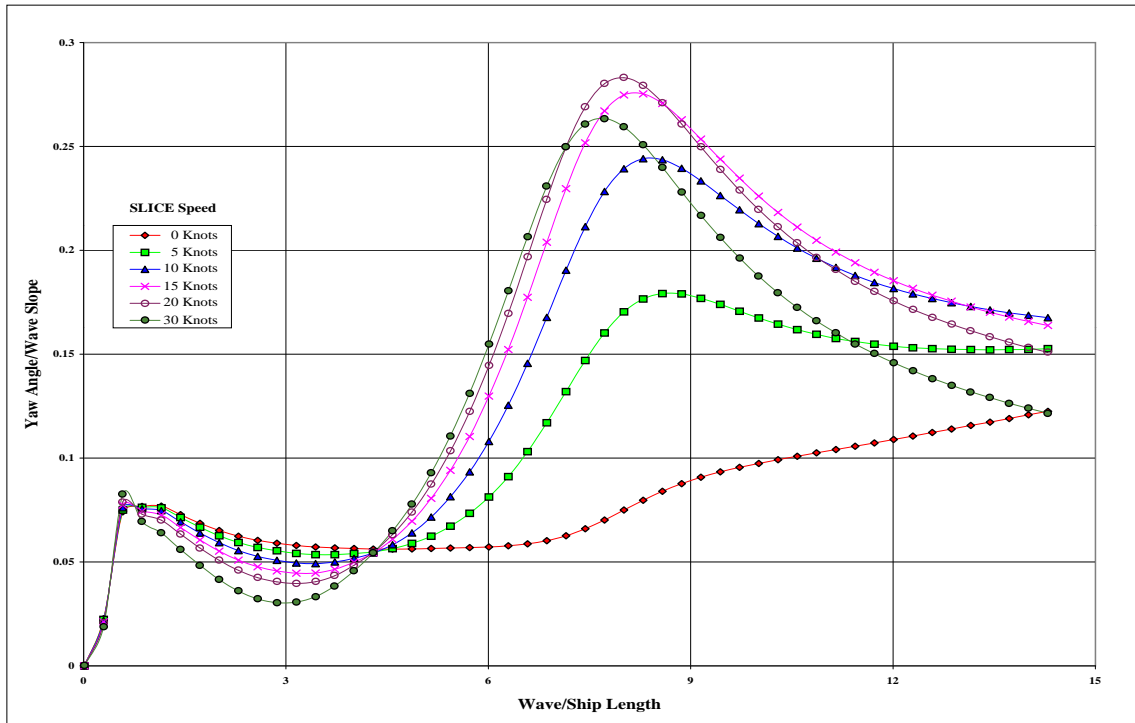


Figure (59). Yaw Characteristics as a Function of SLICE Speed, 90 Degree Wave Angle.

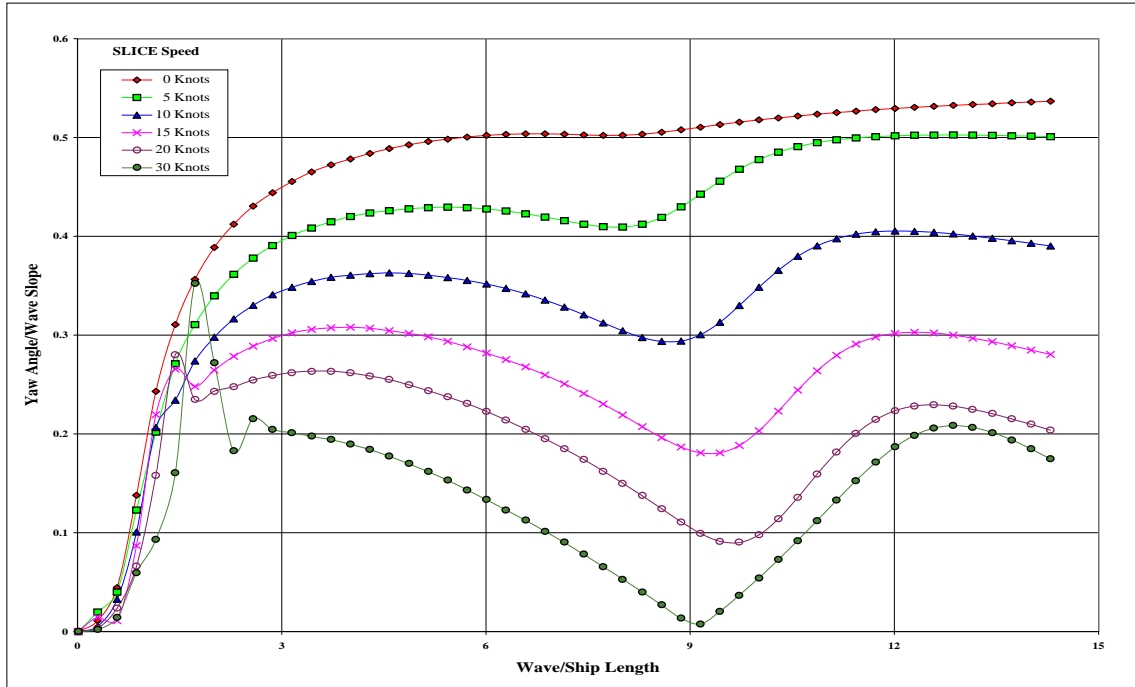


Figure (60). Yaw Characteristics as a Function of SLICE Speed, 120 Degree Wave Angle.

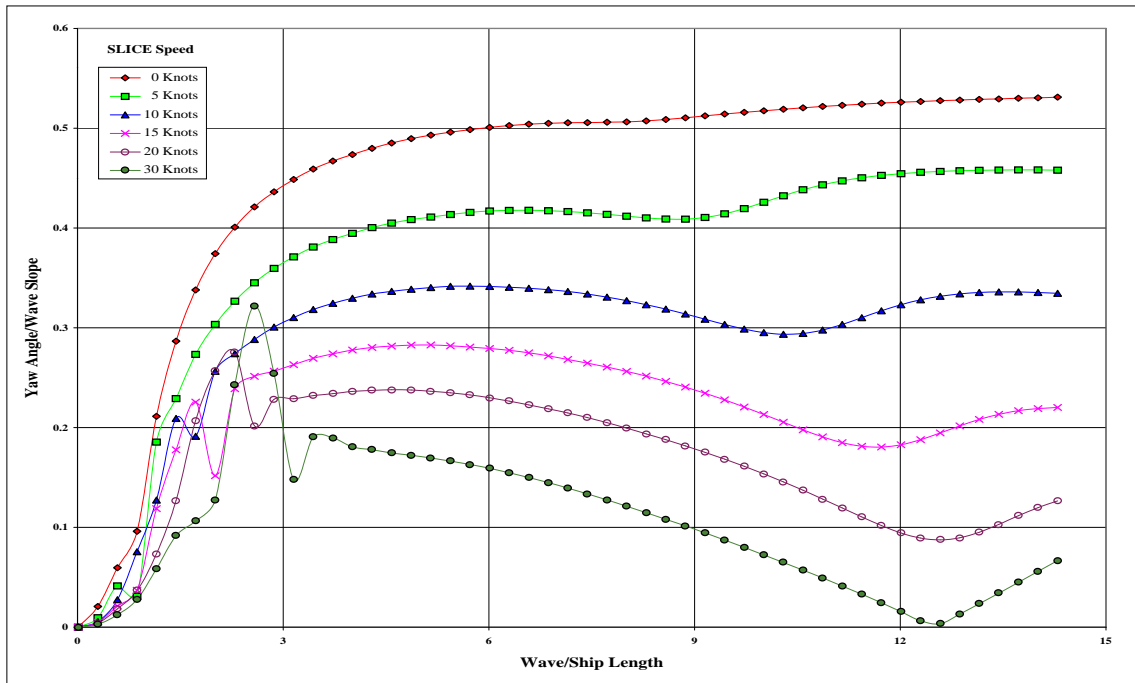


Figure (61). Yaw Characteristics as a Function of SLICE Speed, 150 Degree Wave Angle.

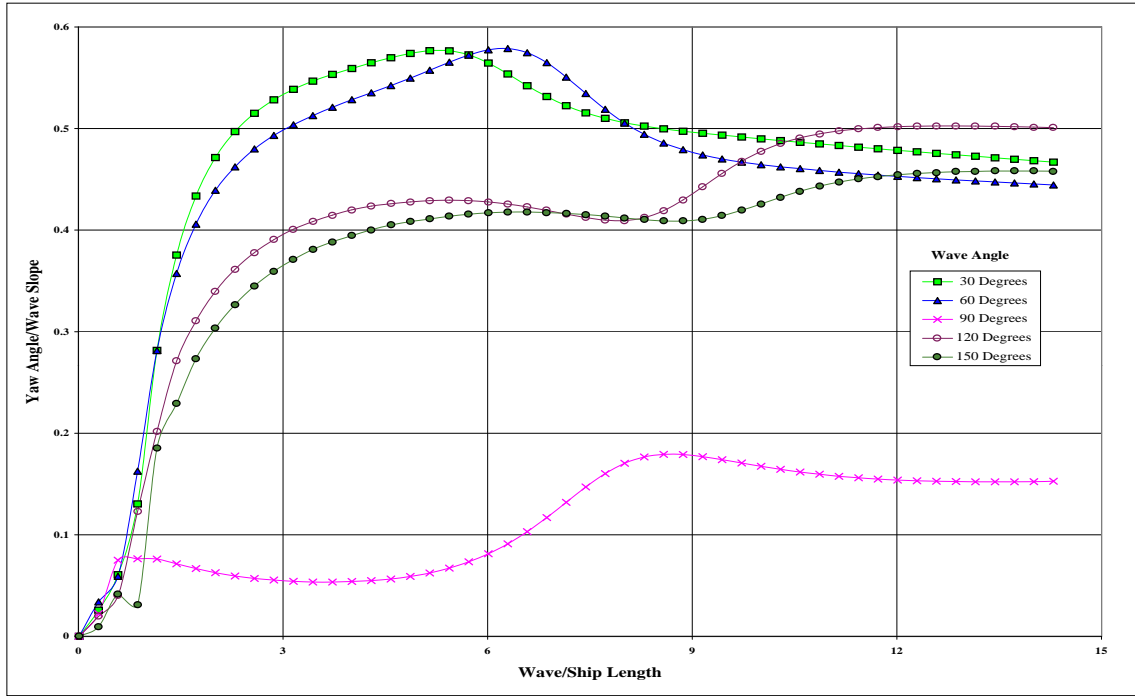


Figure (62). Yaw Characteristics as a Function of Wave Angle, 5 Knots.

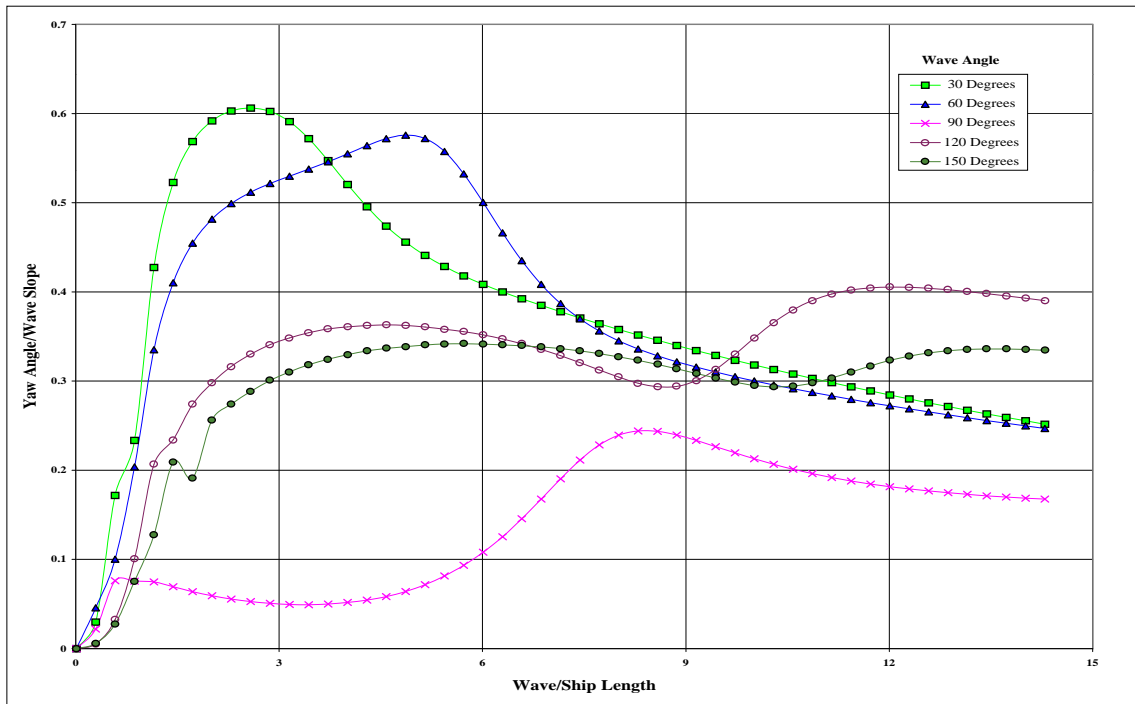


Figure (63). Yaw Characteristics as a Function of Wave Angle, 10 Knots.

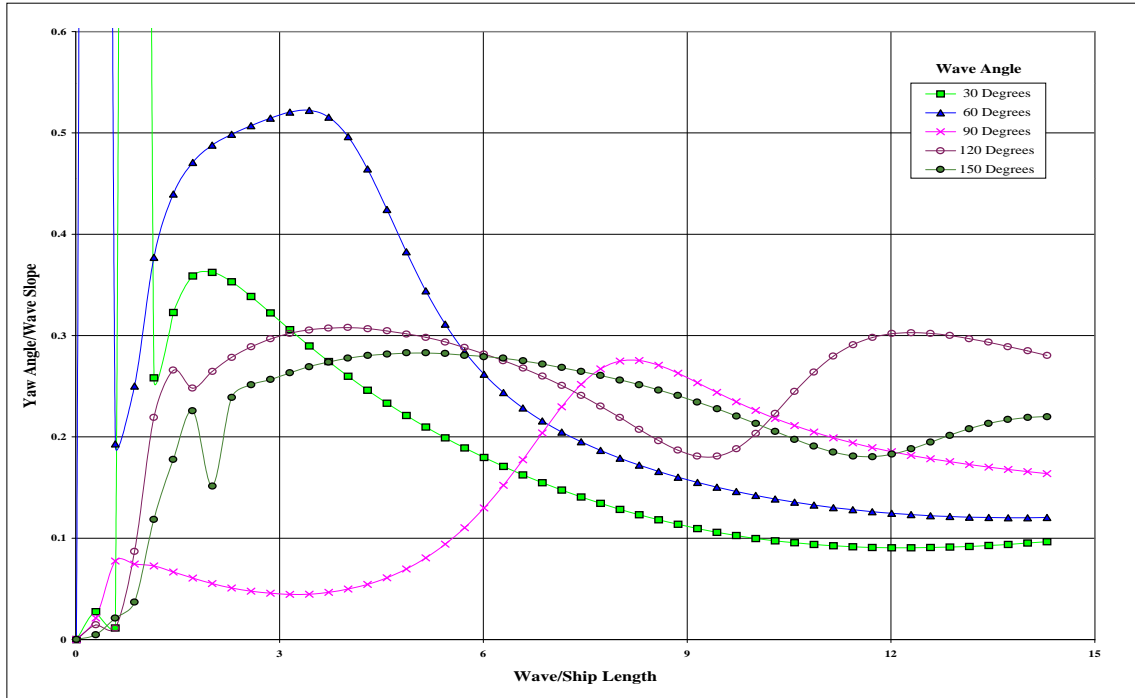


Figure (64). Yaw Characteristics as a Function of Wave Angle, 15 Knots.

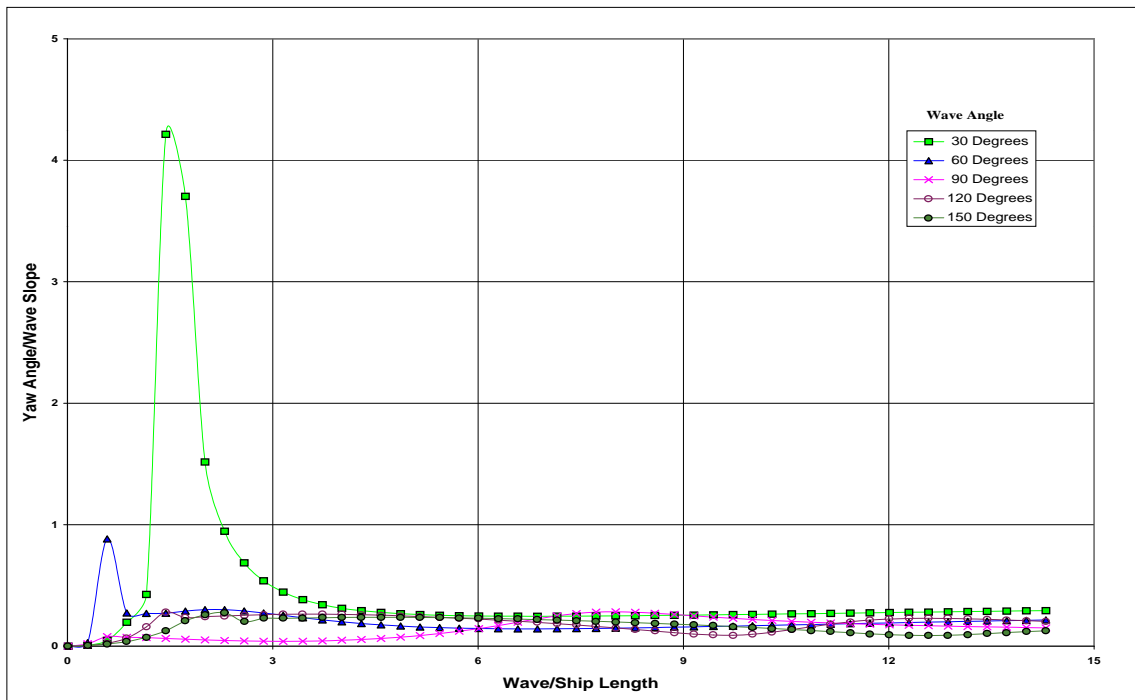


Figure (65). Yaw Characteristics as a Function of Wave Angle, 20 Knots.

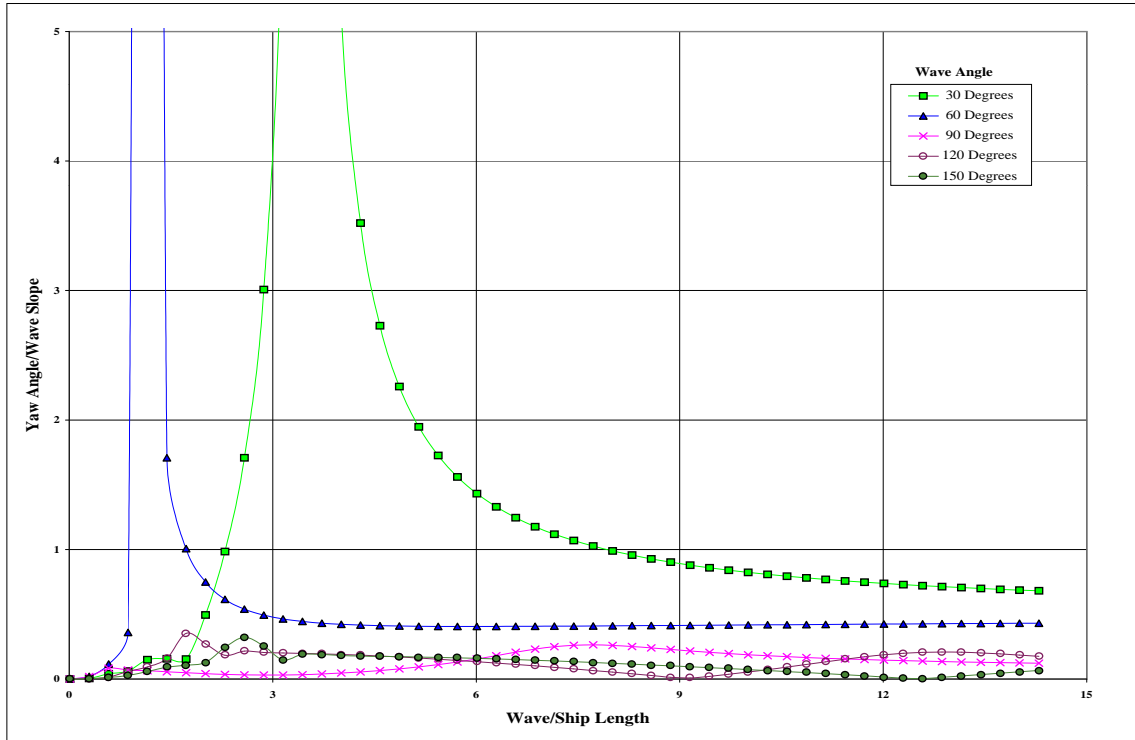


Figure (66). Yaw Characteristics as a Function of Wave Angle, 30 Knots.

In the motions of heave and pitch, the resonant peaks increase in amplitude for wave angles forward of the beam and decrease in amplitude for those aft of the beam as shown in Figures (67) through (90). These vertical plane resonances are a result of the small waterplane area of the SLICE hull, and are characteristic of SWATH vessels. As SLICE speed increases, these peaks move toward higher wave/ship length ratios. This shift makes it more difficult to achieve resonance since a more severe sea is required to excite the system. Table (6) provides an illustration of the relationship between sea severity and wave to ship length ratio. For a conventional SWATH vessel, this resonance is controllable through the use of active and passive surfaces or fins. Figure (2) depicts these surfaces for the SLICE configuration. This study did not include the passive effects of these surfaces due to insufficient data in the available drawings.

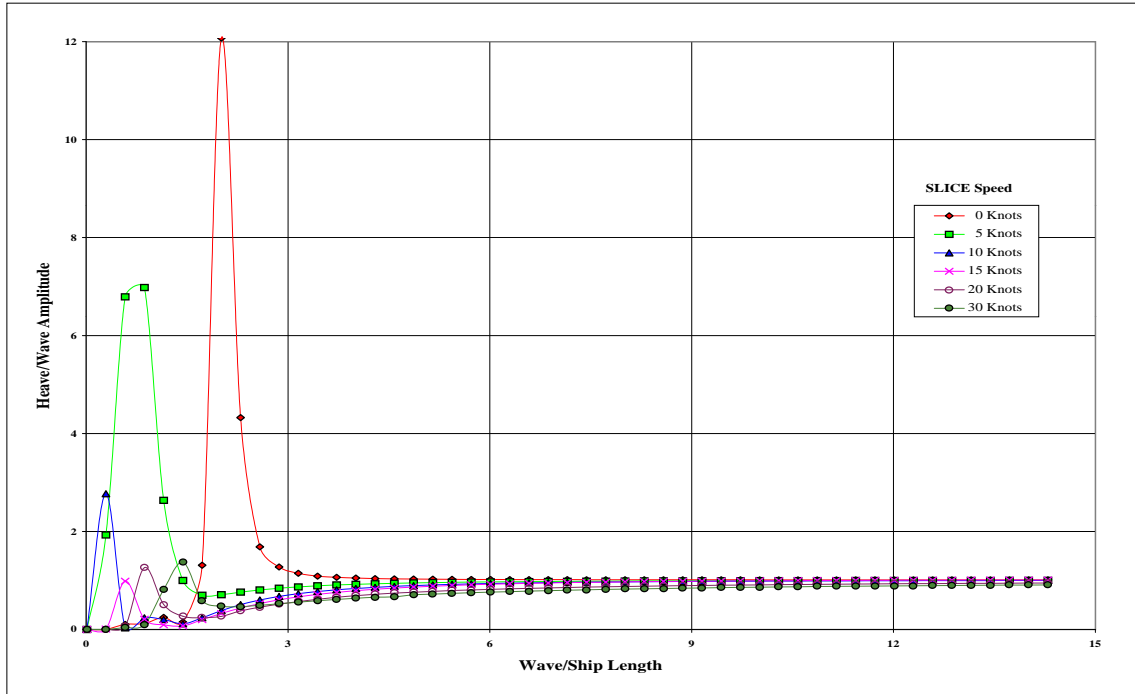


Figure (67). Heave Characteristics as a Function of SLICE Speed, 0 Degree Wave Angle.

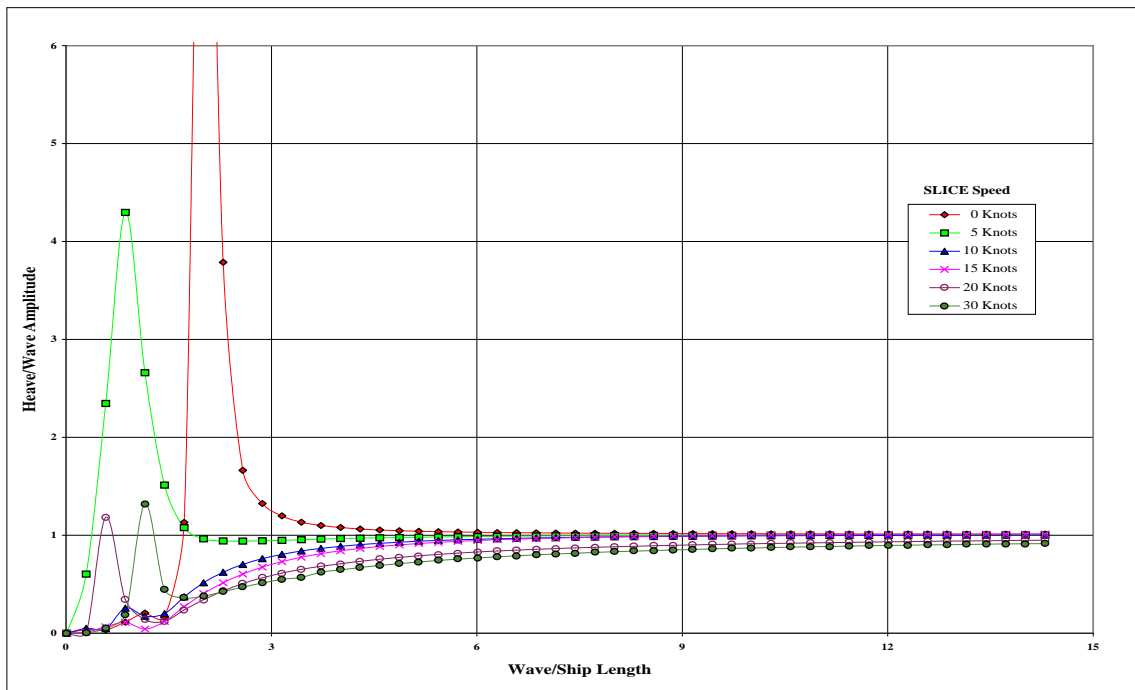


Figure (68). Heave Characteristics as a Function of SLICE Speed, 30 Degree Wave Angle.

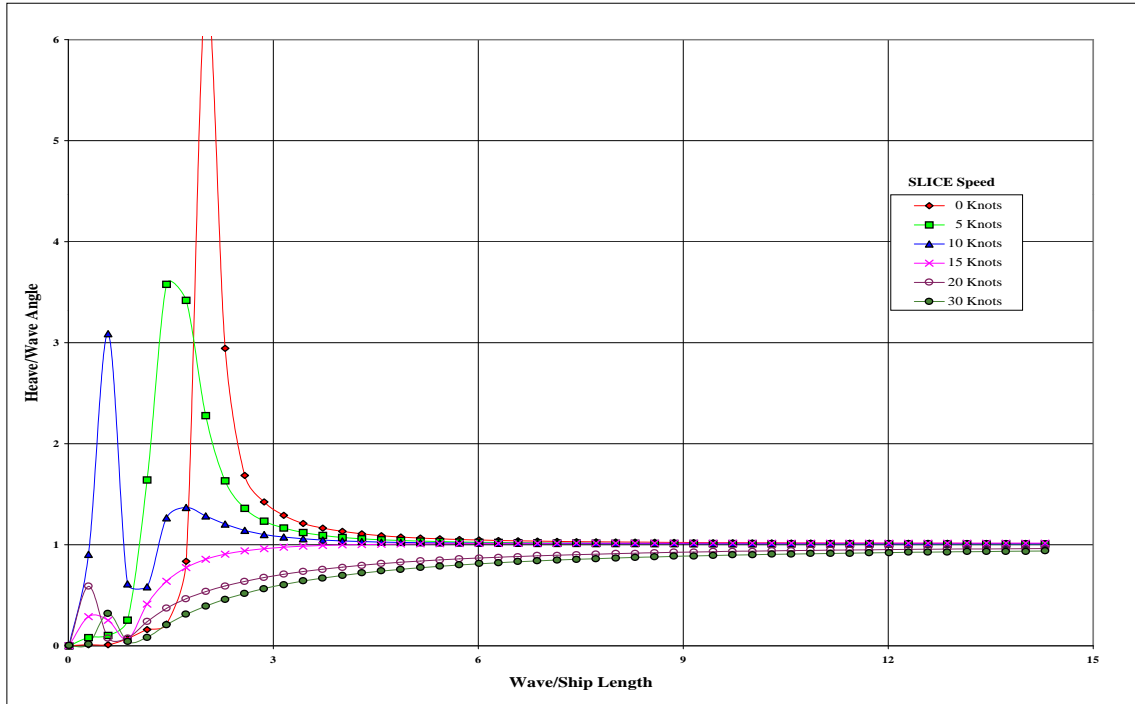


Figure (69). Heave Characteristics as a Function of SLICE Speed, 60 Degree Wave Angle.

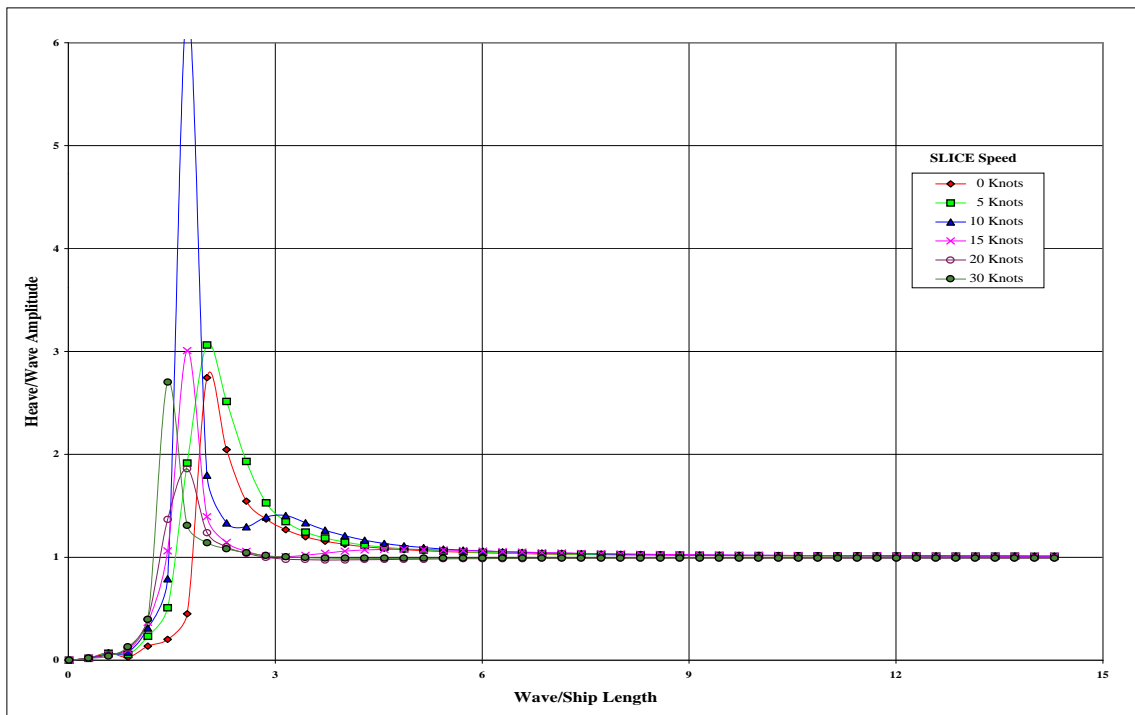


Figure (70). Heave Characteristics as a Function of SLICE Speed, 90 Degree Wave Angle.

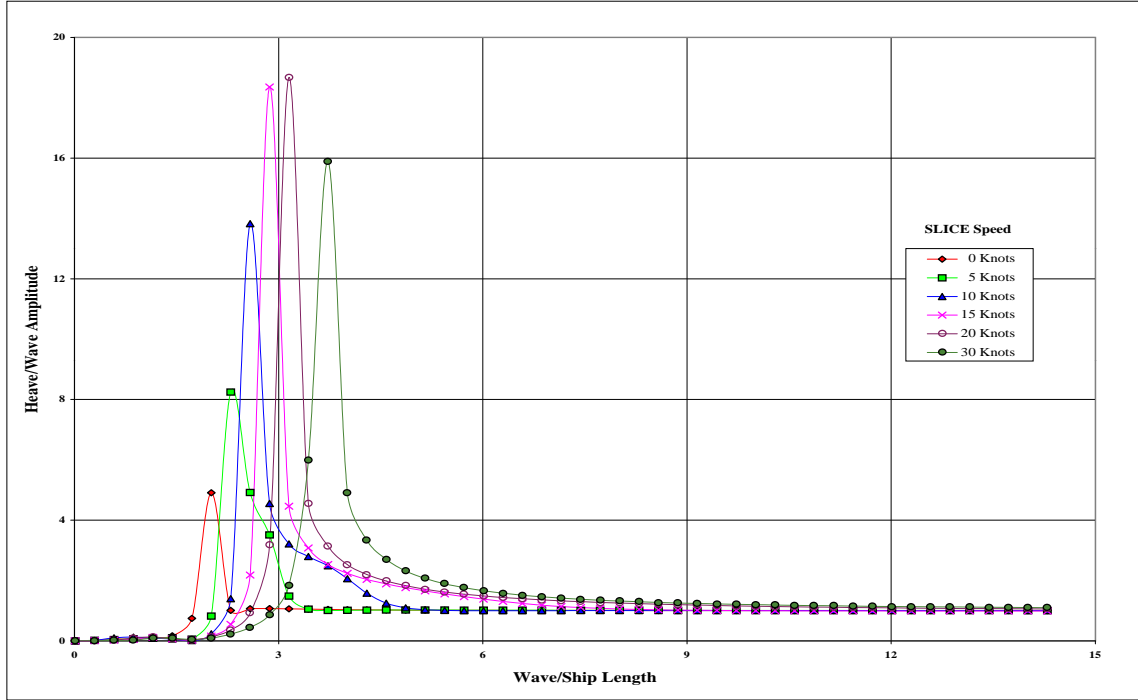


Figure (71). Heave Characteristics as a Function of SLICE Speed, 120 Degree Wave Angle.

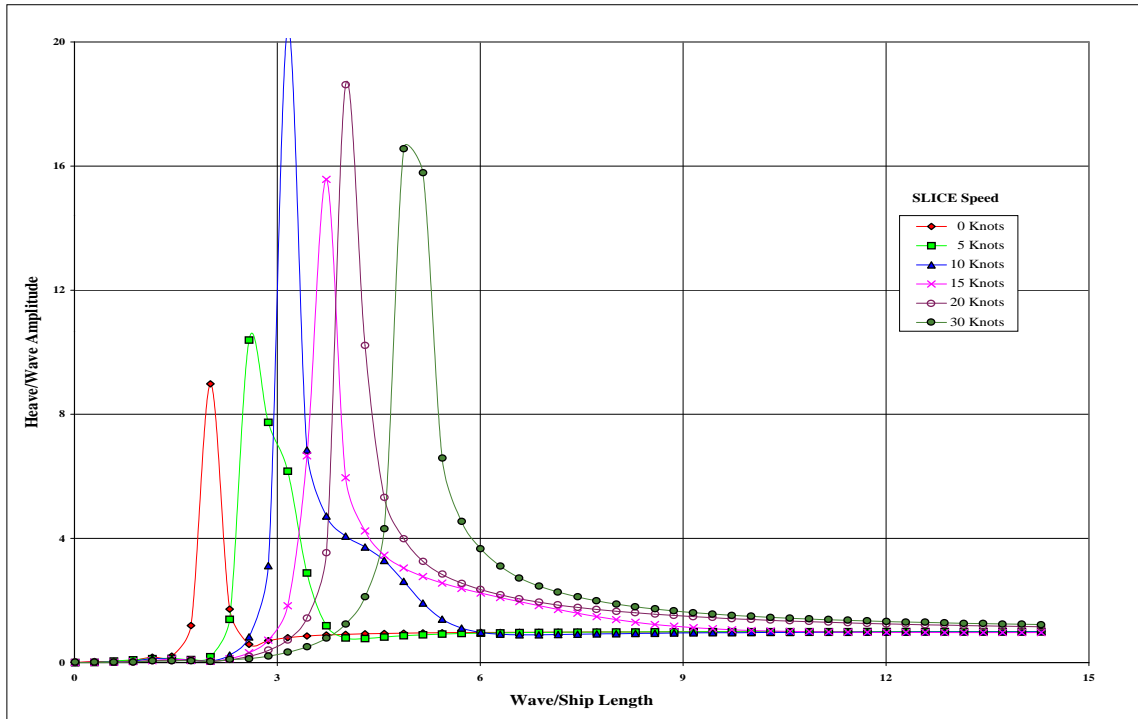


Figure (72). Heave Characteristics as a Function of SLICE Speed, 150 Degree Wave Angle.

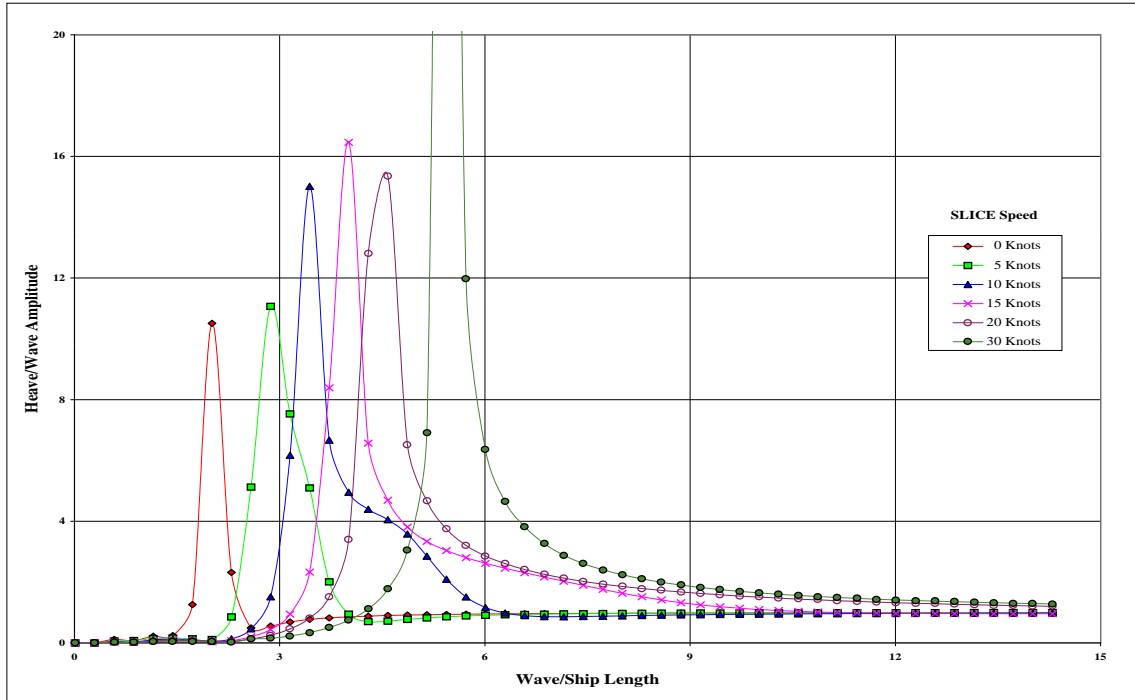


Figure (73). Heave Characteristics as a Function of SLICE Speed, 180 Degree Wave Angle.

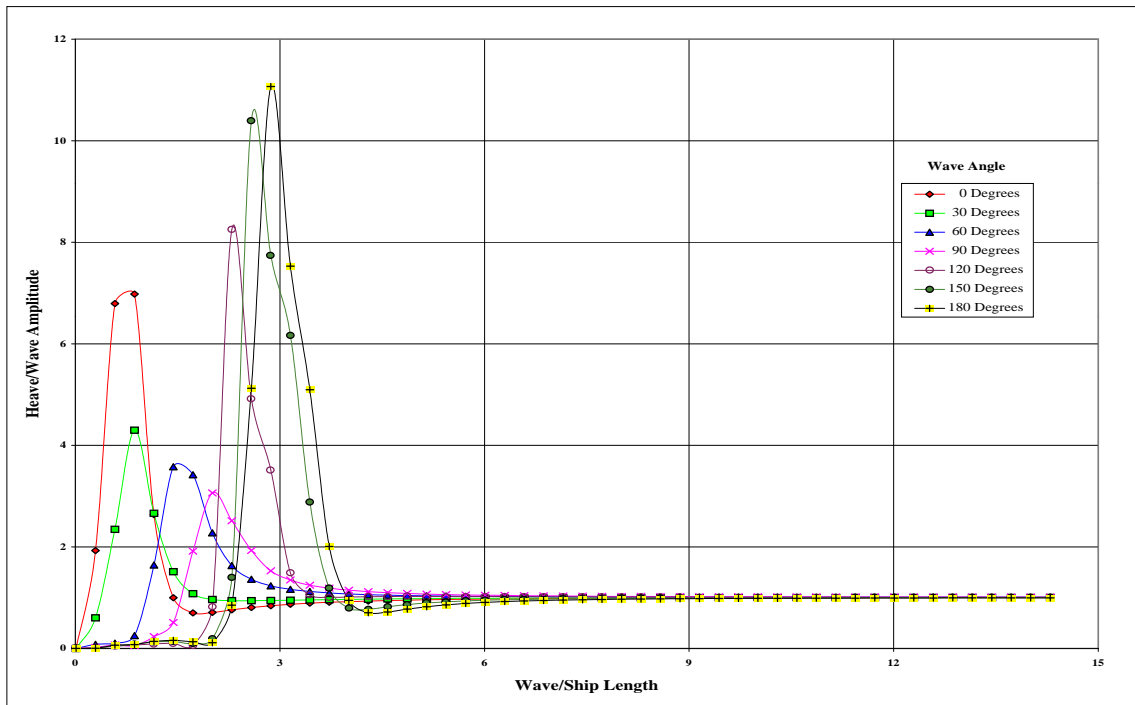


Figure (74). Heave Characteristics as a Function of Wave Angle, 5 Knots.

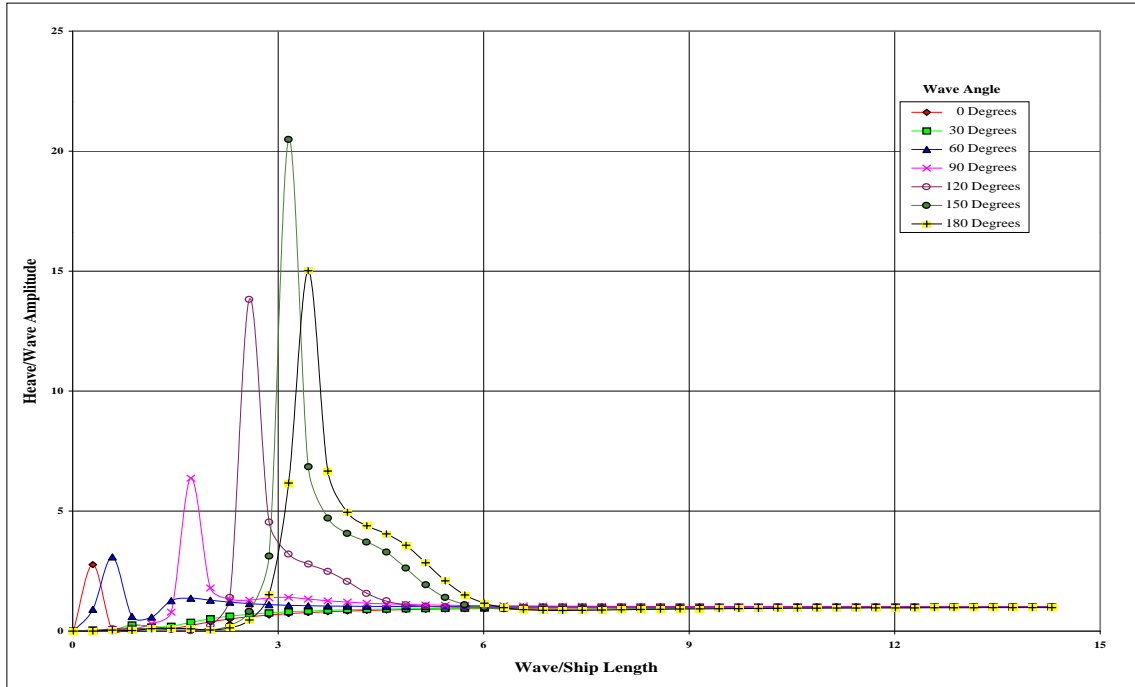


Figure (75). Heave Characteristics as a Function of Wave Angle, 10 Knots.

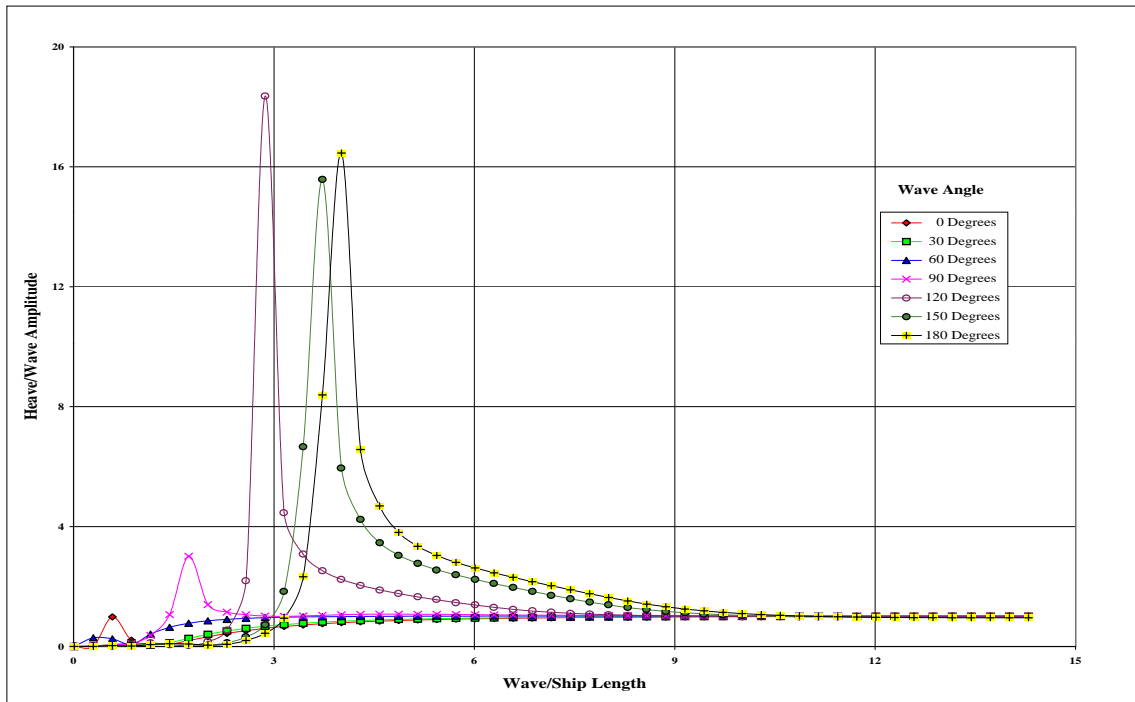


Figure (76). Heave Characteristics as a Function of Wave Angle, 15 Knots.

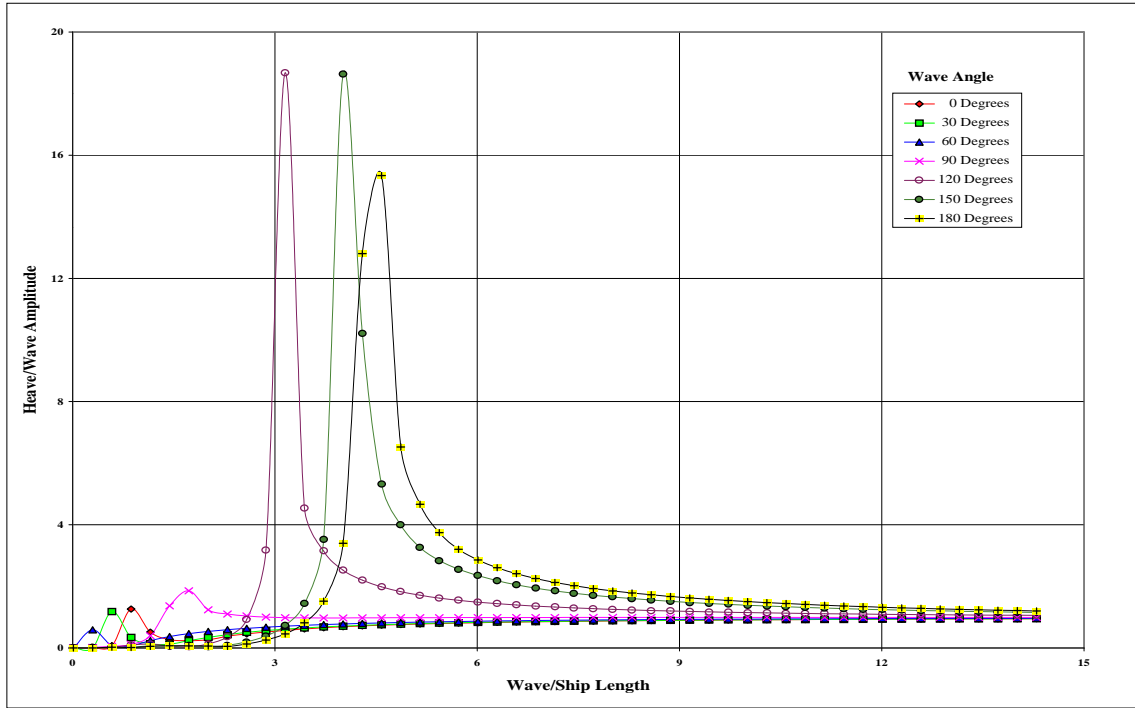


Figure (77). Heave Characteristics as a Function of Wave Angle, 20 Knots.

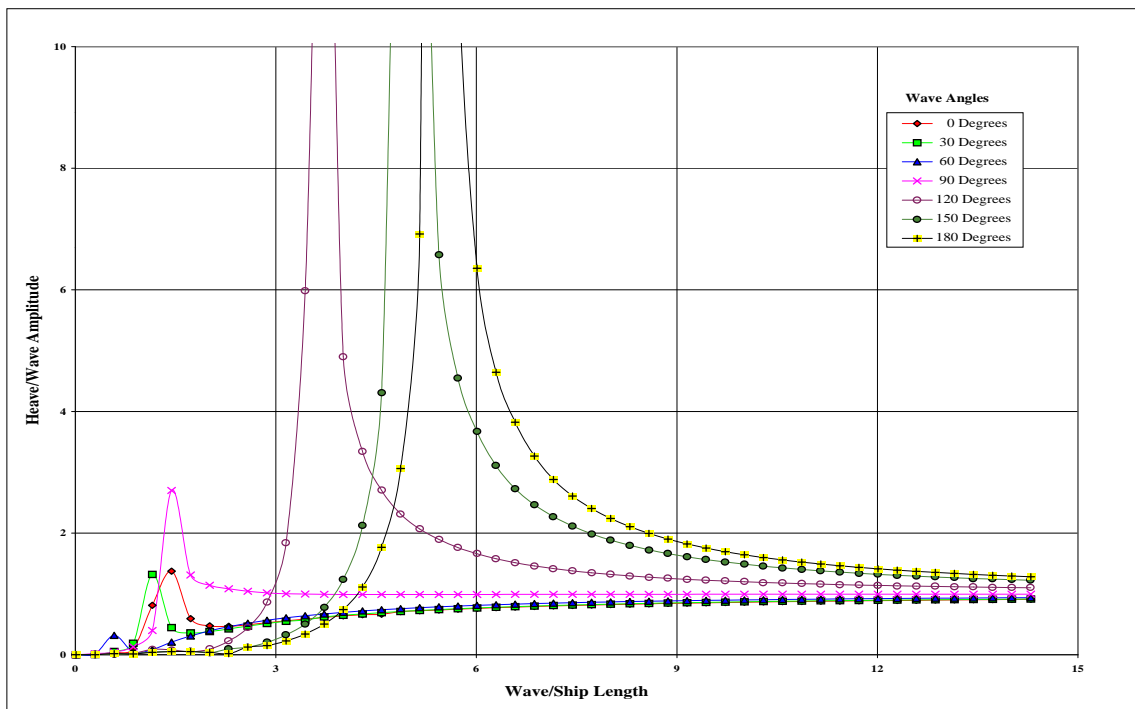


Figure (78). Heave Characteristics as a Function of Wave Angle, 30 Knots.

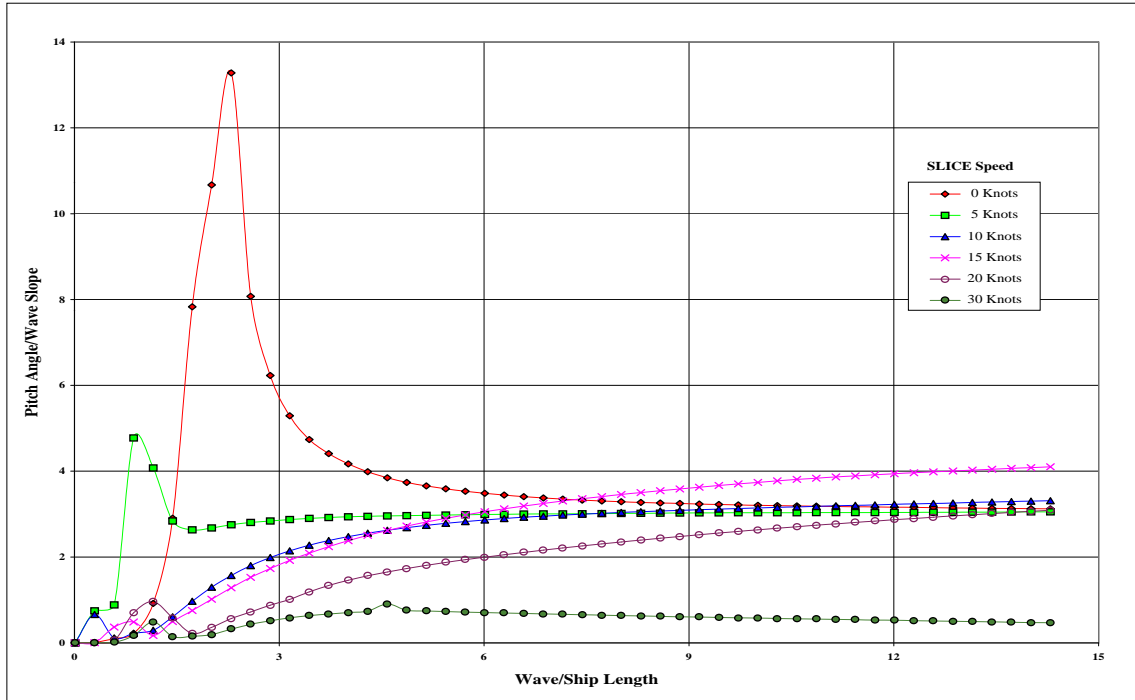


Figure (79). Pitch Characteristics as a Function of SLICE Speed, 0 Degree Wave Angle.

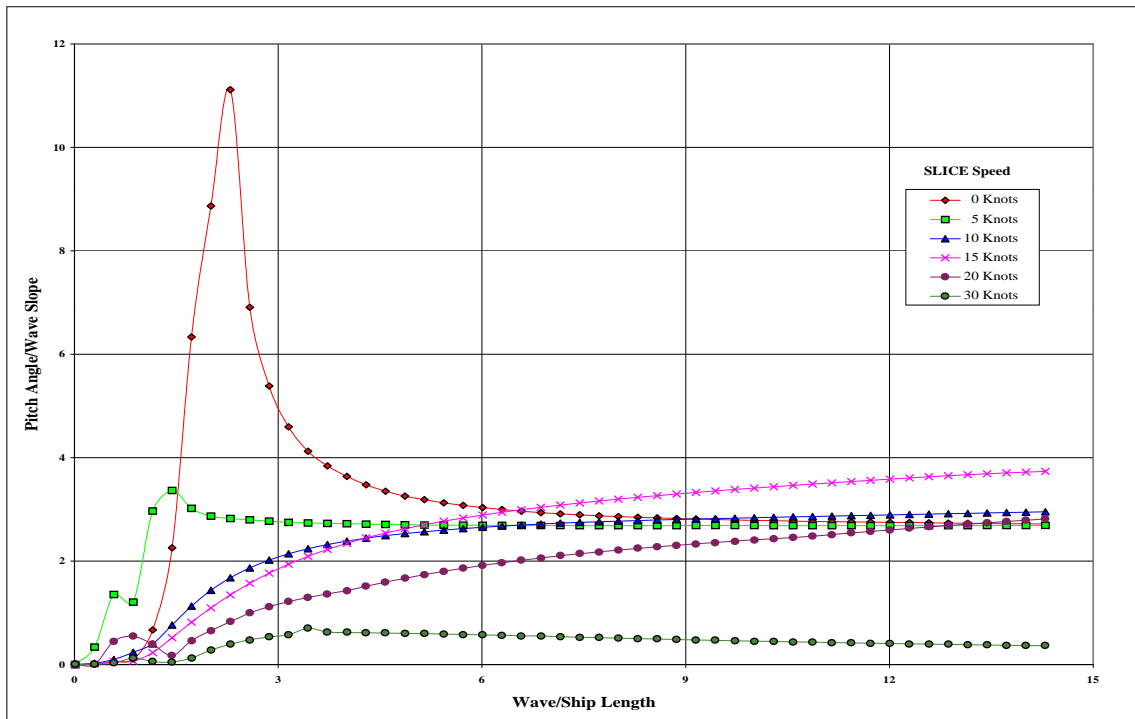


Figure (80). Pitch Characteristics as a Function of SLICE Speed, 30 Degree Wave Angle.

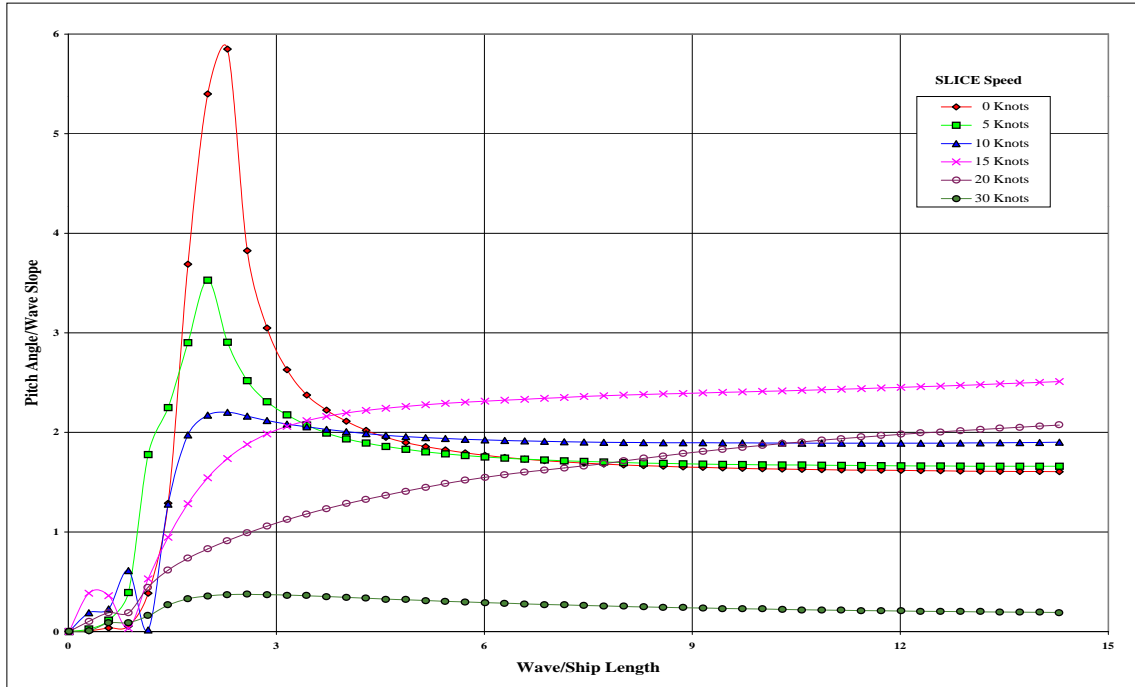


Figure (81). Pitch Characteristics as a Function of SLICE Speed, 60 Degree Wave Angle.

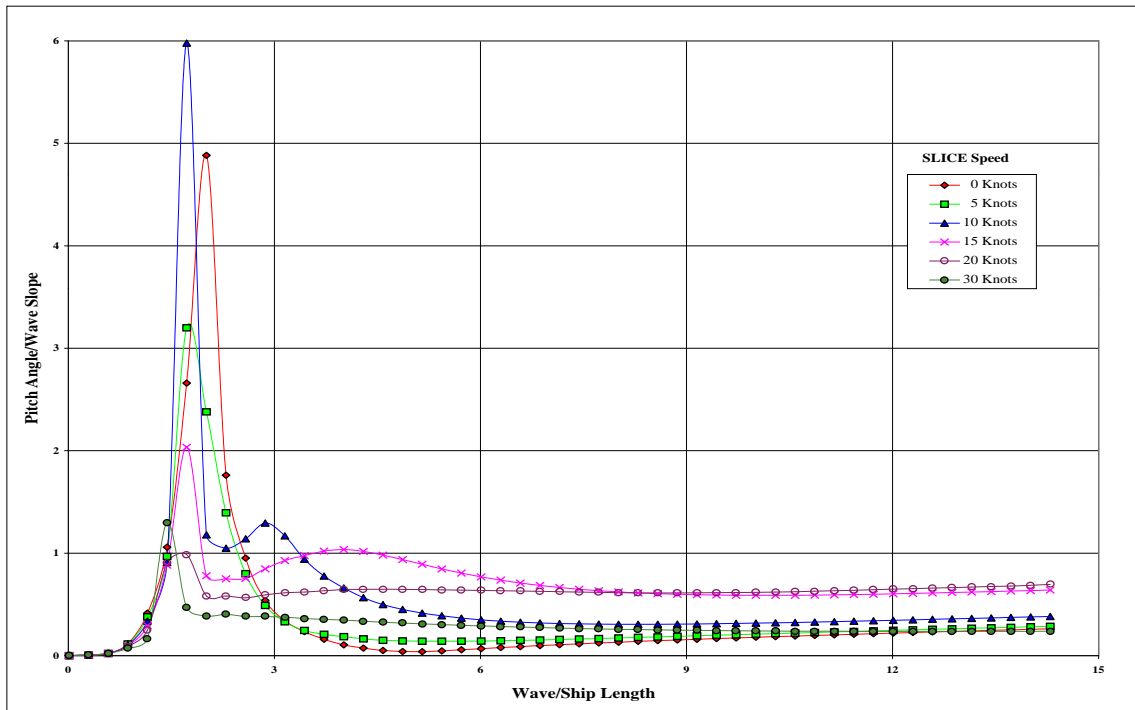


Figure (82). Pitch Characteristics as a Function of SLICE Speed, 90 Degree Wave Angle.

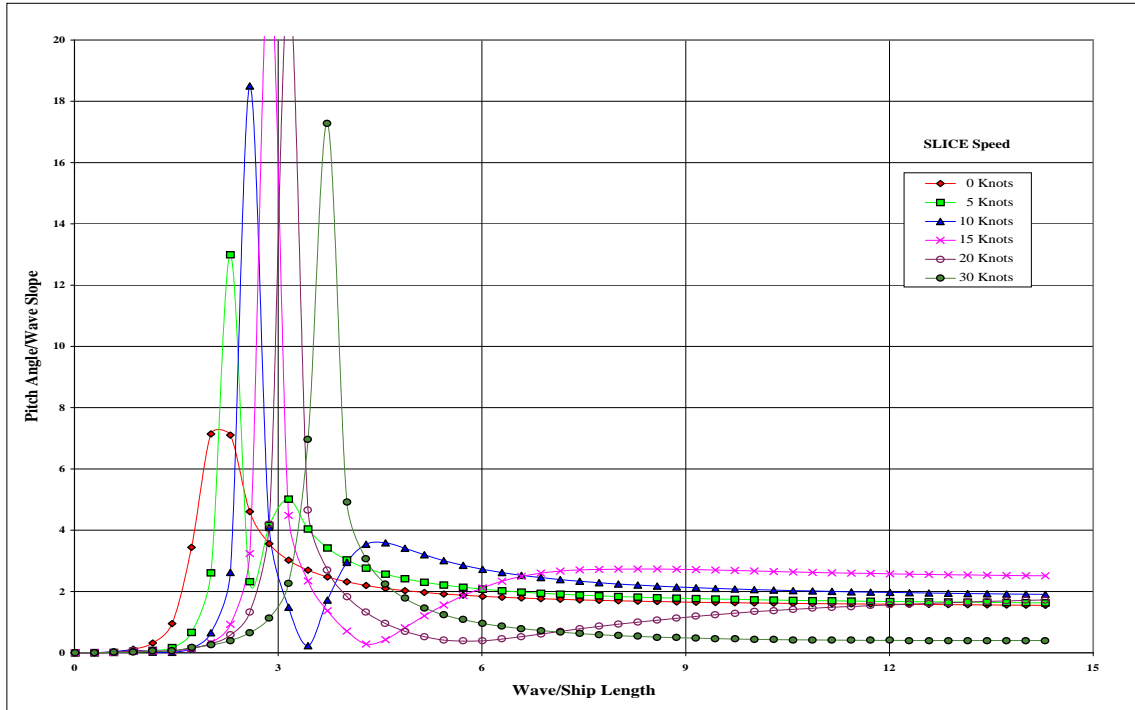


Figure (83). Pitch Characteristics as a Function of SLICE Speed, 120 Degree Wave Angle.

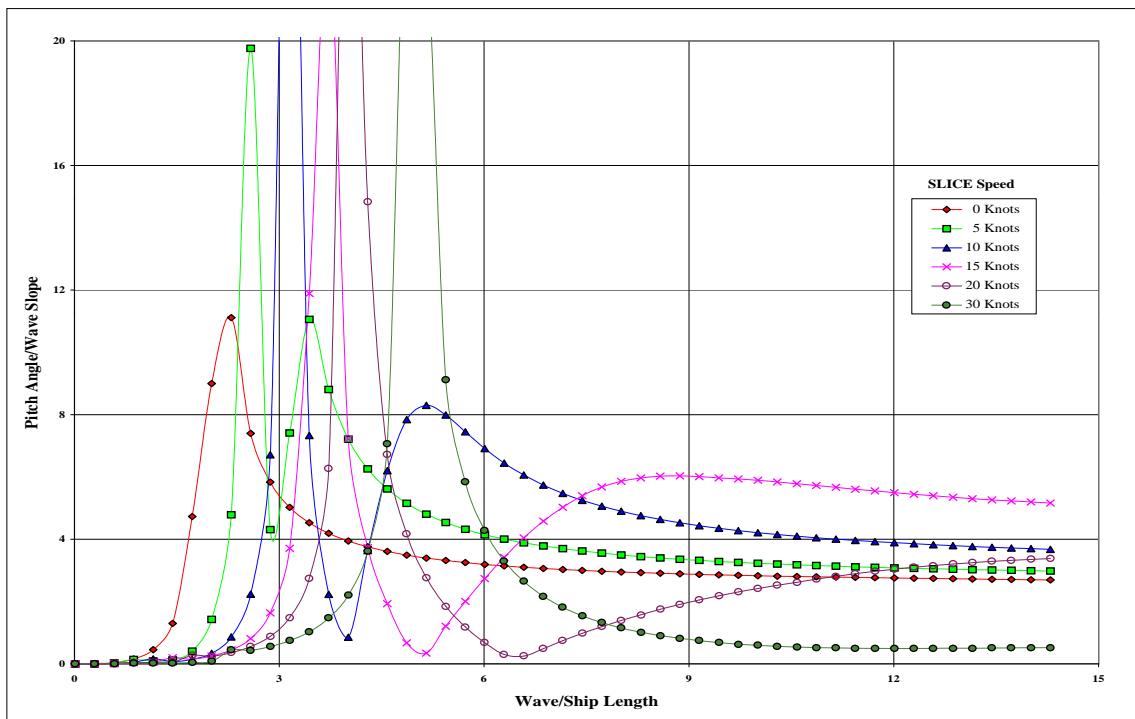


Figure (84). Pitch Characteristics as a Function of SLICE Speed, 150 Degree Wave Angle.

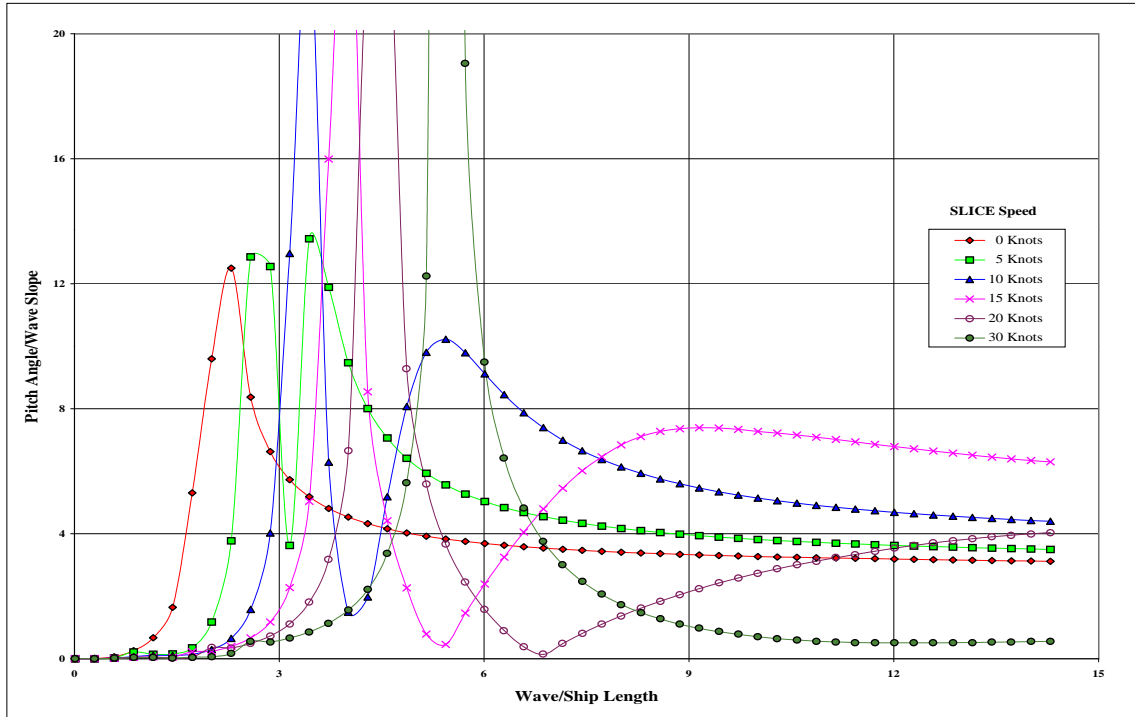


Figure (85). Pitch Characteristics as a Function of SLICE Speed, 180 Degree Wave Angle.

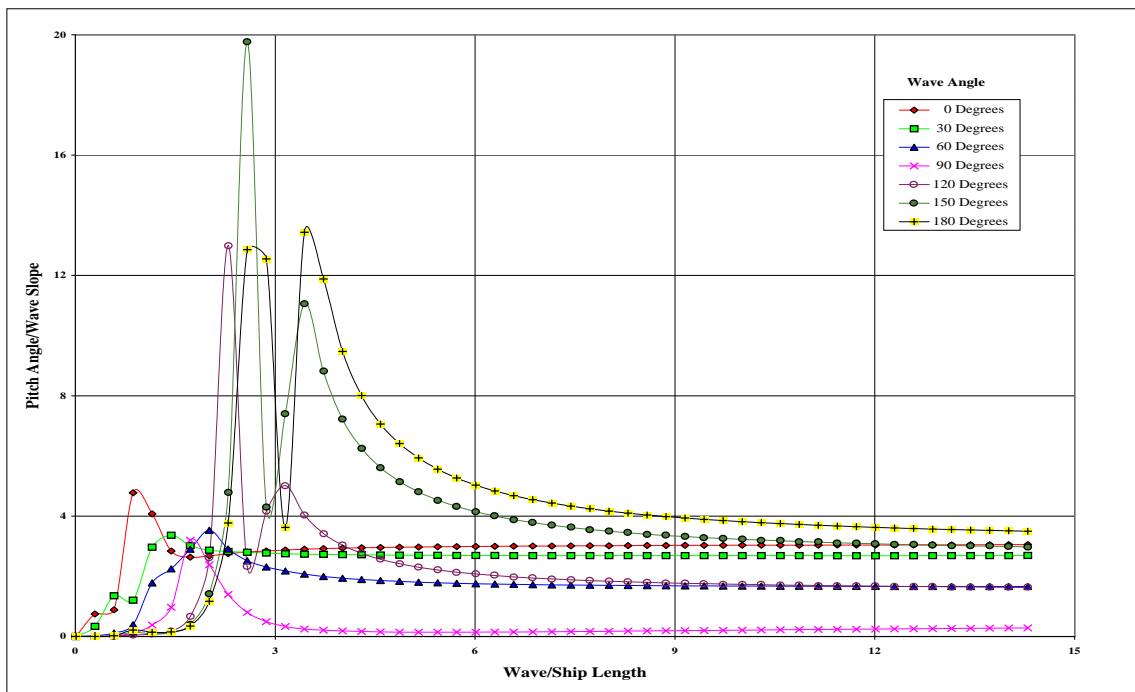


Figure (86). Pitch Characteristics as a Function of Wave Angle, 5 Knots.

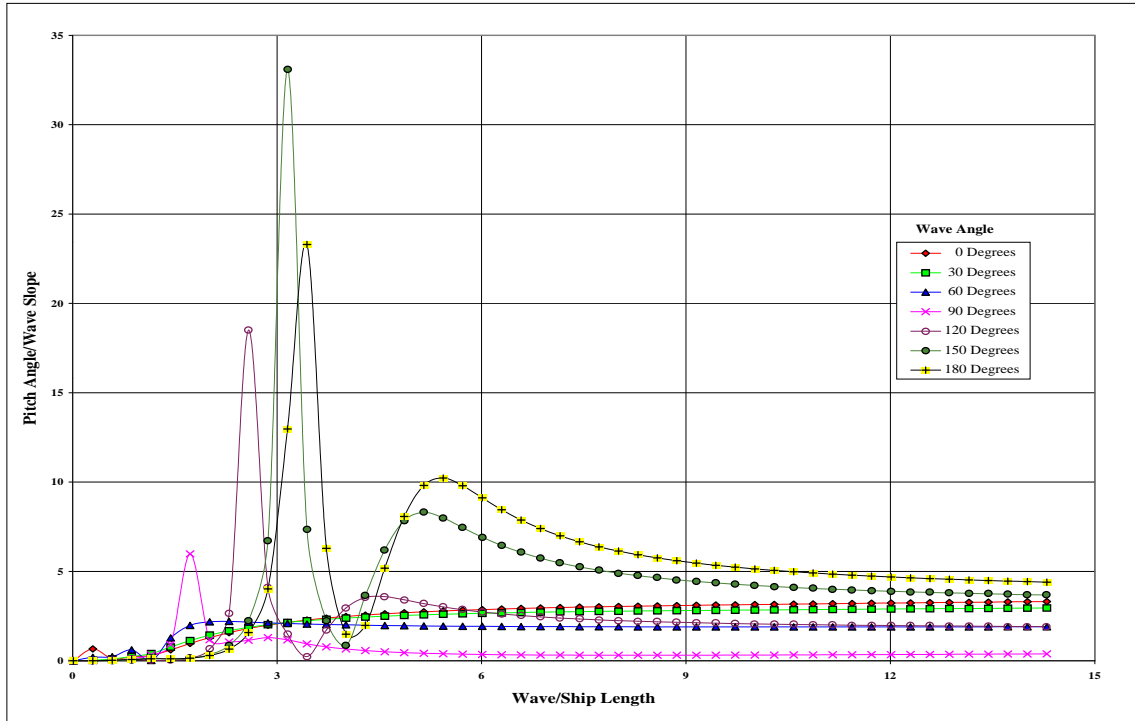


Figure (87). Pitch Characteristics as a Function of Wave Angle, 10 Knots.

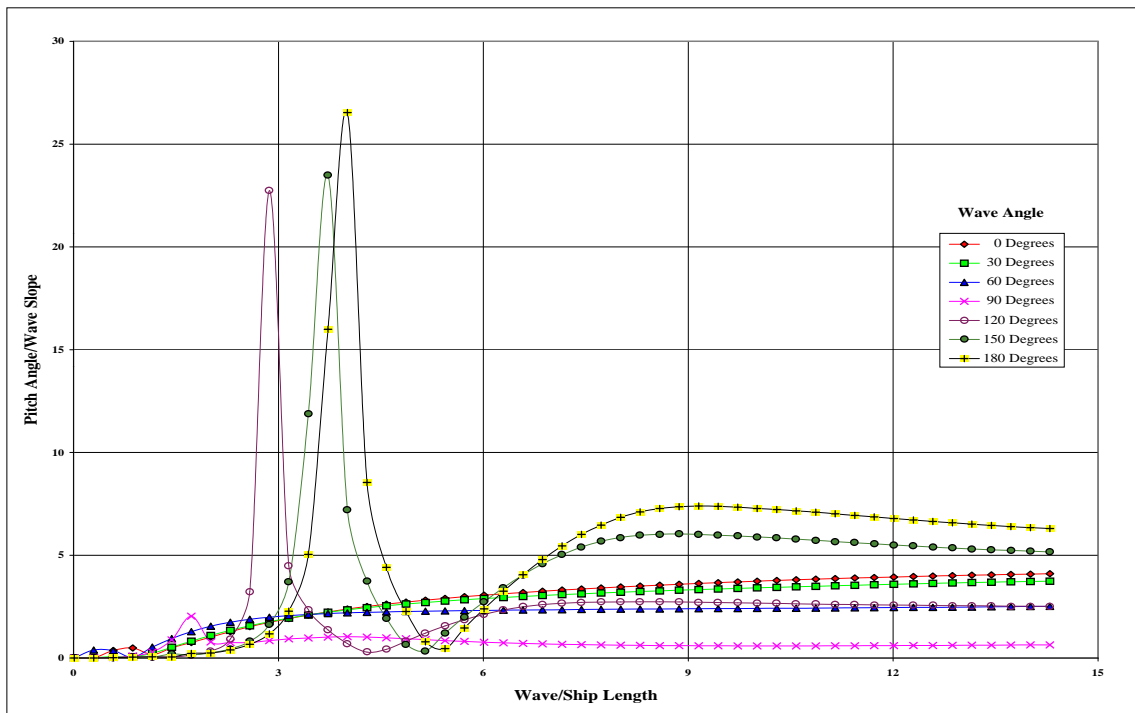


Figure (88). Pitch Characteristics as a Function of Wave Angle, 15 Knots.

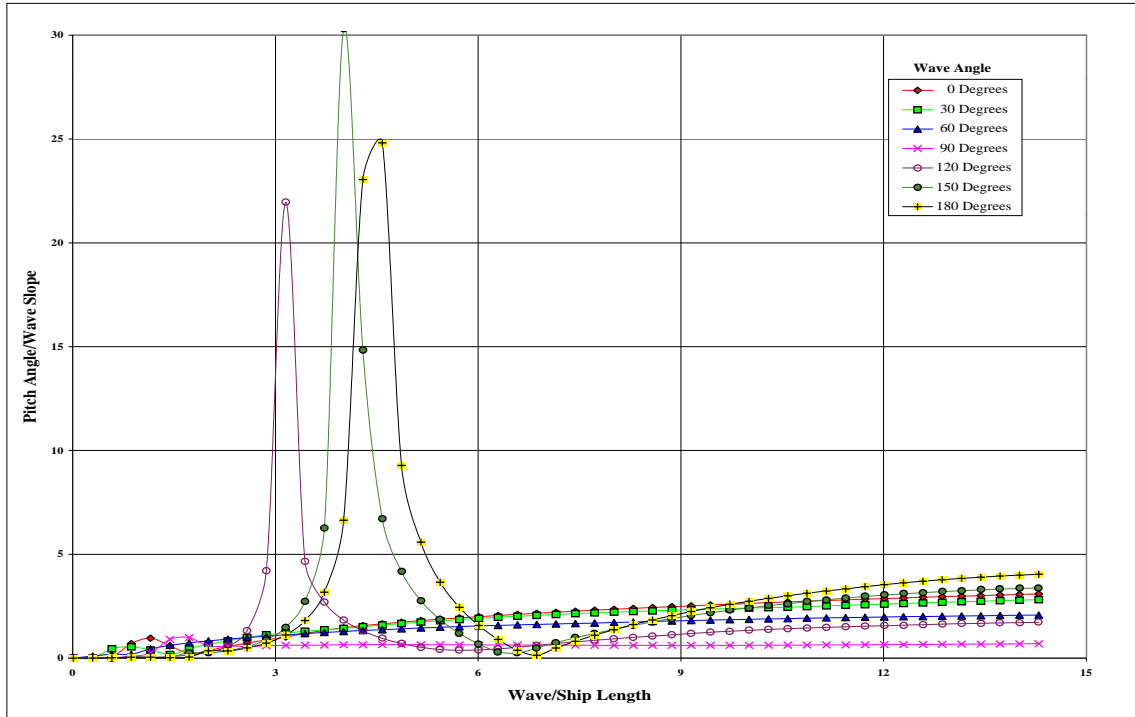


Figure (89). Pitch Characteristics as a Function of Wave Angle, 20 Knots.

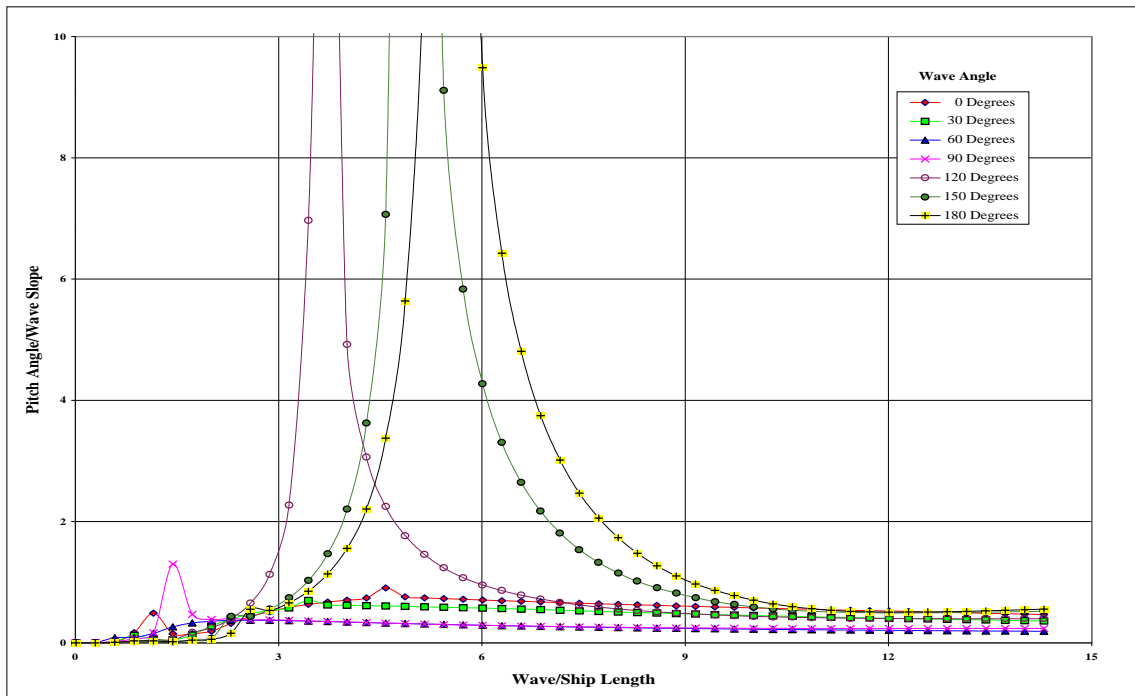


Figure (90). Pitch Characteristics as a Function of Wave Angle, 30 Knots.

It can be assumed, from research on SWATH vessels, that sufficient control of the SLICE will be achieved utilizing the canards (passive fins - forward pods) and stabilizer/rudders (active fins - after pods) (Lee, 1977).

Wind Speed (Knots)	Approximate Sea State	Significant Wave Height (meters)	Average Wavelength (meters)	Average Wavelength (feet)	Wave to Ship Length Ratio
10	2	0.6	22	67.1	0.64
20	4	2.2	89	271.3	2.58
30	6	5.0	200	609.6	5.81
40	7	8.9	355	1082	10.31

Table (6). Relationship between Sea Severity and Wave to Ship Length Ratios. After Papoulias, 1993.

In roll, for wave angles aft of the beam, the peak motions move toward lower wave/ship length ratios. This effect translates to decreased stability in roll for quartering seas, which is common to many surface ships. For wave angles forward of the beam, peaks shift toward higher ratios. Roll amplitudes generally increased in quartering seas for speeds up to 15 knots and then decreased above 15 knots. For seas off the bow (120 and 150 degree wave angles), the opposite effect was noted. However, the shift toward higher wave to ship length ratios makes the likelihood of encountering waves capable of exciting these motions low. In beam seas, motions decreased slightly with increasing speed. Figures (91) through (100).

Resonant behavior as a function of SLICE speed and wave angle is summarized in Figures (101) through (104), for the motions of surge, heave, pitch, and roll. The modes of sway and yaw did not exhibit resonance in the studied wave to ship length range. Discontinuous curves reflect speed and wave angle combinations that did not show resonant behavior in the studied range. These discontinuities, with the exception of the 30 knot peak for roll at a 150 degree wave angle, are limited to wave angles aft of the beam (0, 30, and 60 degrees) and may arise, in part, from negative encounter frequencies. Wave angles forward of the beam show an increasing trend in wave to ship ratios. As wavelength increases, periods of motion also increase, due to lower wave frequency. Therefore, for seas forward of the beam, the SLICE becomes more stable with increasing speed. In beam seas, stability decreases slightly with

increasing speed. For quatrering and following seas, stability decreases until 10 - 15 knots and then increases, except in roll where stability continues to decrease with increasing speed.

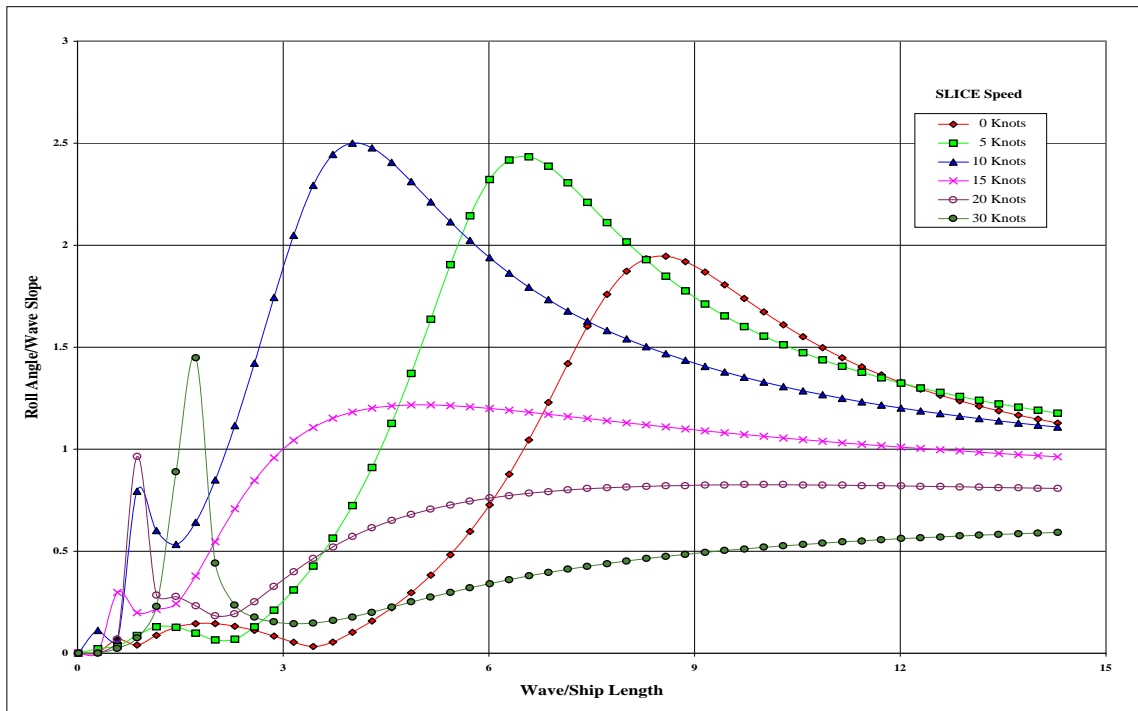


Figure (91). Roll Characteristics as a Function of SLICE Speed, 30 Degree Wave Angle.

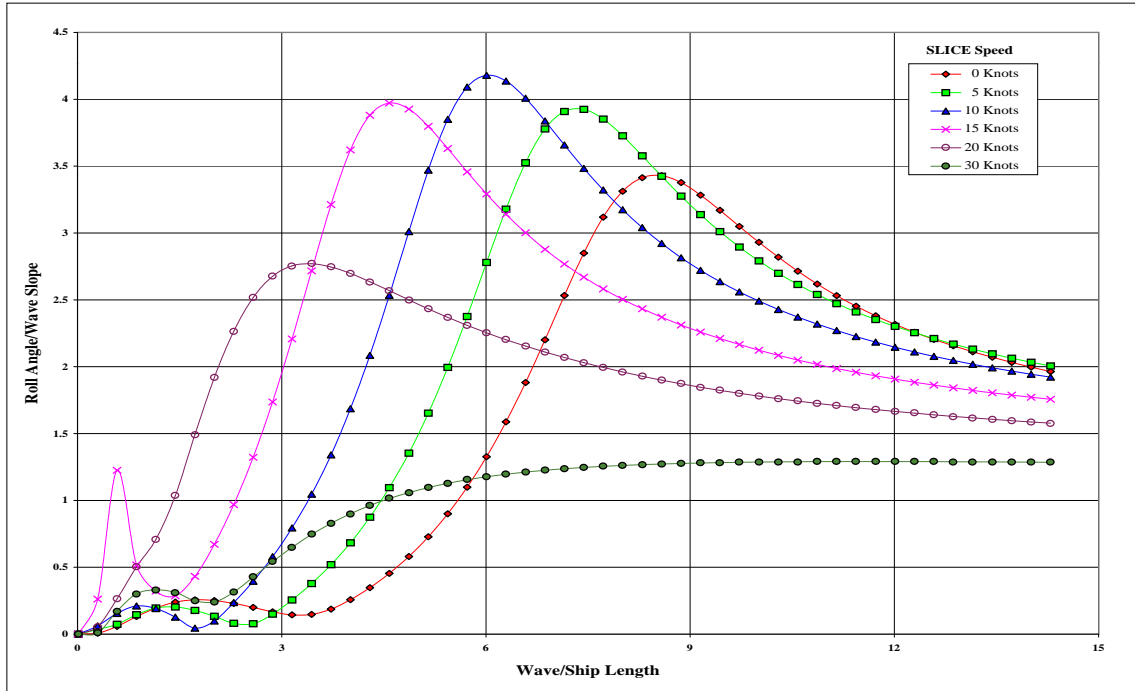


Figure (92). Roll Characteristics as a Function of SLICE Speed, 60 Degree Wave Angle.

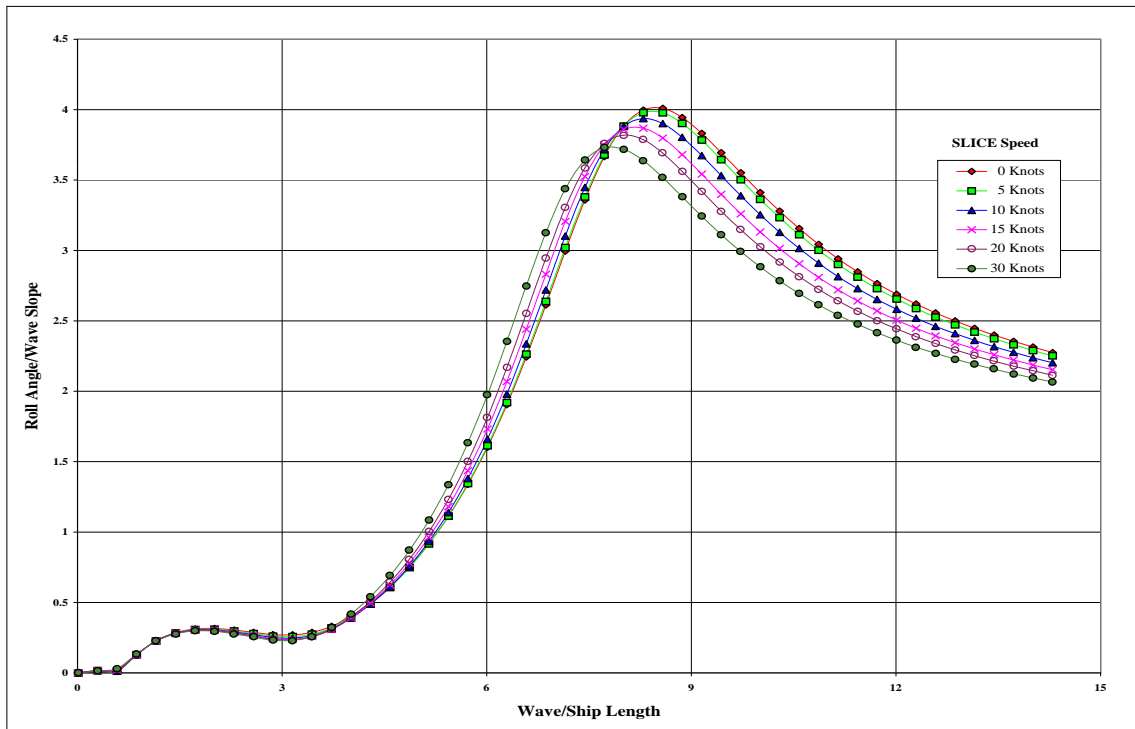


Figure (93). Roll Characteristics as a Function of SLICE Speed, 90 Degree Wave Angle.

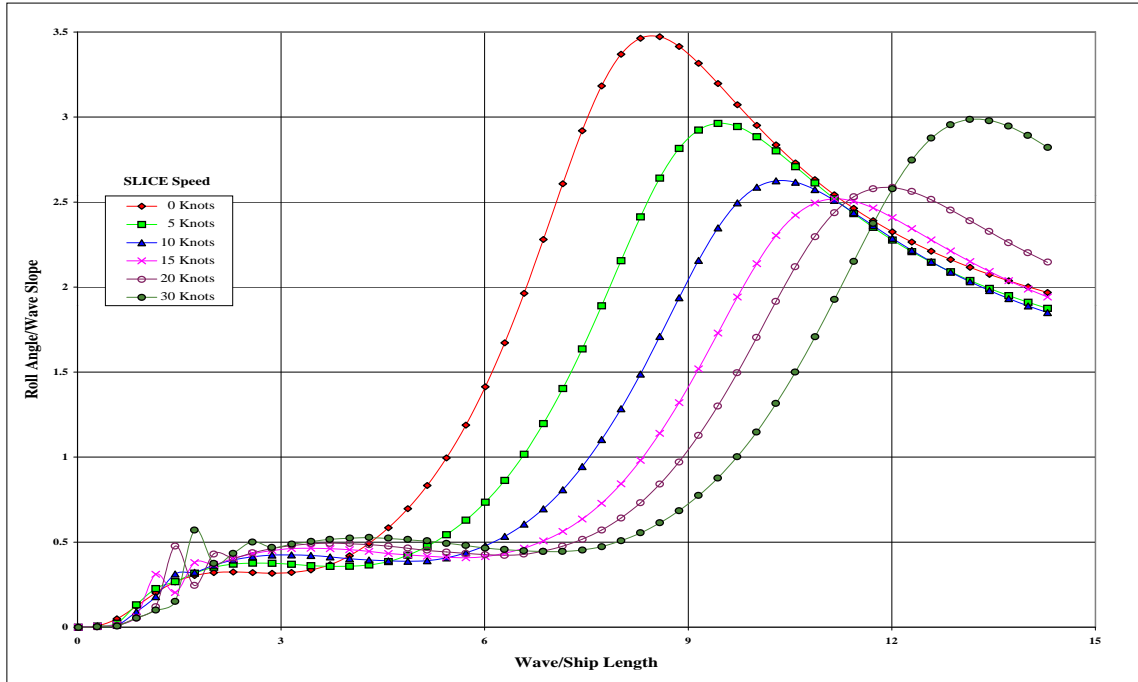


Figure (94). Roll Characteristics as a Function of SLICE Speed, 120 Degree Wave Angle.

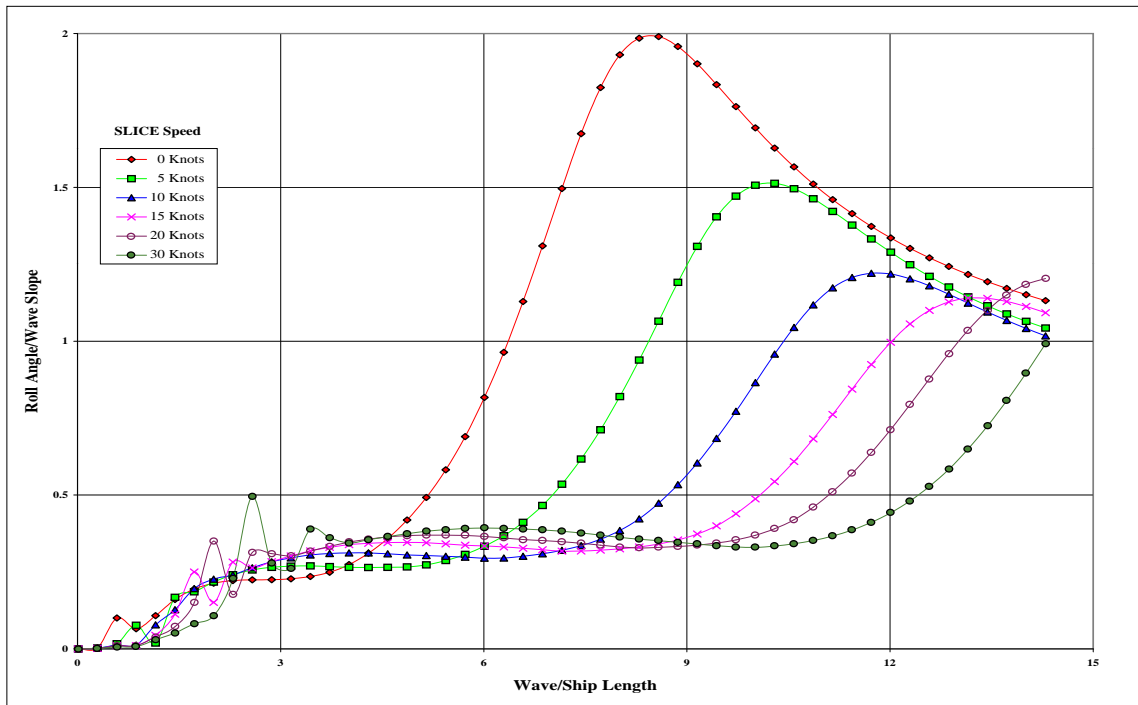


Figure (95). Roll Characteristics as a Function of SLICE Speed, 150 Degree Wave Angle.

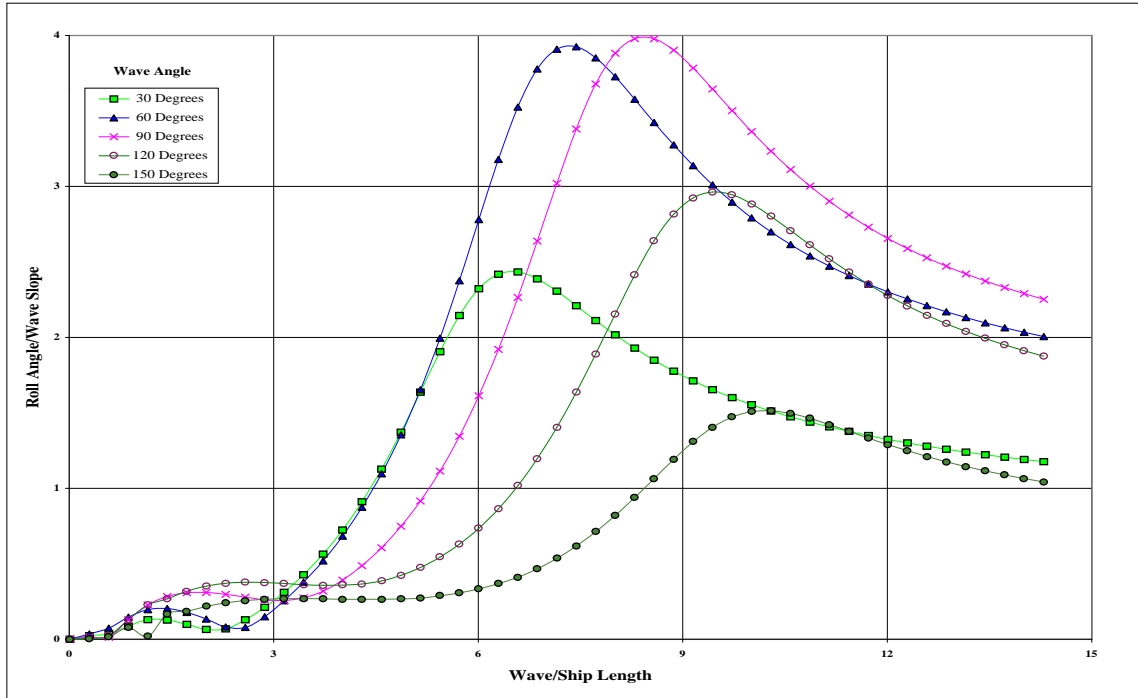


Figure (96). Roll Characteristics as a Function of Wave Angle, 5 Knots.

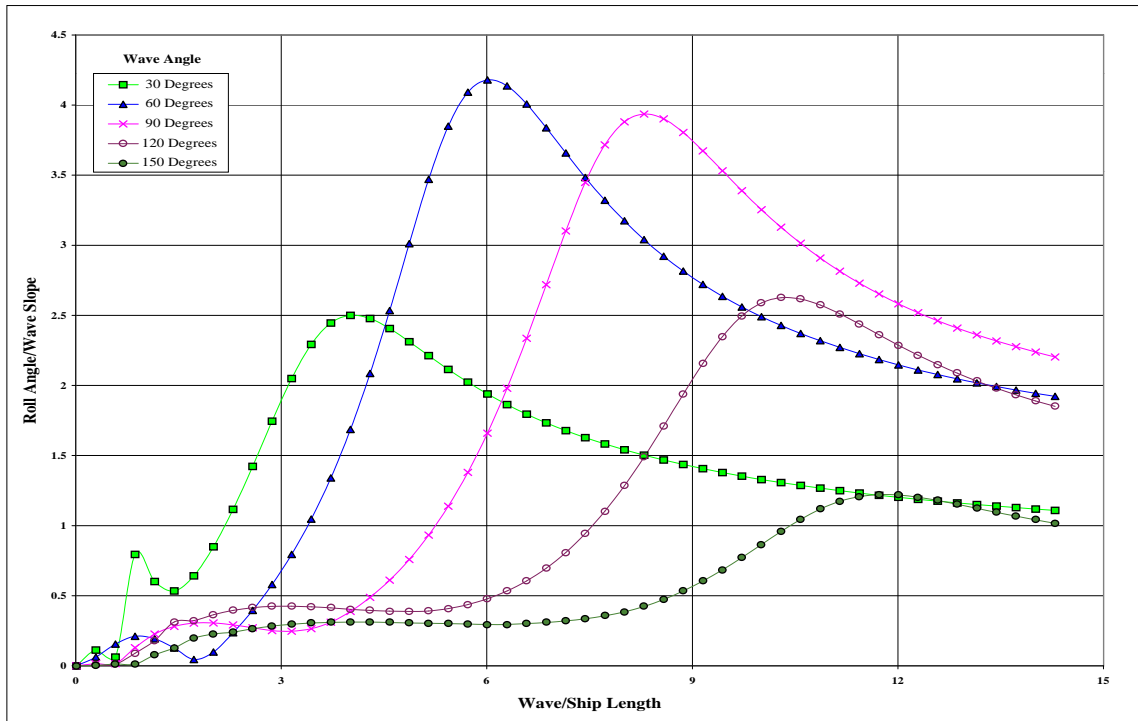


Figure (97). Roll Characteristics as a Function of Wave Angle, 10 Knots.

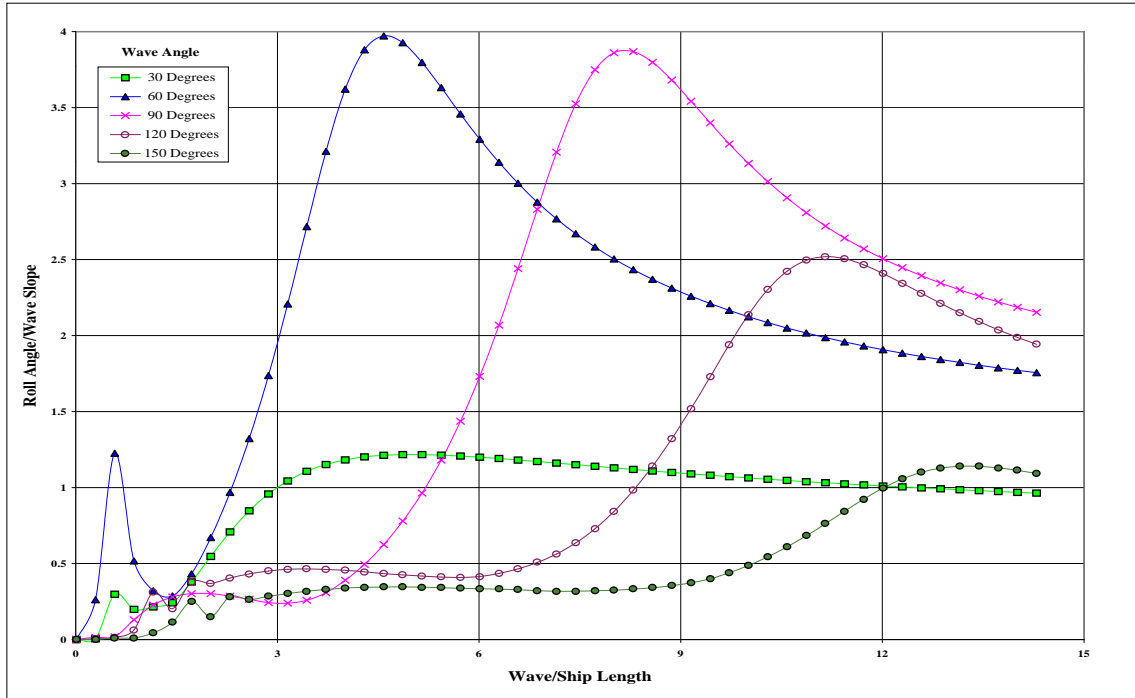


Figure (98). Roll Characteristics as a Function of Wave Angle, 15 Knots.

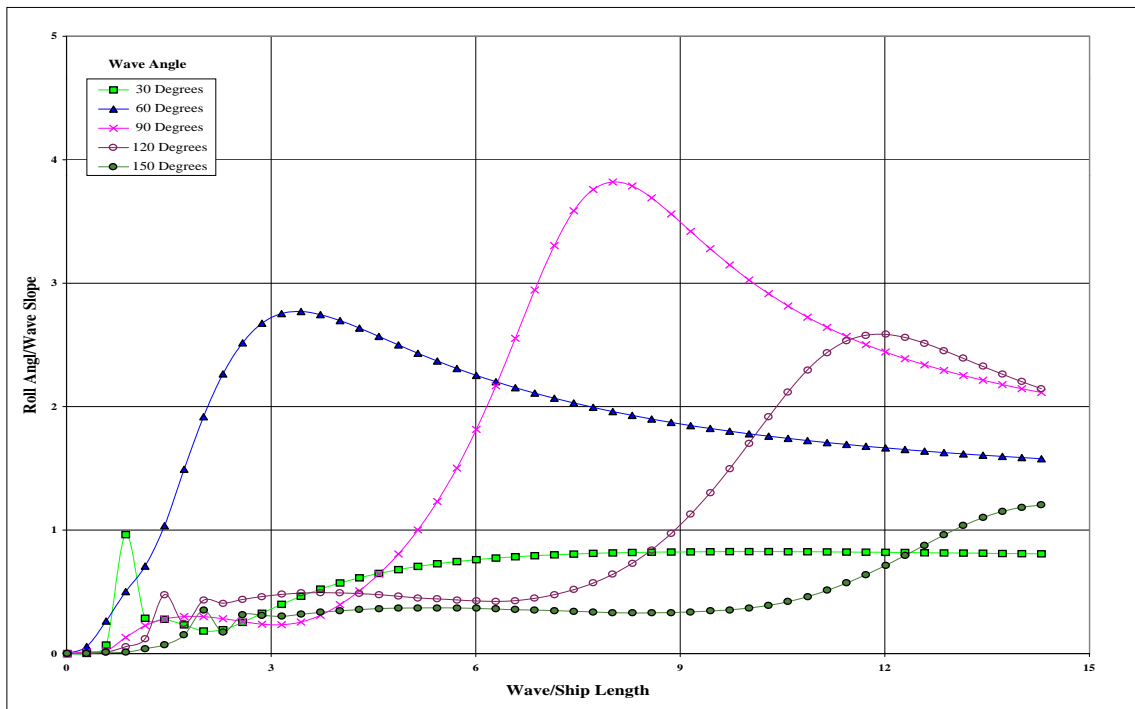


Figure (99). Roll Characteristics as a Function of Wave Angle, 20 Knots.

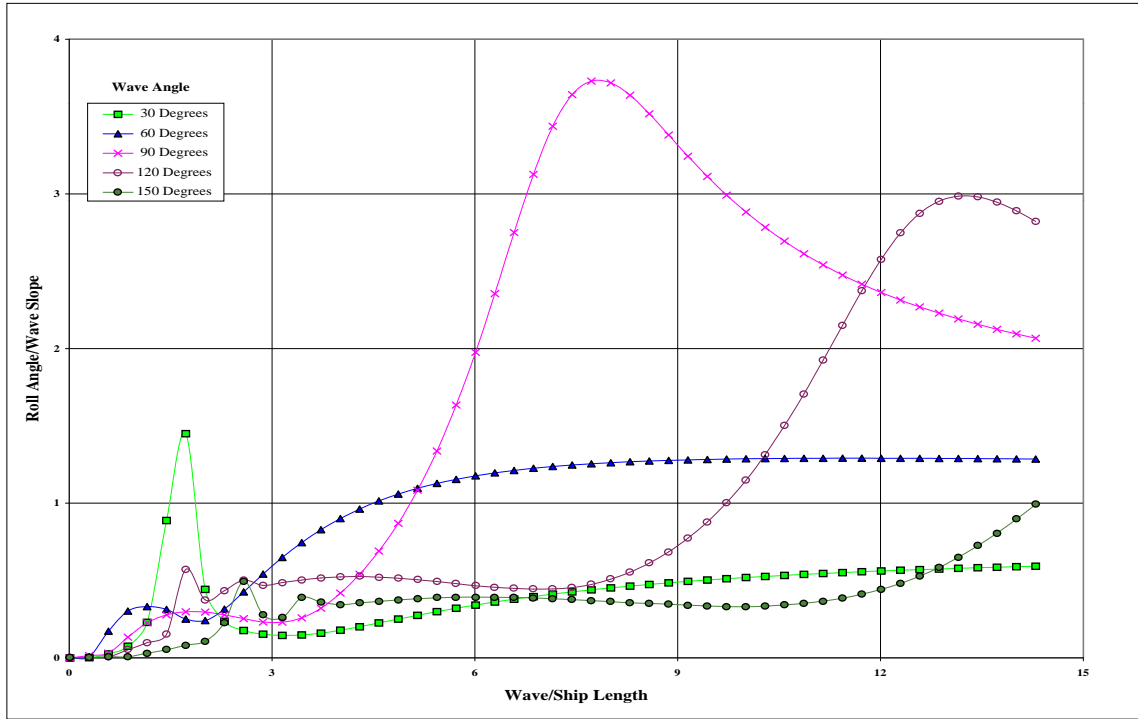


Figure (100). Roll Characteristics as a Function of Wave Angle, 30 Knots.

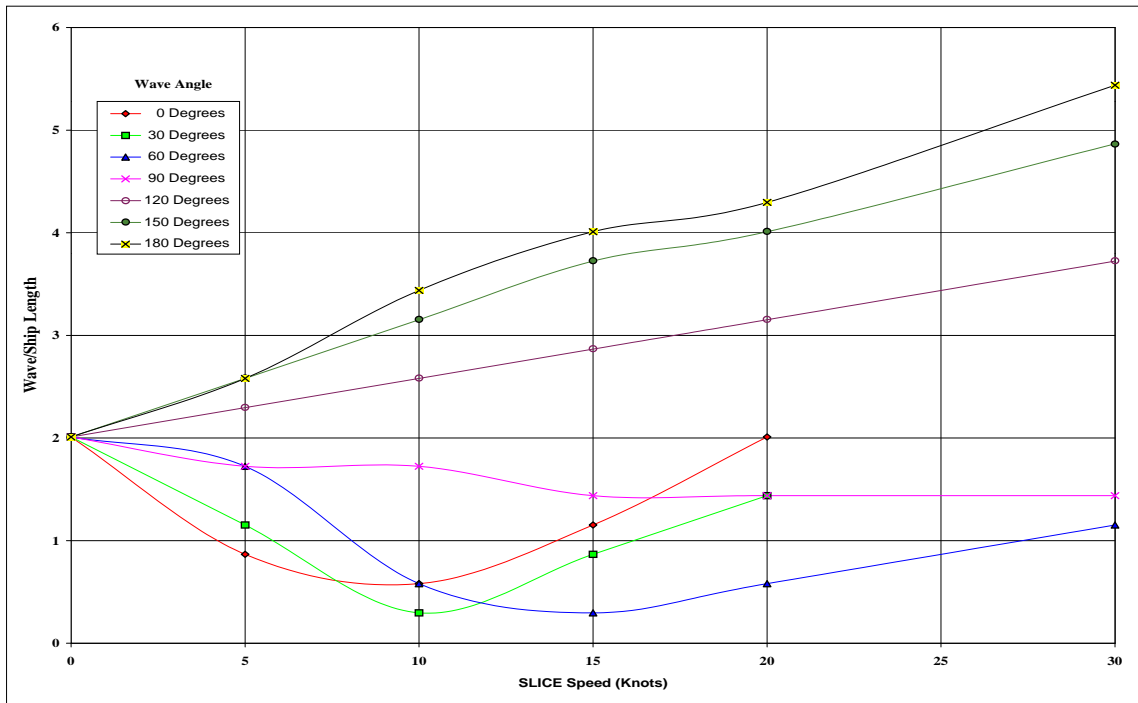


Figure (101). Resonant Peak Locations for Surge.

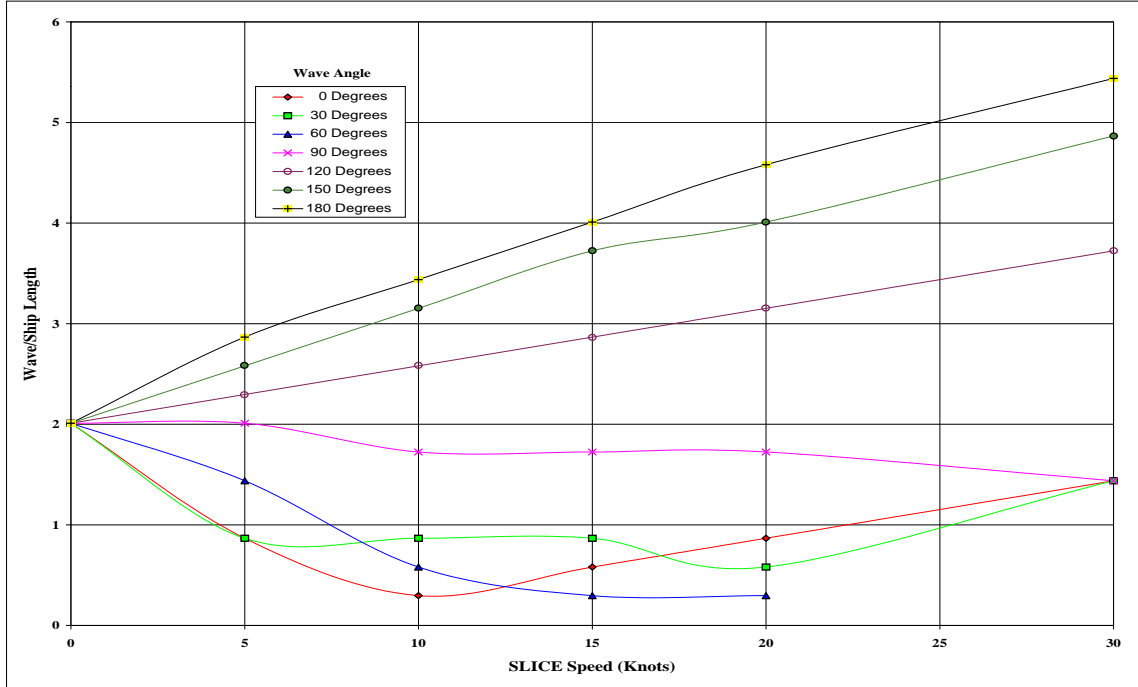


Figure (102). Resonant Peak Locations for Heave.

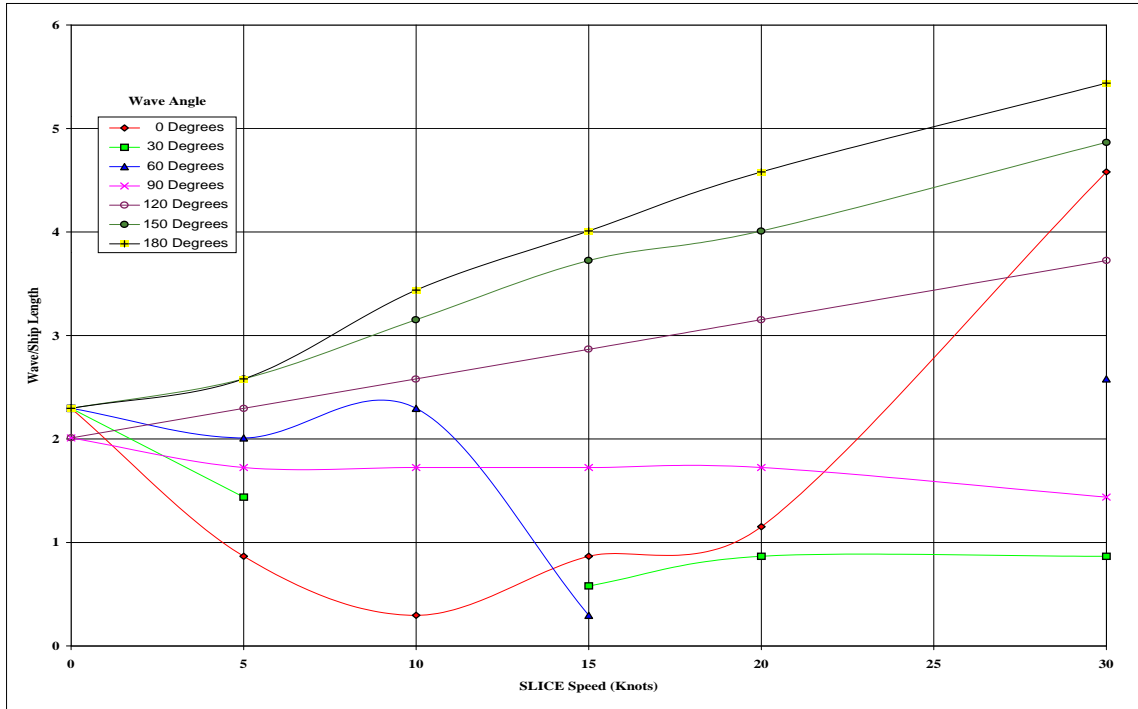


Figure (103). Resonant Peak Locations for Pitch.

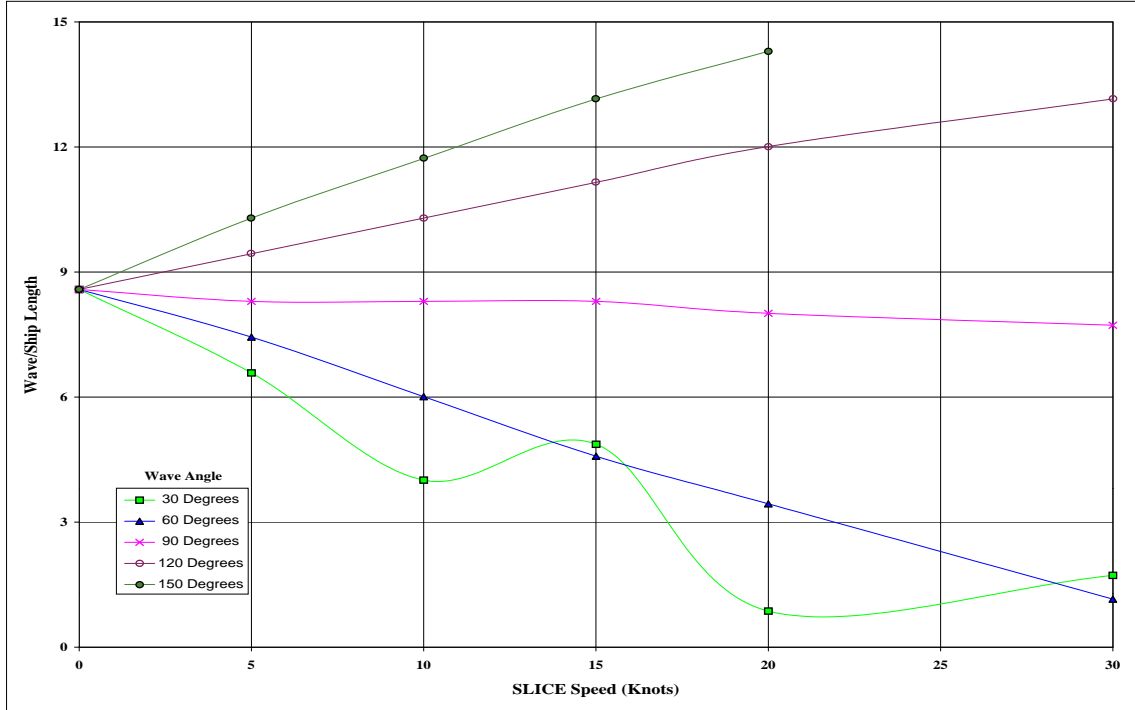


Figure (104). Resonant Peak Locations for Roll.

C. IRREGULAR WAVE RESULTS

The irregular wave analysis concerns itself with the motions as previously described in Table (2); focusing on pitch, roll and vertical accelerations. In pitch and roll, the following data supports the trends described in the preceding regular wave analysis. The data presentation in this section makes the findings more easily understood by using polar plots. Data are presented as significant motion amplitudes in terms of degrees of pitch and roll, and g's of acceleration. Table (7) serves as the legend for these plots.

Figures (105) through (116) show the effect of sea state on the motions of pitch and roll at constant speeds. With the SLICE at rest, these motions increased as the seas grew more severe (sea states two through seven). Motion values for sea state one were negligible.

Generally, as speed increased, pitch motions waned for wave angles aft of the beam and increased for those forward. Pitch becomes unstable, in seas off the bow, above 15 knots; as shown in Figures (117) through (122). The largest amplitudes appear at wave angles between 110 and 180 degrees with some distinctive spikes dispersed throughout the range. Pitch in beam

seas remained relatively constant, in a given sea state. This indicates there might be some cross coupling between pitch and roll.

Color	Constant Sea States	Constant Speeds
Yellow	0 Knots	Sea State 2
Purple	5 Knots	Sea State 3
Turquoise	10 Knots	Sea State 4
Red	15 Knots	Sea State 5
Green	20 Knots	Sea State 6
Blue	30 Knots	Sea State 7

Table (7). Legend for Polar Plots.

Roll motions showed some instability in quartering seas; specifically, wave angles 30 to 70 degrees, as shown in Figures (123) through (128). Roll in beam seas remained constant. In seas off the bow, rolling motion reduced as speed increased at constant sea state. For quartering seas, motions increased with speed. Maximum roll amplitudes occurred in seas of wave angle between 50 and 80 degrees.

Vertical plane accelerations, as depicted in Figures (129) through (140), show the same trends as pitch.

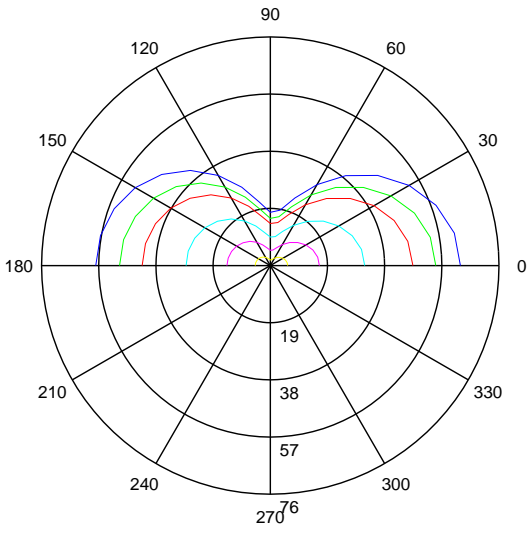
D. SEAKEEPING EVALUATION

Recall from Table (2), the seakeeping criteria adopted for the SLICE ferry application. Maximum significant amplitudes of pitch, roll, and vertical accelerations are set at 3 degrees, 8 degrees, and 0.4 g's respectively. It is obvious, from the data previously presented in Figures (105) through (140), that any evaluation made must contain some discussion to be of merit. Due to the ideal fluid assumption of the strip theory employed in the motion determinations, excessive resonant peaks exist in pitch and vertical acceleration data. Roll data is more accurate due to the damping determination presented in the previous chapter.

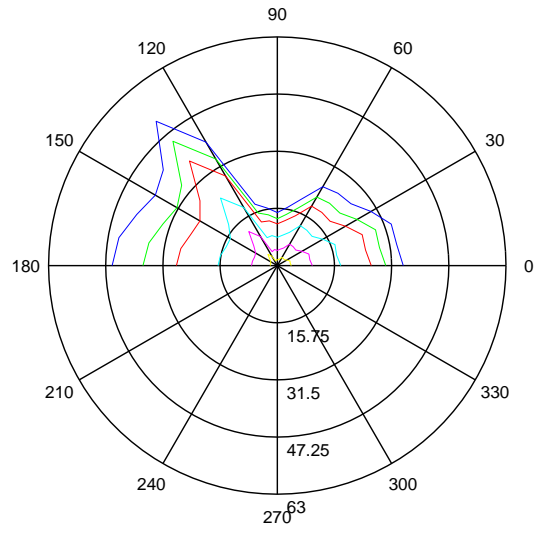
An attempt to filter the data can be made by utilizing previously published SWATH experimental-theoretical results comparisons. Based on the work of C. M. Lee (1976, 1977) and

Y. S. Hong (1986), this correction factor may be as high as 3.0 for pitch, and 1.6 for roll and vertical accelerations. By applying these correction factors to a bandwidth of motion and acceleration data, centered on the resonant frequency, more accurate statistical motion values will result. It must also be remembered that these correction factors will need to be adjusted to accurately reflect the additional damping effects of the control surfaces. In this final point is where the difficulties lie.

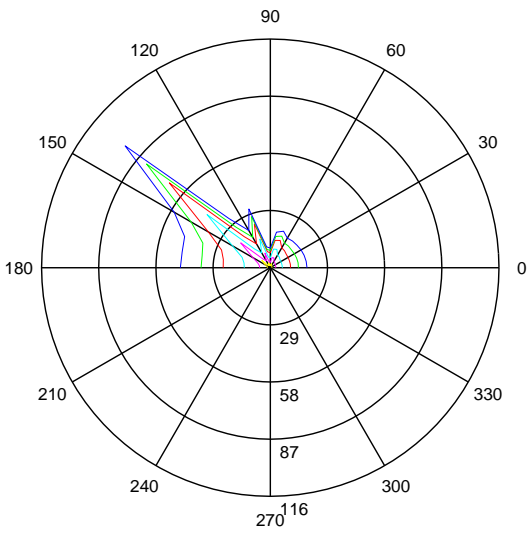
The direction taken in this evaluation was to assume the vertical plane instabilities of heave and pitch could be controlled with the stabilizer/rudders and canards. The increased damping of these modes of motion, through a reduction in excitation forces, will also proportionally reduce the vertical plane accelerations. Therefore, an examination of the roll data should provide a fairly accurate seakeeping evaluation. Based on these assumptions, the SLICE will be within the bounds of our criteria in seas up to sea state four, at all wave angles. Seas to sea state six can be satisfactorily encountered provided quartering and beam seas (30 to 90 degree wave angles) can be avoided. The criteria for roll is obtained in sea state seven for seas within 45 degrees of the bow. However, this is where pitch and vertical accelerations are most severe and might not be controllable to within other set criteria. Refer back to Figures (123) through (128).



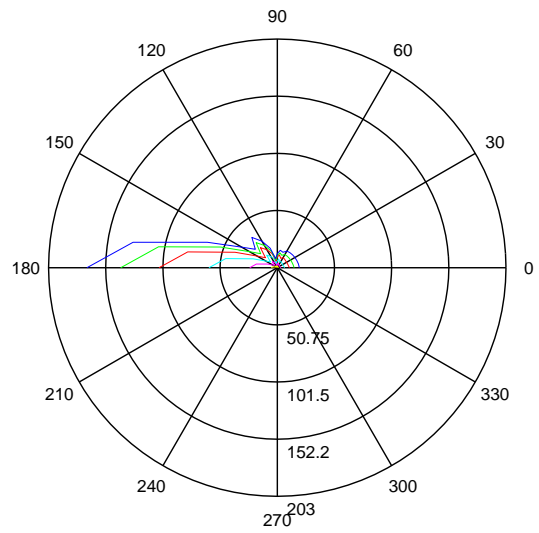
Figure(105). Pitch Characteristics, 0 Knots.



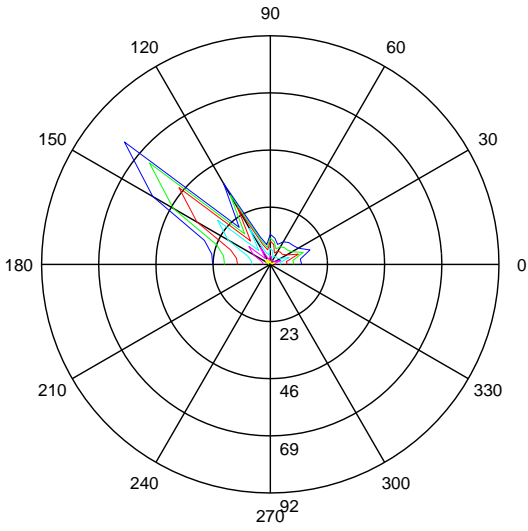
Figure(106). Pitch Characteristics, 5 Knots.



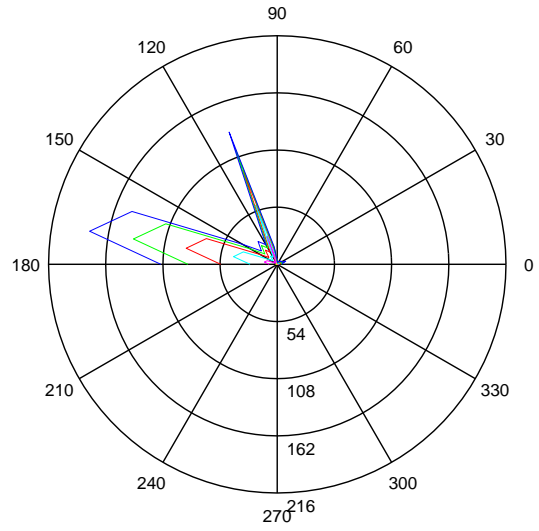
Figure(107). Pitch Characteristics, 10 Knots.



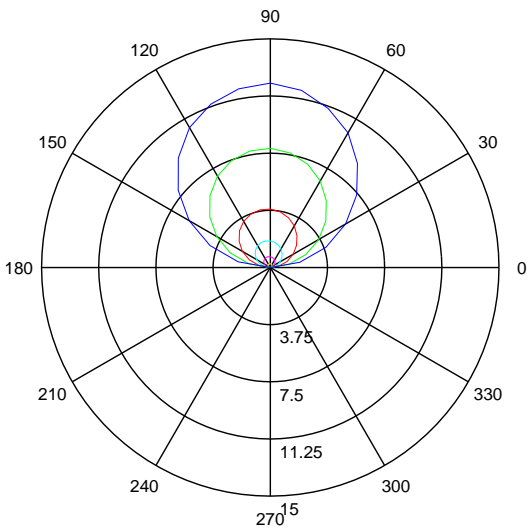
Figure(108). Pitch Characteristics, 15 Knots.



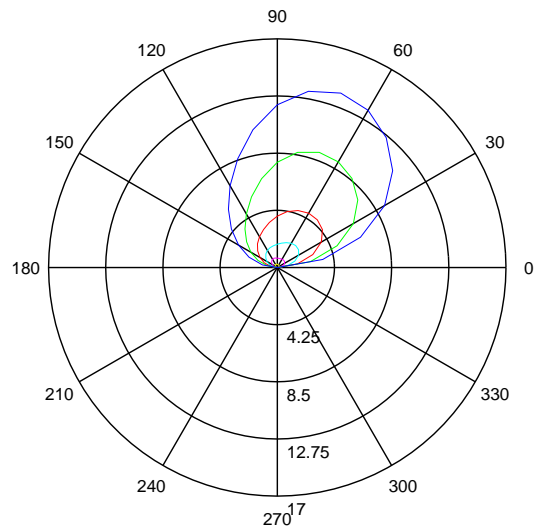
Figure(109). Pitch Characteristics, 20 Knots.



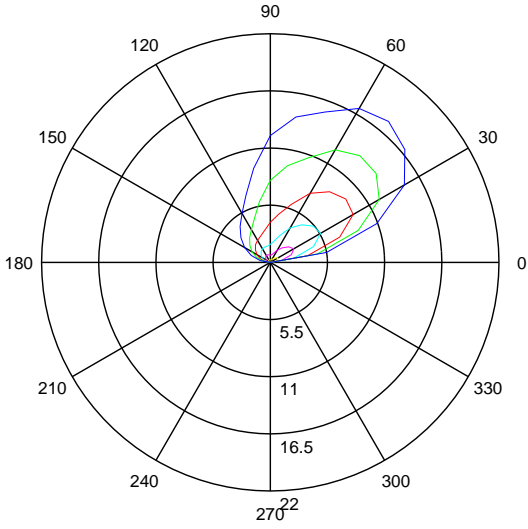
Figure(110). Pitch Characteristics, 30 Knots.



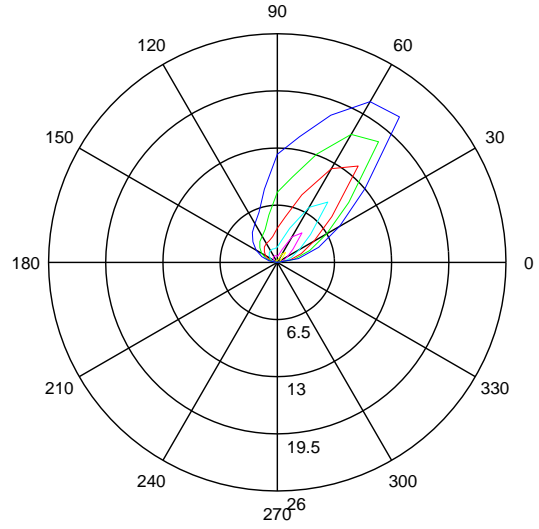
Figure(111). Roll Characteristics, 0 Knots.



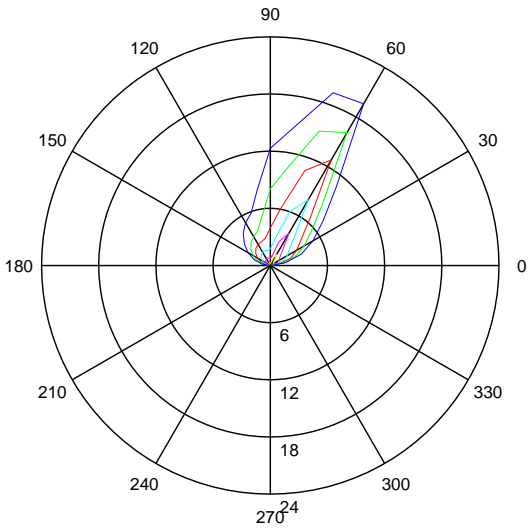
Figure(112). Roll Characteristics, 5 Knots.



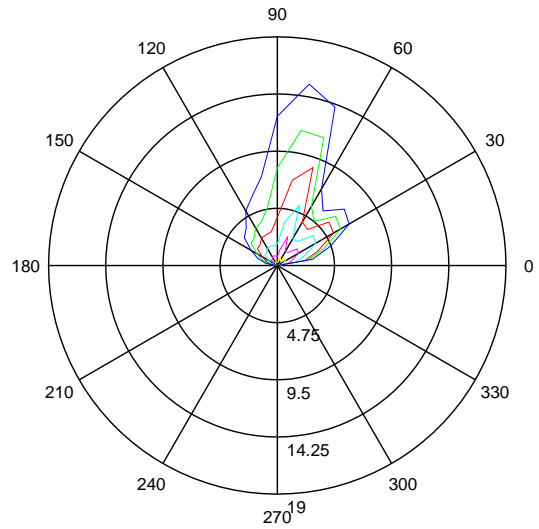
Figure(113). Roll Characteristics, 10 Knots.



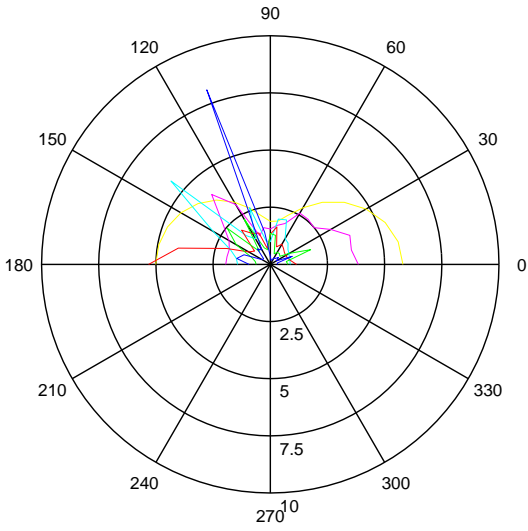
Figure(114). Roll Characteristics, 15 Knots.



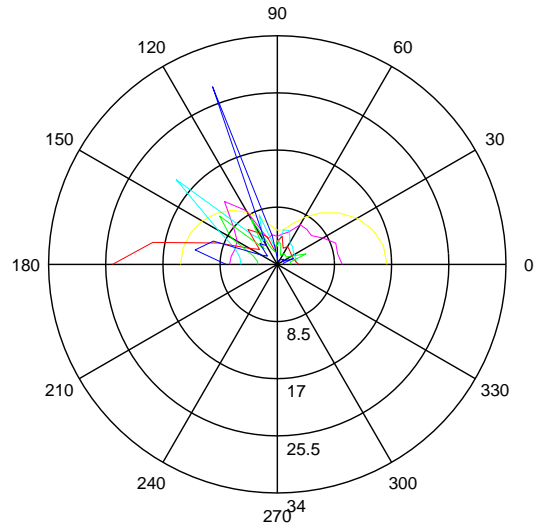
Figure(115). Roll Characteristics, 20 Knots.



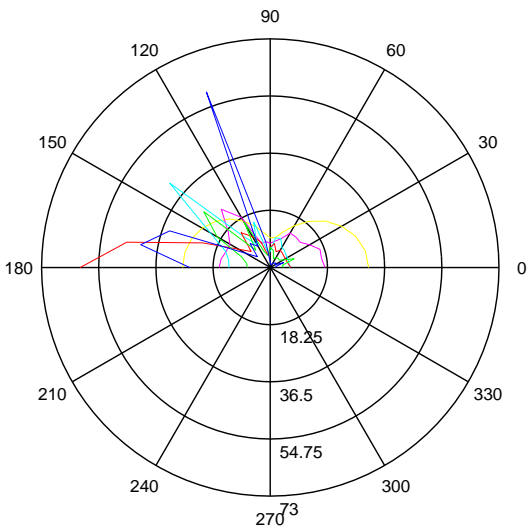
Figure(116). Roll Characteristics, 30 Knots.



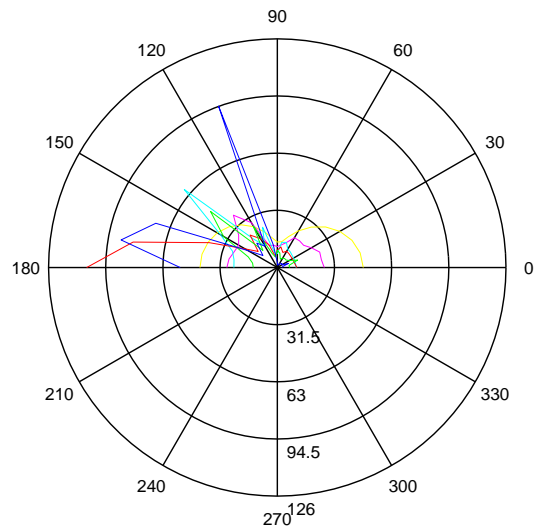
Figure(117). Pitch Characteristics, Sea State 2.



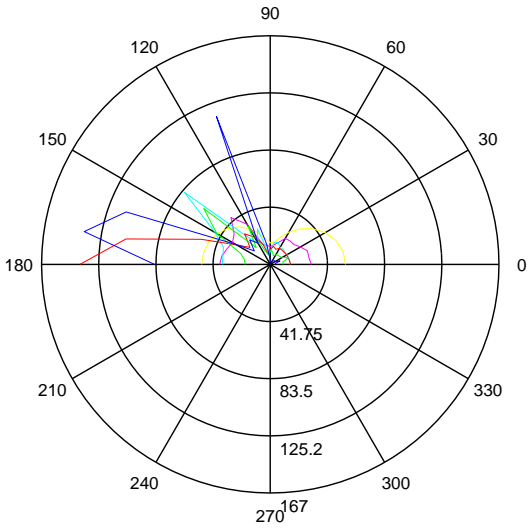
Figure(118). Pitch Characteristics, Sea State 3.



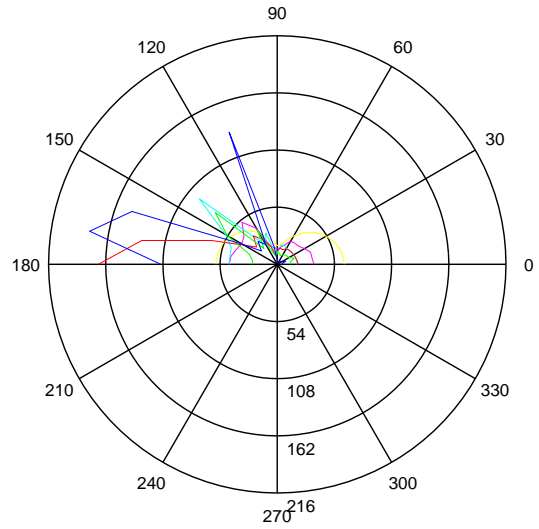
Figure(119). Pitch Characteristics, Sea State 4.



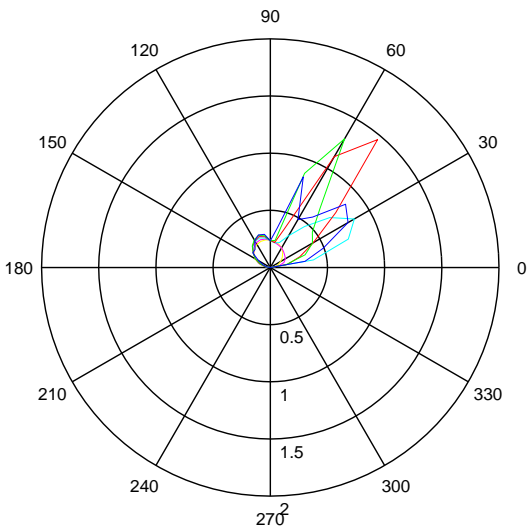
Figure(120). Pitch Characteristics, Sea State 5.



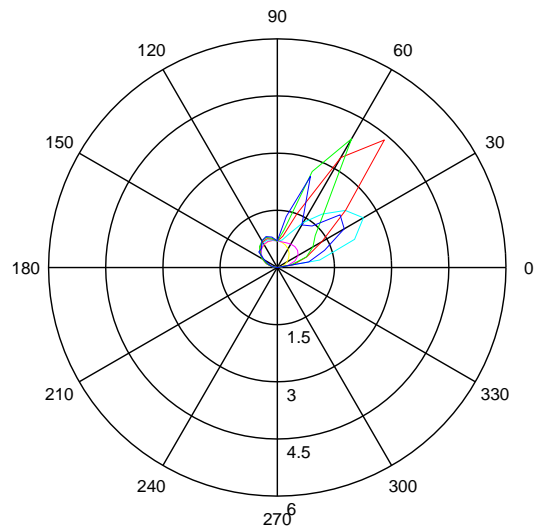
Figure(121). Pitch Characteristics, Sea State 6.



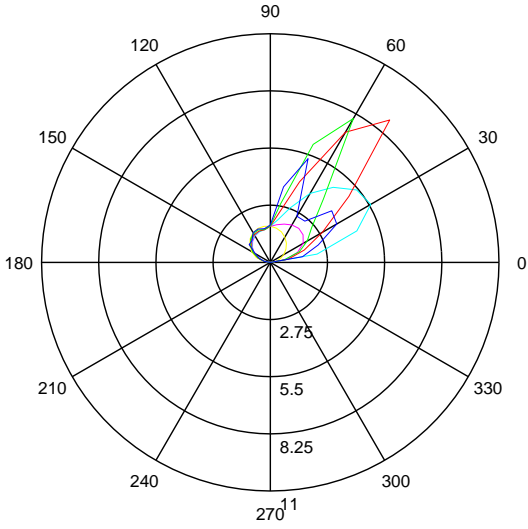
Figure(122). Pitch Characteristics, Sea State 7.



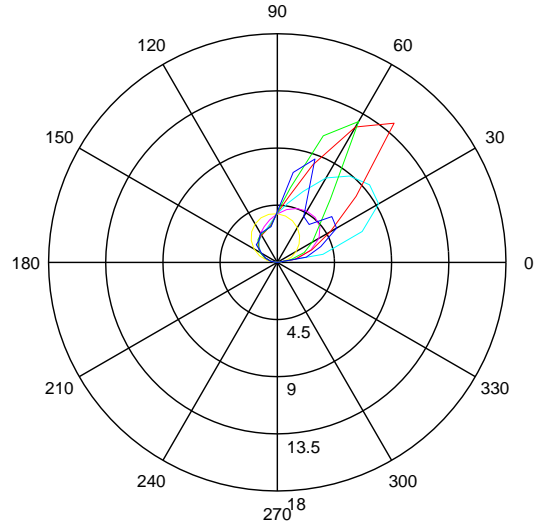
Figure(123). Roll Characteristics, Sea State 2.



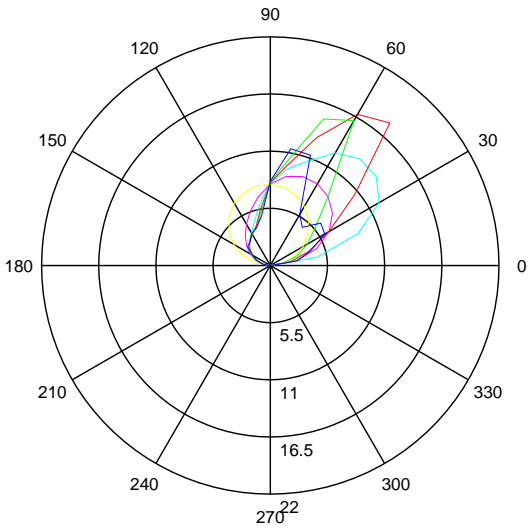
Figure(124). Roll Characteristics, Sea State 3



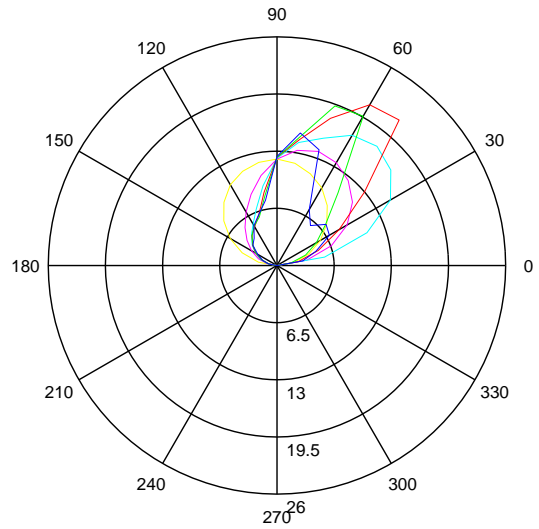
Figure(125). Roll Characteristics, Sea State 4.



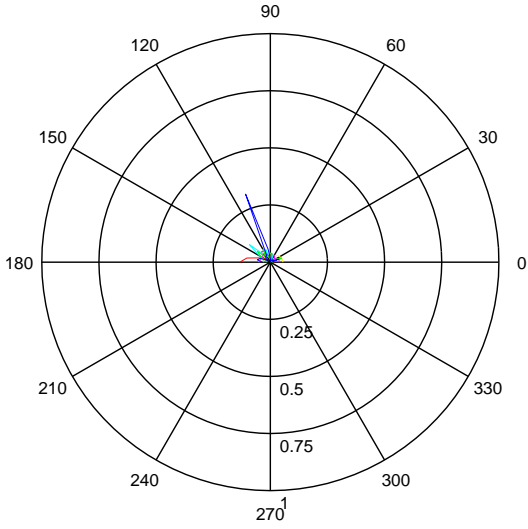
Figure(126). Roll Characteristics, Sea State 5.



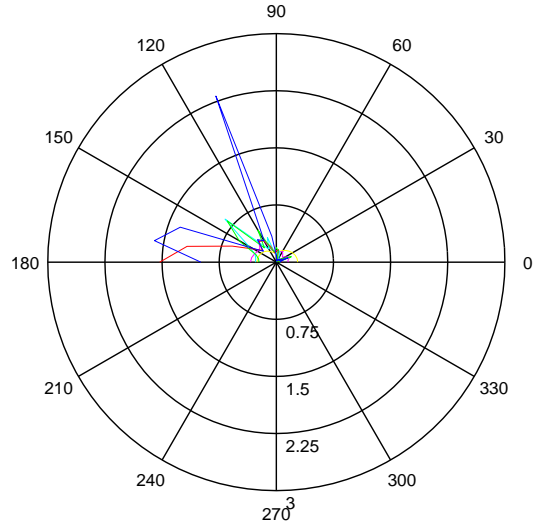
Figure(127). Roll Characteristics, Sea State 6.



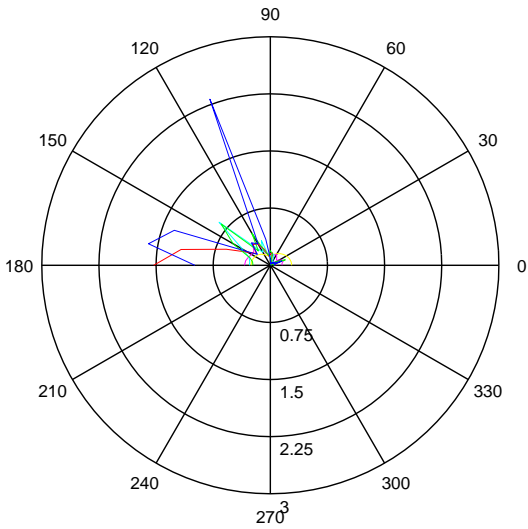
Figure(128). Roll Characteristics, Sea State 7.



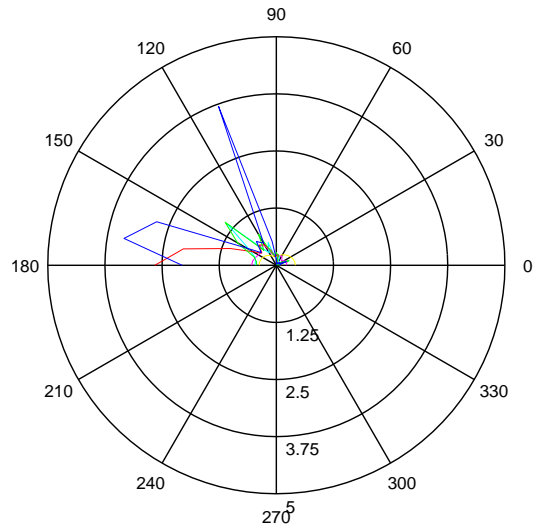
Figure(129). Vertical Acceleration, 0 Knots.



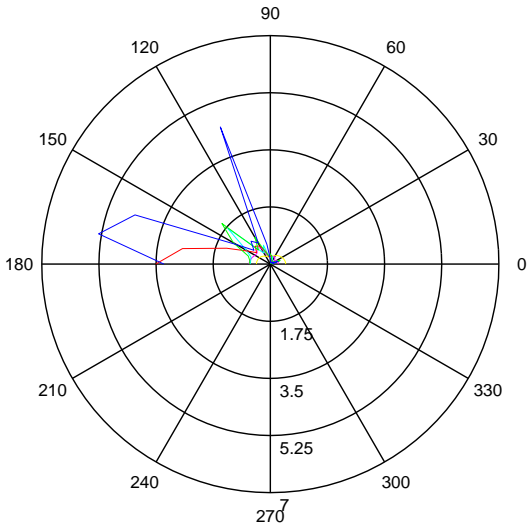
Figure(130). Vertical Acceleration, 5 Knots.



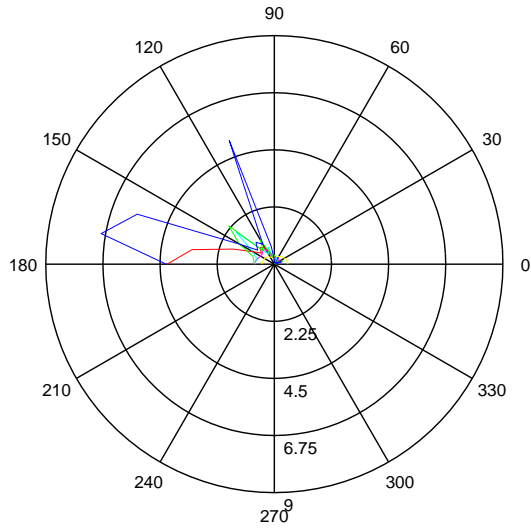
Figure(131). Vertical Acceleration, 10 Knots.



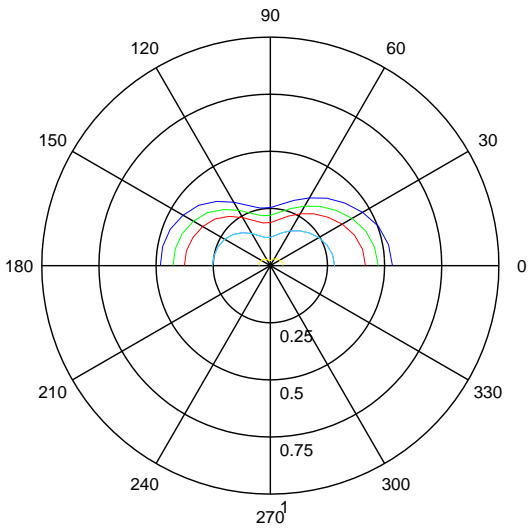
Figure(132). Vertical Acceleration, 15 Knots.



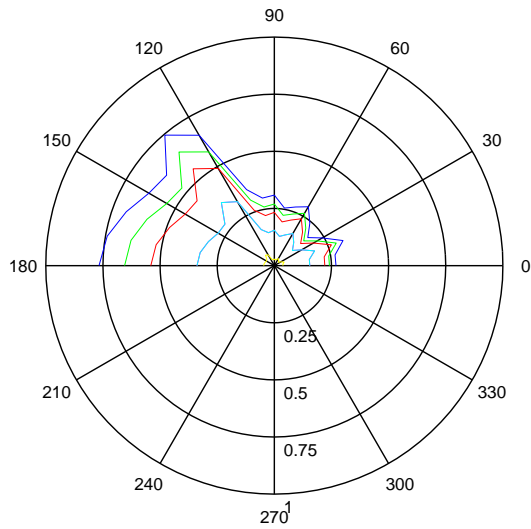
Figure(133). Vertical Acceleration, 20 Knots.



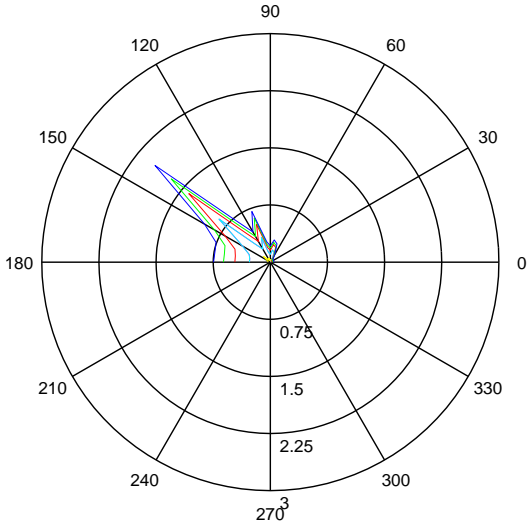
Figure(134). Vertical Acceleration, 30 Knots.



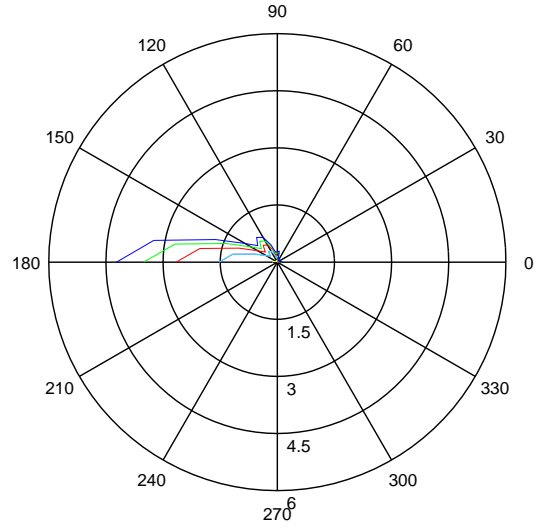
Figure(135). Vertical Acceleration, Sea State 2.



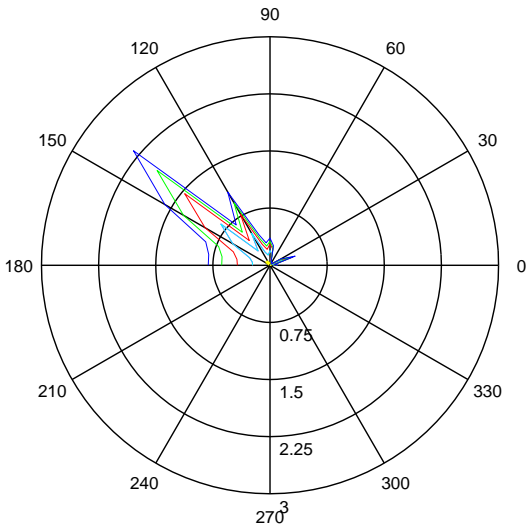
Figure(136). Vertical Acceleration, Sea State 3.



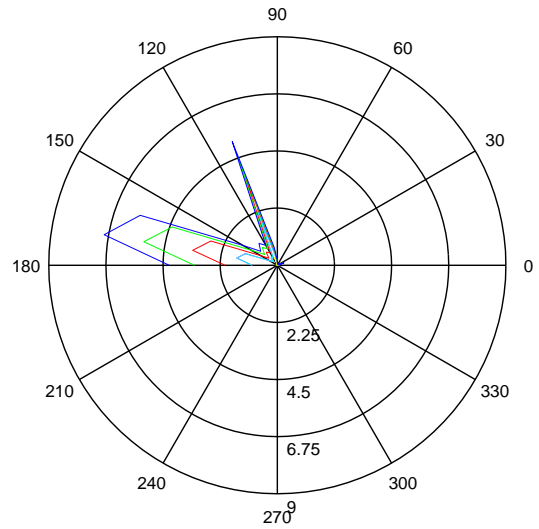
Figure(137). Vertical Acceleration, Sea State 4.



Figure(138). Vertical Acceleration, Sea State 5.



Figure(139). Vertical Acceleration, Sea State 6.



Figure(140). Vertical Acceleration, Sea State 7.

IV. DISCUSSION

A. CONCLUSIONS

This study has shown the SLICE to be a viable design for its intended application provided the inherent vertical plane instabilities can be balanced through the use of active and passive control surfaces. The overall effectiveness of control must be determined before other mission areas, with more stringent criteria, are considered.

This investigation determined the roll damping term to be within the range of 0.02 and 0.3; in terms of percentage of critical damping. The lower bound was adopted from Reilly (1988), and the upper bound was determined as the percentage where roll behavior is no longer underdamped. The modeled value of 0.1 was arrived at in matching data based on scale model experiments.

Ignoring the influence of negative encounter frequencies, the motions of surge, heave, and pitch were maximized in seas forward of the bow. For sway, it was beam seas that excited largest motions. Roll and yaw were greatest in quartering seas. Horizontal plane motions tend to be damped out while vertical plane motions grow larger with increasing speed for wave angles forward of the beam.

Resonant peak locations relate directly to the stability of the platform in a given motion. Peaks were recorded for the motions of surge, heave, pitch, and roll. It was shown that the higher the wave to ship length ratio, the more severe sea conditions needed to be to excite resonant motions. The SLICE shows increased stability, with increasing speed for wave angles forward of the beam. In following and quartering seas, decreased stability is observed at speeds below 15 knots. A slight decrease in stability is apparent in beam seas. It appears that stability increases in quartering seas for speeds above 15 knots, but this is the region where encounter frequencies are likely to be negative, and therefore the data is questionable.

The seakeeping evaluation showed the SLICE to maintain motions within the limits of the criteria for sea state four and below at all speeds and wave angles. The criteria can be

maintained in seas up to state six provided quartering and beam seas are avoided. This range of sea states covers the conditions in which the SLICE would most likely operate on a regular basis.

B. RECOMMENDATIONS

The following is a list of recommendations for further research on the SLICE hull configuration:

Since typical ship designs utilize a ship length much greater than the beam, cross coupling between the modes of pitch and roll is seldom experienced due to the large separation in natural frequencies of these modes. The SLICE design employs roughly a two to one ratio in these dimensions. This makes the natural frequencies of these motions much closer together and increases the possibility that one mode may excite the other. Figures (104) to (122) indicate there might be some coupling of this nature. An investigation into this nonlinear behavior might prove worthwhile.

Establish a computer protocol that will take decompose the bending moment information and formulate it to be used as an applied force/moment set in the I-DEAS finite element model of the SLICE generated by Roberts (1995). This will allow for more realistic modeling of the dynamic loads encountered in a seaway to determine the structural limitations of the design, if any. Previous research could only complete a static analysis. This would require a program more sophisticated than SHIPMO.BM since the wave loads must be distributed along the hull. SHIPMO.BM utilizes a two dimensional potential theory and can only provide loads resolved along the centerline. A three dimensional theory would be required.

LIST OF REFERENCES

- Beck, R. F., and Troesch, A. W., "Documentation and User's Manual for the Computer Program SHIPMO.BM," Report No. 89-2, 1989.
- Fang, M. C., "The Motion of SWATH Ships in Waves," *Journal of Ship Research*, vol. 32 No. 4, pp. 238-245, 1988.
- Fein, J. A., Ochi, M. D., and McCreight, K. K., "The Seakeeping Characteristics of a Small Waterplane Area Twin-Hull Ship," 13th Symposium of Hydrodynamics, 1987.
- Frank, W., "On the Oscillations of Cylinders in or Below the Free Surface of Deep Fluids," Technical Note 69, Hydrodynamics Laboratory, Naval Ship R&D Center, 1967.
- Gilmer, T. C., and Johnson, B., "Introduction to Naval Architecture," United States Naval Institute Press, Annapolis, Md., 1982.
- Himeno, Y., "Prediction of Ship Roll Damping - State of the Art," Report No. 239, Department of Naval Architecture and Marine Engineering, Univ. of Michigan, Ann Arbor, MI, 1981.
- Hong, Y. S., "Heave and Pitch Motions of SWATH Ships," *Journal of Ship Research*, vol. 30 No. 1, pp. 12-25, 1986.
- Lee, C. M., "Theoretical Prediction of Motion of Small Waterplane Area, Twin-Hull (SWATH) Ships in Waves," David W. Taylor Naval Ship Research and Development Center, Report 760046, 1976.
- Lee, C. M., and Curphey, R. M., "Prediction of Motion, Stability, and Wave Load of Small-Waterplane-Area, Twin-Hull Ships," *SNAME Transactions*, vol. 85, pp. 94-130, 1977.
- Lockheed Missile and Space Company, Inc. (LMSC), "SLICE Inboard Profile," Drawing No. P1-100-04, Aug. 1994.
- Lockheed Missile and Space Company, Inc. (LMSC), "SLICE Lines and Offsets," Drawing No. P1-100-01, Sheets 1 and 2, Dec. 1994.
- Lockheed Missile and Space Company, Inc. (LMSC), "SLICE Advanced Technology Demonstration, Final Technical Review," Dec. 1994.
- McCreight, K. K., "Assessing the Seaworthiness of SWATH Ships," *SNAME Transactions*, vol. 95, pp. 189-214, 1987.
- Papoulias, F. A., "Dynamics of Marine Vehicles," Informal Lecture Notes for ME4823, Naval Postgraduate School, Monterey, CA, Summer 1993.
- Peffer, S. B., "Seakeeping Aspects of SLICE Hulls," M.S. Thesis, Naval Postgraduate School, Monterey, CA, 1995.
- Reilly, E. T., Shin, Y. S., and Kotte, E. H., "A prediction of Structural Load and Response of a SWATH Ship in Waves," *Naval Engineers Journal*, pp. 251-264, 1988.

Roberts, D. J., "Structural Response of the SLICE Advanced Technology Demonstrator," M. S. Thesis, Naval Postgraduate School, Monterey, CA, 1995.

Salvesen, N., Tuck, E. O., and Faltisen, O., "Ship Motions and Sea Loads," SNAME Transactions, vol. 78, pp 250-287,

APPENDIX A

Input file, SHIPMO.IN, for running regular and irregular wave analyses on the SLICE hull form. Refer to Appendix A of the SHIPMO.BM User's Manual for format and line content information.

SLICE HULL FORM GENERATED BY D.B. LESH APRIL 1995

```
0 164 0 0 1 0 2 0 1 0 0 0 7 20 1
105.0000 1.9905 32.1740 1.26E-05 1.6557E+02 0.0000
33.0000 -26.0000 1.0000
1 48.6000 0.0000 0
16.5000 0.0000
5 44.8750 0.0000 0
16.0000 0.0000
16.2500 -0.9000
16.5000 -1.8000
16.7500 -0.9000
17.0000 0.0000
8 40.8750 0.0000 0
15.5000 0.0000
15.8000 -2.0000
16.1000 -4.0000
16.1000 -10.0000
16.9000 -10.0000
16.9000 -4.0000
17.2000 -2.0000
17.5000 0.0000
15 39.8750 0.0000 0
15.4000 0.0000
15.6000 -1.5000
15.5500 -7.3100
14.6250 -8.9200
14.5000 -10.0000
14.6250 -11.1000
15.0850 -11.4100
16.5000 -12.0000
17.9000 -11.4100
18.3750 -11.1000
18.5000 -10.0000
18.3750 -8.9200
```

17.4500 -7.3100
17.4000 -1.5000
17.6000 0.0000
11 37.8750 0.0000 0
15.0000 0.0000
15.0000 -5.7500
13.5800 -8.3125
13.3000 -10.0000
14.7000 -11.7900
16.5000 -13.2000
18.2900 -11.7900
19.7000 -10.0000
19.4200 -8.3125
18.0000 -5.7500
18.0000 0.0000
15 33.8750 0.0000 0
14.8750 0.0000
14.8750 -4.8000
14.8500 -4.9100
13.0400 -8.0000
12.5000 -10.0000
13.0400 -12.0000
14.5000 -13.4600
16.5000 -14.0000
18.5000 -13.4600
20.0000 -12.0000
20.5000 -10.0000
20.0000 -8.0000
18.1500 -4.9100
18.1250 -4.8000
18.1250 0.0000
13 23.8750 0.0000 0
15.2000 0.0000
15.2000 -6.9200
13.0400 -8.0000
12.5000 -10.0000
13.0400 -12.0000
14.5000 -13.4600
16.5000 -14.0000
18.5000 -13.4600
20.0000 -12.0000
20.5000 -10.0000
20.0000 -8.0000

17.8000 -6.9200
17.8000 0.0000
13 19.8750 0.0000 0
15.8750 0.0000
15.9100 -6.1200
15.6640 -6.5500
13.0380 -10.0000
13.5000 -11.7300
14.7700 -13.0000
16.5000 -13.4600
18.2300 -13.0000
19.5000 -11.7300
20.0000 -10.0000
17.3400 -6.5500
17.1000 -6.1200
17.1250 0.0000
15 16.8750 0.0000 0
16.4000 0.0000
16.4000 -7.2500
15.0600 -7.5100
14.0100 -8.5600
13.6200 -10.0000
14.0100 -11.4400
15.0600 -12.4900
16.5000 -12.8800
18.0000 -12.4900
19.1000 -11.4400
19.3800 -10.0000
19.1000 -8.5600
18.0000 -7.5100
16.6000 -7.2500
16.6000 0.0000
13 7.1250 0.0000 1
16.5000 -9.2800
16.1400 -9.3800
15.8800 -9.6400
15.7800 -10.0000
15.8800 -10.3600
16.1400 -10.6200
16.5000 -10.7200
16.8600 -10.6200
17.1200 -10.3600
17.2200 -10.0000

17.1200 -9.6400
16.8600 -9.3800
16.5000 -9.2800
1 0.0000 0.0000 1
23.5000 0.0000
1 -10.1250 0.0000 1
23.5000 -10.0000
13 -11.3000 0.0000 1
23.5000 -7.8000
22.4000 -8.0900
21.5900 -8.9000
21.3000 -10.0000
21.5900 -11.1000
22.4000 -11.9100
23.5000 -12.2000
24.6000 -11.9100
25.4000 -11.1000
25.7000 -10.0000
25.4000 -8.9000
24.6000 -8.0900
23.5000 -7.8000
13 -13.3500 0.0000 1
23.5000 -7.1000
22.1000 -7.4800
21.0800 -8.5500
20.6000 -10.0000
21.1800 -11.4500
22.1500 -12.5200
23.5000 -12.9000
25.0000 -12.5200
26.0000 -11.4500
26.4000 -10.0000
26.0000 -8.5500
25.0000 -7.4800
23.5000 -7.1000
15 -16.7900 0.0000 0
22.4000 0.0000
23.4000 -6.0000
21.5000 -6.5400
20.0000 -8.0000
19.5000 -10.0000
20.0000 -12.0000
21.5000 -13.4600

23.5000 -14.0000
25.5000 -13.4600
27.0000 -12.0000
27.5000 -10.0000
27.0000 -8.0000
25.5000 -6.5400
23.6000 -6.0000
24.6000 0.0000
11 -19.1250 0.0000 0
22.1000 0.0000
22.1000 -5.3000
21.3400 -6.6350
19.5000 -10.0000
20.6700 -12.8300
23.5000 -14.0000
26.3300 -12.8300
27.5000 -10.0000
25.6600 -6.6350
24.9000 -5.3000
24.9000 0.0000
13 -25.1250 0.0000 0
21.9000 0.0000
21.9000 -5.0000
21.7500 -5.0500
20.0000 -8.0000
19.5000 -10.0000
20.6700 -12.8300
23.5000 -14.0000
26.3300 -12.3300
27.5000 -10.0000
27.0000 -8.0000
25.2600 -5.0500
24.9000 -5.0000
24.9000 0.0000
13 -32.1250 0.0000 0
22.0000 0.0000
22.0000 -6.8000
22.0250 -6.8800
21.6700 -7.4900
20.3000 -10.0000
21.2400 -12.2600
23.5000 -14.0000
25.7000 -12.2600

26.7000	-10.0000		
25.3300	-7.4900		
25.0000	-6.8800		
25.0000	-6.8000		
25.0000	0.0000		
15	-40.8000	0.0000	0
23.4000	0.0000		
23.4000	-8.8000		
23.0000	-8.9750		
22.5000	-9.4100		
22.3200	-10.0000		
22.5000	-10.5900		
23.0000	-11.0200		
23.5000	-11.8300		
24.0900	-11.0200		
24.5200	-10.5900		
24.6800	-10.0000		
24.5200	-9.4100		
24.0000	-8.9750		
23.6000	-8.8000		
23.6000	0.0000		
1	-46.1250	0.0000	1
23.5000	-10.0000		
9999.0	0.0000		
1.8750	0.0	0.0	
58.8800	0.2210	7.2289	16.5000
54.6800	0.2210	7.2289	16.5000
54.6800	0.2710	8.2937	16.5000
42.5800	0.2710	8.2937	16.5060
42.5800	0.2210	7.2289	16.5060
40.8800	0.2210	7.2289	16.5101
40.8800	0.9063	5.7590	16.5101
37.0800	0.9063	5.7590	16.6123
37.0800	1.1196	2.8272	16.6123
30.6800	1.1196	2.8272	16.6479
30.6800	0.9063	5.7590	16.6479
27.8800	0.9063	5.7590	16.6479
27.8800	1.8746	-1.8491	16.6479
25.8800	1.8746	-1.8491	16.6504
25.8800	2.4336	0.2640	16.6504
16.6800	2.4336	0.2640	16.6166
16.6800	3.8786	1.3690	16.6166
16.1800	3.8786	1.3690	16.6061

16.1800	2.9103	4.8089	16.6061
15.0800	2.9103	4.8089	16.5913
15.0800	3.8303	1.2664	16.5913
12.6800	3.8303	1.2664	16.5591
12.6800	3.2713	0.2268	16.5591
10.6800	3.2713	0.2268	16.5371
10.6800	3.5580	0.7831	16.5371
9.6800	3.5580	0.7831	16.5285
9.6800	4.6180	4.7786	16.5285
8.9800	4.6180	4.7786	16.5220
8.9800	4.2741	5.7263	16.5220
8.3800	4.2741	5.7263	16.5170
8.3800	2.8291	7.0013	16.5170
6.6800	2.8291	7.0013	16.5079
6.6800	1.9091	15.1654	16.5079
5.0800	1.9091	15.1654	16.5000
5.0800	1.5677	14.6222	16.5000
2.5800	1.5677	14.6222	16.5000
2.5800	1.7066	14.1646	16.5000
-7.6300	1.7066	14.1646	23.5000
-7.6300	1.4199	15.5850	23.5000
-8.2300	1.4199	15.5850	23.5000
-8.2300	1.2810	16.2290	23.5000
-10.5300	1.2810	16.2290	23.5000
-10.5300	1.6034	11.6142	23.5000
-13.6300	1.6034	11.6142	23.6038
-13.6300	3.5304	-0.2817	23.6038
-19.6300	3.5304	-0.2817	23.6046
-19.6300	1.6034	11.6142	23.6046
-20.5300	1.6034	11.6142	23.6046
-20.5300	1.8334	9.2979	23.6046
-26.1300	1.8334	9.2979	23.5921
-26.1300	2.0534	7.1596	23.5921
-29.1300	2.0534	7.1596	23.5765
-29.1300	2.5276	7.0734	23.5765
-29.6300	2.5276	7.0734	23.5720
-29.6300	1.4676	-0.9558	23.5720
-30.8300	1.4676	-0.9558	23.5658
-30.8300	1.2376	0.1396	23.5658
-34.8800	1.2376	0.1396	23.5352
-34.8800	1.0176	2.4744	23.5352
-40.8800	1.0176	2.4744	23.5087
-40.8800	0.5434	-1.2131	23.5087

-42.8800 0.5434 -1.2131 23.5063
-42.8800 0.2210 7.2289 23.5063
-46.1250 0.2210 7.2289 23.5000
0.0000 246.9000 5924.8000 -296.2000 740.6000 987.5000 987.5000
7 7.1200 16.5000 -10.0000
5.0000 1.0000 1501.0000 30.0000 0.0000 50.0000 8.3333
0.1000
0.0000 180.0000 30.0000
0.0

The following changes are made to the above file when conducting the irregular wave analysis:

Input Line for Card 2:

0 164 0 5 1 0 1 0 0 0 1 0 7 20 1

Input Line for Card 11:

1.0000 0.4000 2.4000 0.1000 0.0000 50.0000 8.3333

Input Line for Card 13:

0.0000 180.0000 10.0000

Input Line for Card 14:

0.9500 7.0000

INITIAL DISTRIBUTION LIST

		No. Copies
1.	Defense Technical Information Center Cameron Station Alexandria, VA 22304-6145	2
2.	Dudley Knox Library, Code 52 Naval Postgraduate School Monterey, CA 93943-5000	2
3.	Chairman, Code ME Department of Mechanical Engineering Naval Postgraduate School Monterey, CA 93943-5000	1
4.	Professor Fotis A. Papoulias, Code ME/PA Department of Mechanical Engineering Naval Postgraduate School Monterey, CA 93943-5000	6
5.	Naval Engineering Curricular Office, Code 34 Naval Postgraduate School Monterey, CA 93943-5100	1
6.	LT Donald B. Lesh 1271 Leahy Rd. Monterey, CA 93940	2